

Material Analysis and Testing Report

Wilson Tunnel Plenum and Hanger Rods

September 6, 2022



Developed For: State of Hawaii Department of Transportation
District of Oahu



Prepared By:



Joshua Steiner
Report by: Joshua Steiner, PE

Job No.: S220477HI

Ikaika Kincaid
Reviewed by: Ikaika Kincaid, PE

EXECUTIVE SUMMARY

This report summarizes the findings of the Wilson Tunnel Plenum materials destructive testing analysis. Samples for the analysis were collected by CONSOR Engineers, LLC (CONSOR). The Wilson Tunnel plenum slab is the focus of this analysis due to degradation and fracture of the stainless-steel plenum hanger rods with corrosion induced stress risers. The purpose of this analysis is to determine the condition of the concrete plenum slab and atmospheric factors contributing to the hanger rod degradation. The results of these findings were used to develop repair, retrofit, and mitigation solutions to extend the service life of the tunnel structure.

Samples were collected from the inbound and outbound tunnel plenums to examine potential causes of degradation. Samples retrieved include: 12 concrete cores from along the length of the plenum slab (6 in each tunnel), a stainless-steel hanger rod sample taken from a fractured rod that has been retrofitted, and a dust sample from the outbound plenum. Samples were collected on April 12 and 13, 2022; and sent to American Engineering Testing for physical and chemical analysis. The full laboratory findings report is included in Appendix B, which included the following analysis: chloride ion content testing on the concrete core samples, petrographic analysis on 8 of the 12 concrete core samples, X-ray diffraction (XRD) and microscopy on the dust sample and Scanning Electron Microscopy (SEM) on the steel hanger rod sample.

Based on the results of testing the concrete plenum slab concrete, the previously hypothesized beach sand (with high chloride content) in the concrete mix does not seem the likely cause of the corrosion induced fractures of the hanger rods (results from the report conducted by others, *Investigation into Fractures of Stainless Steel Hanger Rods in Hawaii's Wilson Tunnel*, January 2016, also attached with this report in Appendix C). The results of the chloride ion penetration and petrographic analysis support that the top of slab has corrosive properties due to carbonation and chloride content, but the corrosive levels diminish rapidly below the top 1 in. of the slab. It is suspected that the chloride is being deposited by the humid, salty air in the plenum, through condensation. Over many years this condensation process has pooled at the base of the hanger rods, which has led to development of corrosion cells at the interface with the concrete plenum slab. Additionally, the concrete exposed to the atmosphere is carbonating. As the carbonation in the atmosphere is impregnated into the outer surface of the concrete surface, it leaches into the concrete and slowly creating a corrosive environment for embedded steel. Review of failed hanger rods supports this theory which showed corrosion of the rod was limited to the interface region of the rod and concrete with negligible corrosion noted at deeper locations along the rod.

TABLE OF CONTENTS

1	Purpose of Inspection	1
2	Site Description	1
3	Sample Collection Methodology.....	3
4	Inspection and Laboratory Analysis Findings.....	4
4.1	Summary of Findings.....	4
4.2	Detailed Laboratory Analysis Results.....	5
4.2.1	Concrete Composition	5
4.2.2	Physical Defects	5
4.2.3	Concrete Carbonation.....	5
4.2.4	Chloride Ion Content.....	5
4.3	Dust Sample Laboratory Analysis.....	7
4.4	Stainless Steel Rod Laboratory Analysis.....	7
5	Repair Recommendations.....	8
Appendix A	Photos	A-1
Appendix B	Laboratory Test Results.....	B-1
Appendix C	2016 TFHRC Laboratory Test Results	C-1
Appendix D	E&I Rod Fracture Survey Report	D-1

1 PURPOSE OF INSPECTION

The Wilson Tunnel plenum slab is the focus of this analysis due to degradation and fracture of the plenum hanger rods with corrosion induced stress risers. The purpose of this analysis is to determine what material and atmospheric factors may be contributing to the hanger rod degradation. The findings identified were used to develop repair, retrofit, and mitigation solutions to extend the service life of the tunnel structure.

2 SITE DESCRIPTION

The Wilson Tunnel inbound and outbound bores were constructed in 1952 and 53, and currently carry the Likelike Highway (Route 63) connecting Honolulu to Kane’ohe on the island of Oahu (Figure 1). The tunnel bore construction was completed in 2 phases with the current inbound bore completed prior to the outbound bore.

The tunnel bores have ventilation plenums for extraction of tunnel atmosphere via a vertical ventilation shaft with ventilation fans that pull air from the plenums creating negative pressure in the bores which draws fresh air from both ends of the tunnels. The ventilation plenum is separated from the roadway with a cast in place concrete ceiling slab that is supported by the tunnel liner on either side of the roadway and an intermediate supporting series of stainless-steel hanger rods that suspend the ceiling slab from the top of the tunnel liner (Figure 2). The inbound and outbound plenums have a total of 730 hanger rods which are spaced approximately 8 ft apart.



Figure 1: Location Map - Sourced from Google Earth.

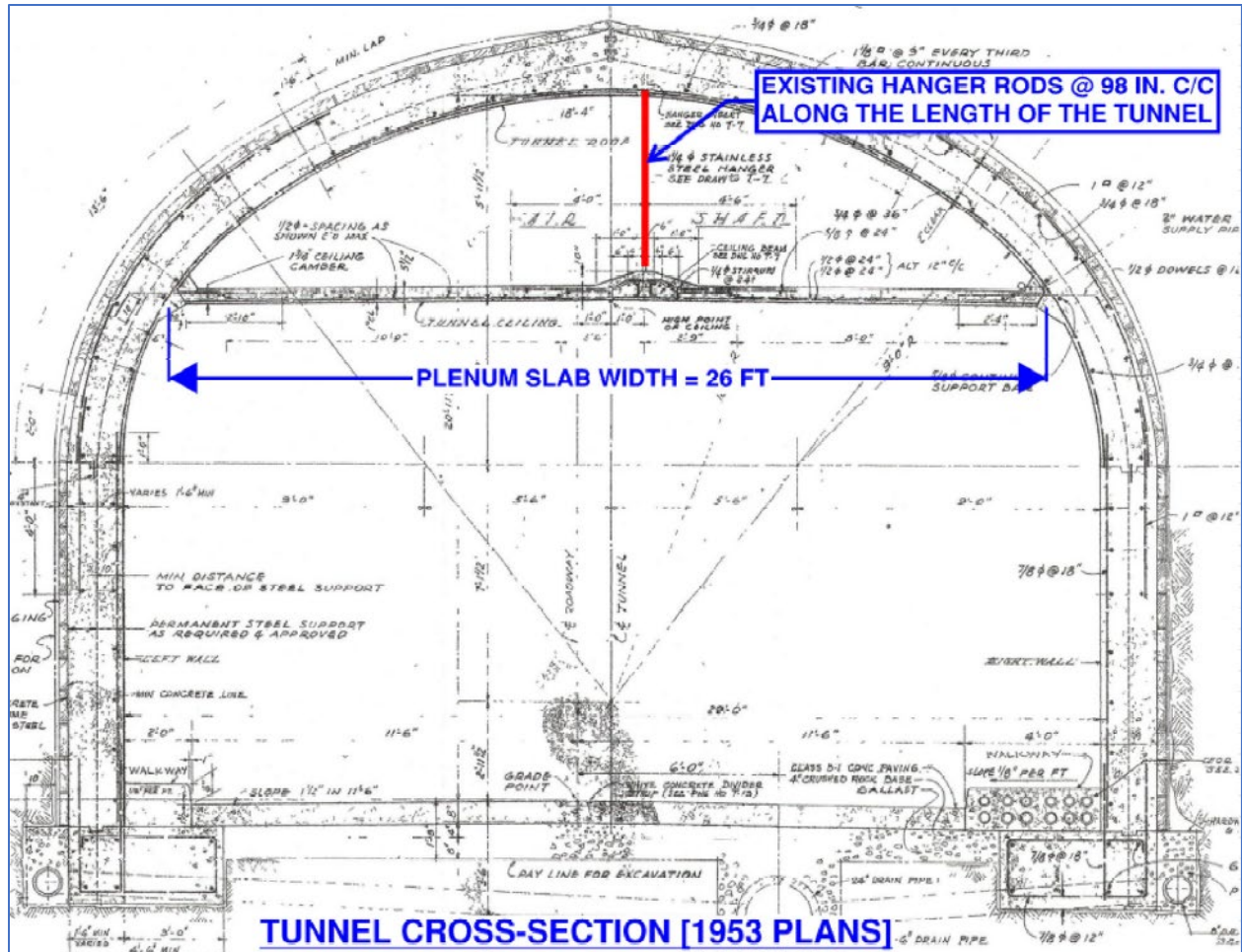


Figure 2: Example of typical tunnel cross-section.

3 SAMPLE COLLECTION METHODOLOGY

CONSOR collected samples for analysis on April 12 and 13, 2022 by a four-person inspection team experienced in the inspection and design of various infrastructure, and the collection of materials samples. The dust sample was collected from the top of the plenum slab in the outbound tunnel bore at Hanger Rod 85. The stainless-steel hanger rod sample was an approximately 6-inch portion cut from fractured rod (Rod 41, inbound bore, Kaneohe side) adjacent to the fracture. The concrete cores were collected by first using a hand-held ground penetrating radar (GPR) device to scan and locate reinforcement and then coring into the plenum slab from the top. The core samples are 2.75 in. diameter x up to 4 in. long. Following core removal, the core holes were filled with non-metallic, non-shrink, cementitious grout. Table 1 identifies the core samples and locations.

Additionally, Engineering & Inspections Hawaii, Inc. (E&I) conducted a survey of all the existing rods in both plenum bores to determine the condition of each rod (their report is attached in Appendix D). The rods were cleaned with wire wheels and visually inspected, with random rods tested with dye penetrant testing. The rods were categorized according to the following conditions:

1. Least severe; visible signs of early stages of mild corrosion and / or pitting is present.
2. Moderate; visible signs of moderate corrosion and / or pitting is present, but no visible signs of cracking detected.
3. Severe; visible signs of cracking detected (complete fractures noted when present).

Table 1: Concrete Core Sample Locations

Bore	Sample #	Location
Outbound	1	Between Rods 1 & 2 (30 in. from Rod 2, 22 in. from rod centerline)
	2	Between Rods 31 & 32 (41 in. from Rod 32, 23 in. from rod centerline)
	3	Between Rods 86 & 87 (28 in. from Rod 86, 13 in. from rod centerline)
	7	Between Rods 3 & 4 (51 in. from Rod 4, 22 in. from rod centerline)
	8	Between Rods 98 & 99 (21 in. from Rod 99, 23 in. from rod centerline)
	9	Between Rods 170 & 171 (16 in. from Rod 171, 21 in. from rod centerline)
Inbound	4	Between Rods 17 & 18 (31 in. from Rod 18, 41 in. from rod centerline)
	5	Between Rods 66 & 67 (31 in. from Rod 66, 41 in. from rod centerline)
	6	Between Rods 107 & 108 (21 in. from Rod 107, 37 in. from rod centerline)
	10	Between Rods 195 & 196 (33 in. from Rod 195, 42 in. from rod centerline)
	11	Between Rods 115 & 116 (14 in. from Rod 115, 42 in. from rod centerline)
	12	Between Rods 3 & 4 (31 in. from Rod 4, 51 in. from rod centerline)

4 INSPECTION AND LABORATORY ANALYSIS FINDINGS

4.1 SUMMARY OF FINDINGS

The core samples were analyzed using a variety of methods to examine the existing concrete for both construction and degradation defects. The samples were categorized in varying condition from good to poor due to cracking, spalling, shrinkage, and carbonation. Cracking was not present in all samples collected, but when cracks were observed they were identified as both the result of temperature and shrinkage cracks as well as structural cracks which were consistent with cracks that occurred later in the life of the concrete.

The top inch of concrete in the inbound bore typically has chloride ion levels above the concentration required to initiate corrosion of reinforcing steel, however these levels typically drop below the required concentration at 1 in. depth and greater. The lower level of chlorides throughout in the interior of the slab indicates that the chlorides are slowly penetrating the concrete from the outside inward and that the proposed chlorides introduced by the “beach sand” identified in the previous analysis, are not the source of the corrosion deterioration.

During the inspections it was noted that the depth of concrete carbonation typically ranged from 0 in. to 0.7 in., with two outliers up to 3.5 in. deep which was along cracks in the concrete. This depth of carbonation is typically shallower than the reinforcement and would not be a significant factor in steel reinforcement deterioration.

The humidity in the plenum ranged from 70% to 88% and the temperature ranged from 72°F to 78°F. Additional humidity and temperature monitoring throughout the year/seasons would provide information on the range and potential to reach dew point. Dew forms when the temperature of a surface cools down to a temperature that is cooler than the dew point of the air next to it. When this happens water vapor will condense into droplets. As the moisture and air within the plenum increases, the stainless-steel rods remain colder than the air, thus dew forms on the rods which then collects at the base.

Additionally, the concrete from around the portion of the extracted rod showed corrosion staining at the top 2 in. of the surrounding concrete, and the fracture occurred just below the surface (Photo 5).

The fracture survey by E&I resulted in the following quantities of rods in conditions 1 through 3. Note that the E&I findings have been updated based on repairs performed since the survey.

Table 2: Rod fracture survey quantity summary

		Condition	Total	
Inbound	0	Repaired Rod	61	18%
	1	Signs of mild corrosion or pitting	0	0%
	2	Signs of moderate corrosion or pitting	0	0%
	3	Signs of cracking detected	279	82%
			Total	340
Outbound	0	Repaired Rod	2	1%
	1	Signs of mild corrosion or pitting	106	28%
	2	Signs of moderate corrosion or pitting	44	12%
	3	Signs of cracking detected	222	59%
			Total	374

The higher chloride ion contents and percentages of “Condition 3” rods in the inbound tunnel compared to the outbound tunnel appear to indicate that this is a partially atmospheric driven issue. The vehicles entering the inbound tunnel from the windward side will push more humid, saltier air into the inbound bore than vehicles entering from the leeward side, which will push a relatively more benign atmosphere into the outbound tunnel. Extrapolating from the above information, the probable failure mechanism for the rods fracturing is the development of a corrosion cell around the bottom portion of the hanger rods at the interface with the plenum concrete.

1. Humid, salty air enters the plenum. Salt is deposited on the surface of the concrete leading to higher chloride ion content in the top 1 in.
2. The humid air condenses on the steel hanger rods and the water and chloride ion content at the rod/concrete interface forms a corrosion cell.
3. The corrosion cell leads to corrosion induced fracturing of the hanger rod.

Detailed laboratory results are presented below, and the full concrete laboratory analysis is presented in Appendix B. The E&I Rod Fracture Survey Report is presented in Appendix D.

4.2 DETAILED LABORATORY ANALYSIS RESULTS

4.2.1 Concrete Composition

Concrete cores were extracted from the top of the plenum slab at 12 locations throughout the inbound and outbound bores (6 cores per bore). The concrete is typically a mixture of Portland cement, quarried and crushed basalt coarse aggregate, and a combined fine aggregate containing natural carbonate sand and crushed basalt.

4.2.2 Physical Defects

Analysis of the concrete cores discovered some porous aggregate that likely held excess moisture content that was released into the concrete during curing, causing a soft paste layer adjacent to the weathered aggregate reducing the local cement/aggregate bond strength.

Concrete cracks were noted in several cores, ranging from surficial microcracks to macrocracks. Several samples were noted as having the top layer spalled, but these spalls occurred primarily during core extraction. Table 3 summarizes the physical defects observed in the cores.

4.2.3 Concrete Carbonation

Carbonation in concrete is a chemical reaction between the calcium hydroxide in the concrete and carbon dioxide in the atmosphere that occurs primarily in humid conditions. This chemical reaction (beginning at the exposed surface and working inward) reduces the alkaline environment of the concrete and leaves the reinforcing steel susceptible to corrosion. Concrete carbonation was noted in varying depths between samples. The depth of carbonation was significantly deeper at locations of cracking which allowed the atmosphere to penetrate more deeply into the concrete. Table 3 summarizes the carbonation depths.

4.2.4 Chloride Ion Content

Chloride ion content measures the concentration of chlorides in the concrete, with a concentration of 0.05% typically being sufficient to initiate corrosion. The concrete core samples were analyzed for chloride content to determine concentration of chlorides throughout the depth of the concrete based upon

previous reports that attributed corrosion to the use of beach sand in the original concrete mix. The result of the analyses shows that the concentration is typically higher at the surface of the concrete, and is typically less than the 0.05% corrosion initiation threshold below the top inch of the concrete. The diminishing concentration with depth into the concrete signals that if beach sand was used, it did not significantly increase the corrosion probability, and that the high concentration at the surface is likely due to salt deposited from the atmosphere. Table 3 summarizes the chloride ion contents for the cores.

Table 3: Summarized core laboratory analysis results

	Sample #	Physical Defect	Carbonation Depth	Chloride Ion Content	
				Depth (in.)	% by Mass
OUTBOUND BORE	1	Macrocrack with related microcracks indicative of structural cracking.	0 to 0.4 in. (up to 3.5 in. along the macrocrack)	0-1	0.010
				1-2	0.004
				2-3	0.003
	2	N/A	N/A	0-1	0.019
				1-2	0.015
				2-3	0.010
	3	Cracking not observed.	0 to 0.04 in.	0-1	0.016
				1-2	0.004
				2-3	0.004
7	Cracking not observed	0.35 to 0.67 in.	0-1	0.037	
			n/a	-	
			n/a	-	
8	N/A	N/A	0-1	0.026	
			1-2	0.004	
			2-3	0.006	
9	Shrinkage cracking consistent with early life cracking that is not likely structural in nature, but has deeper carbonation	1.06 to 1.18 in.	0-1	0.022	
			1-2	0.010	
			2-3	0.008	
INBOUND BORE	4	Shallow spalling and delamination could be result of removal of core or structural cracking adjacent to core location.	0.04 to 0.31 in.	0-1	0.038
				1-2	0.007
				n/a	-
	5	N/A	N/A	0-1	0.038
				1-2	0.021
				n/a	-
	6	Shallow spalling and delamination could be result of removal of core or structural cracking adjacent to core location.	0.47 to 0.71 in.	0-1	0.059
				n/a	-
				n/a	-
	10	Cracking not observed	0.04 to 0.4 in.	0-1	0.035
				1-2	0.009
				2-3	0.004
11	N/A	N/A	0-1	0.075	
			1-2	0.042	
			2-3	0.028	
12	Cracking not observed	0 to 0.2 in.	0-1	0.053	
			1-2	0.006	
			2-3	0.005	

* Cores 2, 5, 8, 11 tested for chloride ion content only.

** No chloride content measurements available for samples that were too short.

4.3 DUST SAMPLE LABORATORY ANALYSIS

The X-ray Diffraction analysis of the dust sample obtained from the Outbound bore plenum adjacent to hanger rod 85 noted mineral content that largely indicated that a large percentage of the material was magnetite which is a strongly magnetic iron oxide-based material that has many applications including use as brake components. Remaining dust sample material consisted of several minerals that are commonly found in fine aggregates used in concrete.

4.4 STAINLESS STEEL ROD LABORATORY ANALYSIS

The Scanning Electron Microscopy and Laser Induced Breakdown Spectroscopy of the stainless-steel rod sample analysis determined the sample to be made of 304 stainless steel (18/8). This result contrasts with the determination of 303 stainless steel in the January 2016 analysis by TFHRC (see Appendix C), although it is possible that differing grades of steel were used because the drawings only indicate “stainless steel”.

The black build up of corrosion product on the rod was comprised of oxides from the steel substrate and a component of chlorine which indicates that chloride is an active contributor to the corrosion of the stainless-steel rod. In this instance, the chlorides found on the rods, within the corrosion buildup, could have only occurred through atmospheric buildup. In both the current and 2016 analyses, chlorides were determined to be in higher concentrations at the fracture sites, while the 2016 analysis also indicated higher levels of sulfate (likely from sulfur in the rod metallurgy).

The total quantity of rod fractures according to the E&I survey is presented below. Note that the E&I findings have been updated based on repairs performed since the survey (repairs performed on rods with complete fractures).

Table 4: Rod fracture survey quantities

		Condition	Kaneohe		Town		Total	
Inbound	0	Repaired Rod	57	25%	4	4%	61	18%
	1	Signs of mild corrosion or pitting	0	0%	0	0%	0	0%
	2	Signs of moderate corrosion or pitting	0	0%	0	0%	0	0%
	3	Signs of cracking detected	171	75%	108	96%	279	82%
			Total	228	100%	112	100%	340
Outbound	0	Repaired Rod	1	0%	1	1%	2	1%
	1	Signs of mild corrosion or pitting	8	3%	98	79%	106	28%
	2	Signs of moderate corrosion or pitting	31	12%	13	10%	44	12%
	3	Signs of cracking detected	210	84%	12	10%	222	59%
			Total	250	100%	124	100%	374

5 REPAIR RECOMMENDATIONS

Based on the core sample analysis and chloride ion testing the driving factors for corrosion are atmospheric based, and not the result of internal concrete composition. CONSOR recommends the following to aid in the future preservation of the concrete plenum and the stainless-steel hanger rods as well as protection against additional corrosive contamination of the existing concrete.

- Given the large number of hanger rods in a severe condition, retrofit the plenum slab to be supported by a new hanger rod system.
- Pressure wash the interior of the plenums on an annual basis to remove existing dirt and debris that may contain corrosive contaminants as well as trap moisture on surfaces in a manner that would accelerate corrosion. This also includes cleaning the rod of any debris and soot buildup along the rods and at the base.
- Patch concrete spalls throughout top of the concrete plenum slab.
- Clean and coat the existing stainless-steel hanger rods and install high-build epoxy cones at the base of the rods to direct moisture away from the rod/concrete interface.
- Coat the top surface of the plenum with a 100% solids, reactive, breathable, penetrating silane sealer to protect against water and chloride intrusion. Some of these products will need to be reapplied, depending on manufacturers recommendations.
- Run the tunnel ventilation system regularly to provide an air exchange and discourage settling of any chlorides and contaminants and remove moisture and humidity buildup.

Appendix A

Photos

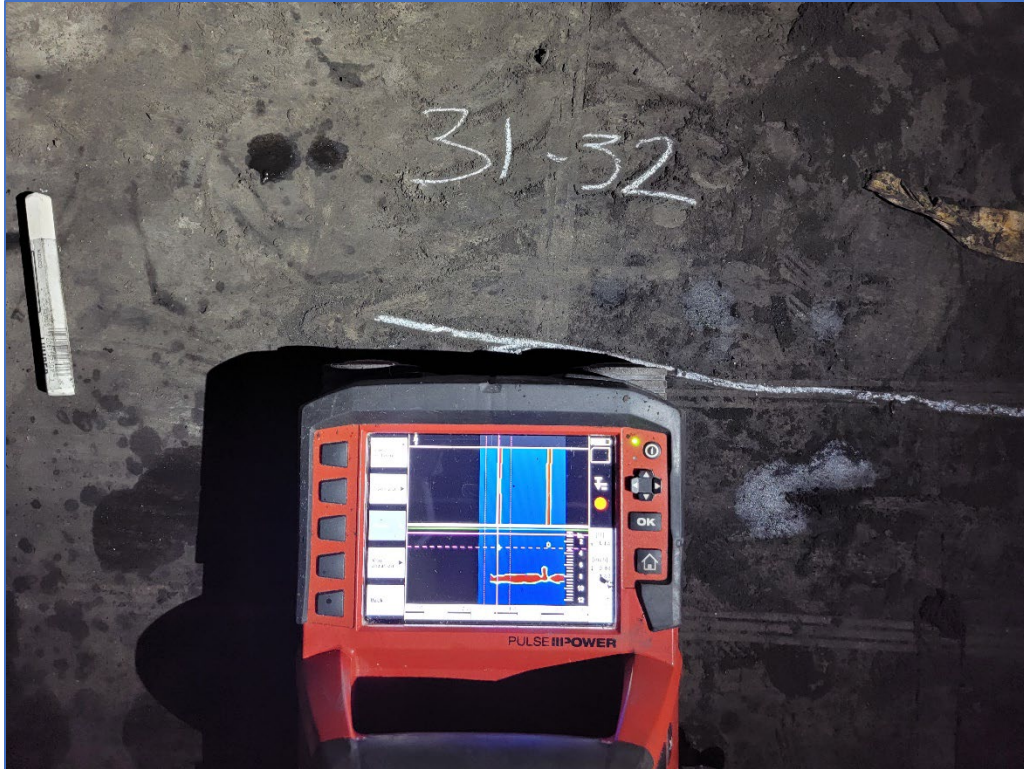


Photo 1: Concrete GPR scanner to locate embedded reinforcement to avoid impact with core drill.



Photo 2: Core sample collection.



Photo 3: Typical sample hole after core extraction (Core 1 shown).



Photo 4: Typical core hole filled with cementitious grout (Core 11 shown).



Photo 5: Fractured rod with corrosion in the top 2 in. (Rod 41, inbound bore, Kaneohe side).

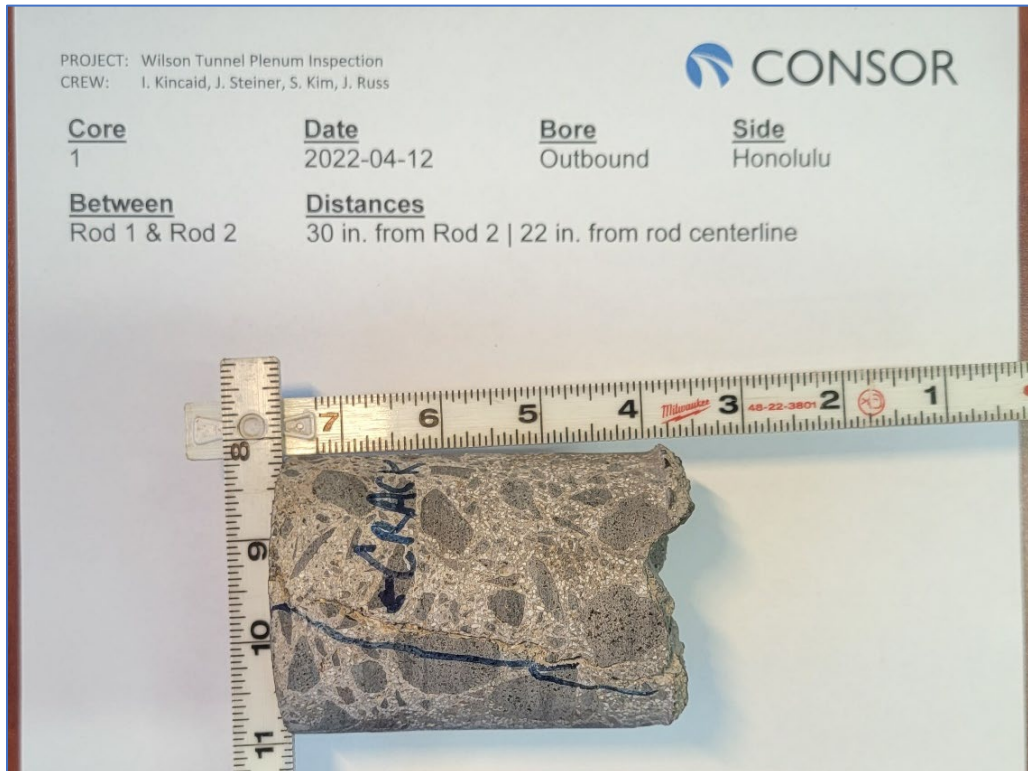


Photo 6: Core 1 after extraction.



Photo 7: Core 2 after extraction.



Photo 8: Core 3 after extraction.



Photo 9: Core 4 after extraction.



Photo 10: Core 5 after extraction.

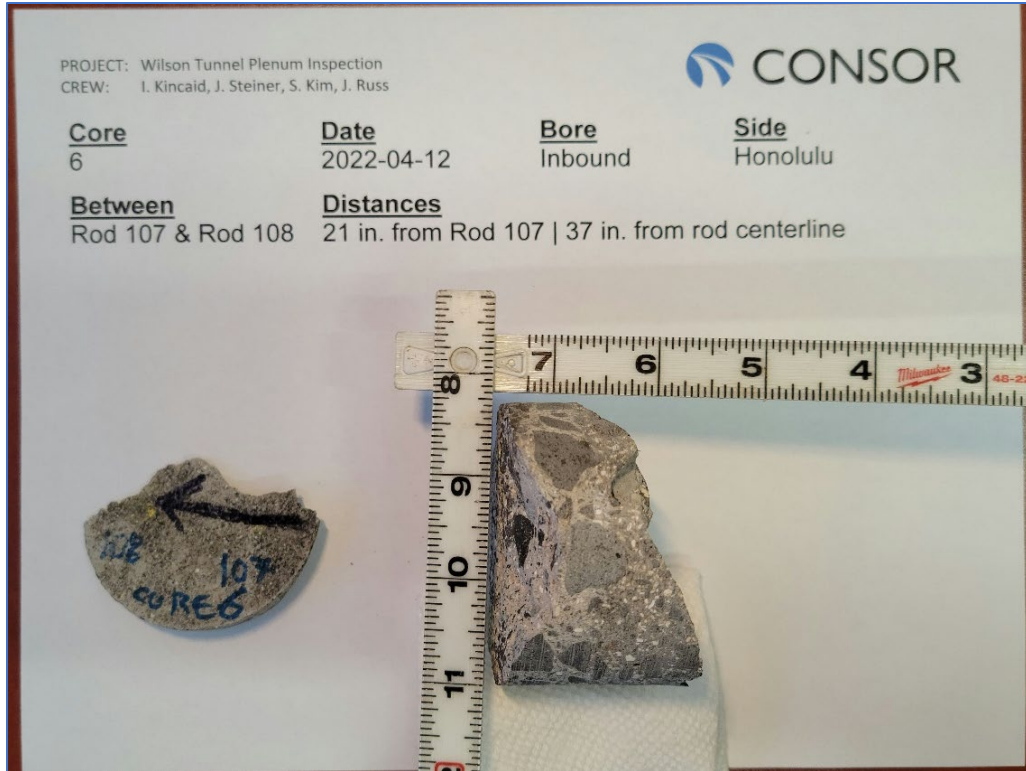


Photo 11: Core 6 after extraction.



Photo 12: Core 7 after extraction.



Photo 13: Core 8 after extraction.



Photo 14: Core 9 after extraction.



Photo 15: Core 10 after extraction.



Photo 16: Core 11 after extraction.

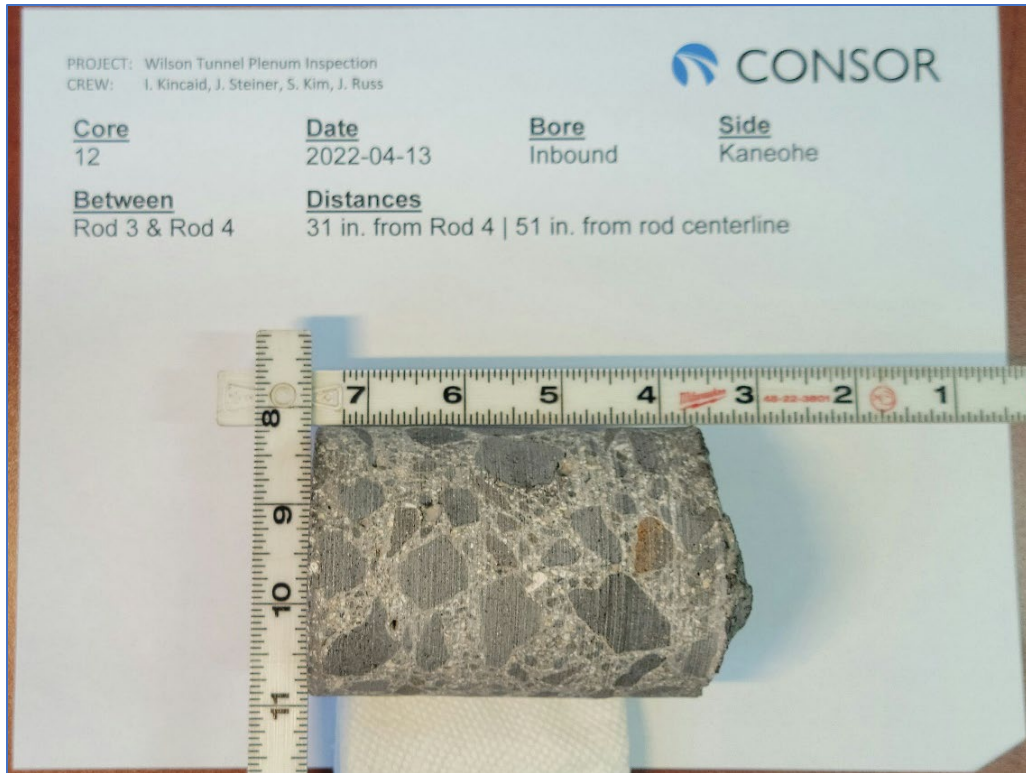


Photo 17: Core 12 after extraction.

Appendix B

Laboratory Test Results



REPORT OF CHLORIDE ANALYSIS

Project:

Wilson Tunnel Plenum Inspection

Reported To:

Conzor Engineers, LLC
737 Bishop Street, Suite 2530
Honolulu, HI 96813

AET Project No.: P-0012413**Attn:** Joshua Steiner**Date:** May 20, 2022

INTRODUCTION

This report presents the results of laboratory work performed by our firm on twelve (12) concrete core samples submitted to us by Joshua Steiner of Consor Engineers, LLC on April 22, 2022. The scope of our work was limited to documenting the water-soluble chloride content of the cores, if possible, at depths of 0-1, 1-2, and 2-3 inches in accordance with ASTM C1218.

TEST PROCEDURES

Laboratory testing was performed on May 16, 2022, and subsequent dates in accordance with ASTM C1218-20, "Standard Test Method for Water-Soluble Chloride in Mortar and Concrete." The core samples were cut at the designated depths, crushed, dried in an oven, and processed to pass a U.S.A. Standard Test Sieve No. 20. Results presented in Table 1 are reported on a dry weight 105 °C basis.

REMARKS

The test sample(s) will be retained for a period of at least sixty days from the date of this report. Unless further instructions are received by that time, the sample(s) may be discarded. The test results relate only to the sample(s) tested. No warranty, expressed or implied, is made.

Report Prepared by:

American Engineering Testing, Inc.

Handwritten signature of Kattie Reamer in black ink, positioned above a horizontal line.

Kattie Reamer

Chemist I

Report Reviewed by:

American Engineering Testing, Inc.

Handwritten signature of Cyler Hayes in black ink, positioned above a horizontal line.

Cyler Hayes

Senior Chemist / Chemistry Lab Managerchayes@teamAET.com

Work: 651-603-6605

550 Cleveland Avenue North | Saint Paul, MN 55114**Phone (651) 659-9001 | (800) 972-6364 | Fax (651) 659-1379 | teamAET.com | AA/EEO**

This document shall not be reproduced, except in full, without written approval from American Engineering Testing, Inc.

TEST RESULTS

Table 1 – Water-Soluble Chloride Content

<u>Sample Identification</u>		<u>Sample Depth, in.</u>	<u>By Mass of Sample</u>	
			<u>%</u>	<u>ppm (mg/kg)</u>
Outbound	Core 1	0 - 1	0.010	100
		1 - 2	0.004	40
		2 - 3	0.003	30
	Core 2	0 - 1	0.019	190
		1 - 2	0.015	150
		2 - 3	0.010	100
	Core 3	0 - 1	0.016	160
		1 - 2	0.004	40
		2 - 3	0.004	40
	Core 7	0 - 1	0.037	370
		1 - 2	0.026	260
		2 - 3	0.004	40
Core 8	0 - 1	0.026	260	
	1 - 2	0.004	40	
	2 - 3	0.006	60	
Core 9	0 - 1	0.022	220	
	1 - 2	0.010	100	
	2 - 3	0.008	80	
Inbound	Core 4	0 - 1	0.038	380
		1 - 2	0.007	70
	Core 5	0 - 1	0.038	380
		1 - 2	0.021	210
	Core 6	0 - 1	0.059	590
		1 - 2	0.035	350
		2 - 3	0.009	90
	Core 10	0 - 1	0.004	40
		1 - 2	0.009	90
		2 - 3	0.004	40
	Core 11	0 - 1	0.075	750
		1 - 2	0.042	420
2 - 3		0.028	280	
Core 12	0 - 1	0.053	530	
	1 - 2	0.006	60	
	2 - 3	0.005	50	



REPORT OF PETROGRAPHIC ANALYSIS

Project:

Wilson Tunnel Plenum Inspection

Reported To:

Conzor Engineers, LLC
737 Bishop Street, Suite 2530
Honolulu, HI 96813

AET Project No.: P-0012413**Attn:** Joshua Steiner**Date:** May 27, 2022

INTRODUCTION

This report presents the results of laboratory work performed by our firm on twelve concrete core samples, one dust sample, and one stainless steel rod sample submitted by Joshua Steiner of Consor Engineers, LLC on April 22, 2022. We understand the concrete cores were obtained from the above reference project location. Core 1 through Core 6 were taken from the Honolulu side and cores 7 through 12 were taken from the Kaneohe side. The age of the concrete was unknown to us. We understand that corrosion of the stainless steel hanger rods supporting the tunnel plenum has been documented however, the concrete samples received did not include any rebar members or corrosion product. The scope of our work was limited to performing petrographic analysis on eight of the core samples, Core 1, Core 3, Core 4, Core 6, Core 7, Core 9, Core 10, and Core 12 to document the general overall condition of the concrete, X-ray diffraction (XRD) testing and microscopy on the dust sample, and scanning electron microscopy (SEM) on the steel rod sample. Chloride ion content testing was also performed on the core samples, and the results were reported separately.

CONCLUSIONS

Based on our observations and analysis:

1. The concrete in sample Core 1 was in poor condition due to a macrocrack and related microcracks oriented at high angle to the outer surface which appeared structural in nature. Several microcracks branch from the macrocrack and the cracking propagates through a few coarse aggregate particles; consistent with cracking formed later in the life of the concrete. The macrocrack was of consistent width through the length of the core, also indicative of structural cracking.
2. The condition of samples Core 4 and Core 6 was poor due to shallow spalling or delamination of up to 60% of the outer surface of each sample which was possibly structural in nature. Spalling

550 Cleveland Avenue North | Saint Paul, MN 55114

Phone (651) 659-9001 | (800) 972-6364 | Fax (651) 659-1379 | teamAET.com | AA/EEO

This document shall not be reproduced, except in full, without written approval from American Engineering Testing, Inc.

of the concrete occurred at low angle to the outer surface, was shallowest near the center of the core surface and deepest at the cored edge of the samples. The spalled surface proceeds through several coarse and fine aggregates and may be the result of prying the concrete from the core hole during sample procurement. The observed spalling could also be part of a larger or nearby structural cracking.

3. The concrete in sample Core 9 was in fair condition due to drying shrinkage/ carbonation shrinkage observed concentrated within the outer 39 mm (9/16") of the concrete. The microcracks occurred in various orientations and proceeded around aggregate particles, an indication that they formed early in the life of the concrete. Carbonation of the concrete in sample 9 was the deepest of the concrete samples examined except along the macrocrack in Core 1. Assuming the concretes are of the same age, the variation in carbonation depths between samples, ranging from negligible to 30 mm (1-3/16") is likely due to variable exposure to carbon dioxide emissions from vehicles.
4. The remaining samples, Core 3, Core 7, Core 10, and Core 12, were in good condition. None of the concrete samples exhibited any evidence of gross deterioration mechanisms or extensive cracking/fractures. The samples were of varying lengths, with Core 7 measuring only 51 mm (2") in length. The fractured inner surfaces of the samples appear fresh and did not exhibit carbonation.
5. Each of the concretes was visually similar and was made with portland cement, quarried and crushed basalt coarse aggregate, and a combined fine aggregate containing natural carbonate sand and crushed basalt. A few weathered basalt coarse aggregate particles were observed in each of the samples. Several of the weathered particles were surrounded by a thin rim of soft paste, likely the result of these relatively porous aggregates retaining more water than the non-weathered particles when brought to SSD at the time of batching. The water was then wicked from the aggregate by the paste, creating a higher w/cm zone. The concretes each contained a small amount of spherical entrained-sized air voids either entrained during mixing or due to a low dose of air entraining admixture.
6. The dust sample "from OB Rod 85" was a fine, dark gray powder. In powder mount review, approximately 80% of the sample was opaque material with smaller amounts of carbonate, feldspar, quartz and pyroxene. The majority of the opaque material was magnetite - a dark gray, submetallic, strongly magnetic mineral. Orange-red iron oxide particles and few white particles (possibly chert) were also observed within the opaque material. The opaque particles were generally the largest particles within the powder. X-ray diffraction of the material from the dust sample which passed through a #200 sieve identified calcite, albite (feldspar), augite (pyroxene), quartz, gypsum, magnetite, and weddellite (calcium oxalate). The minerals albite, augite, magnetite, are commonly found in basalt. Calcite is the main constituent of the natural fine aggregate used in these concretes. Weddellite is found in some corals and maybe from the fine aggregate. Quartz, gypsum and may also be present in the fine aggregate.

7. Scanning electron microscopy and elemental analysis found the corroded SS Rod sample to be made of 304 stainless steel (18/8). Laser Induced Breakdown Spectroscopy confirmed the chemistry (17.06% Cr, 7.04% Ni, 74.6% Fe, and balance of Si, V, Mn, & Cu). Corrosion product was comprised of oxides from the steel substrate with a component of chlorine (Cl). The presence of Cl in the corrosion product indicates chloride as actively contributing to the corrosion of the steel.

SAMPLE IDENTIFICATION

Sample Type: Hardened Concrete Cores

<u>Sample ID</u>	<u>Diameter</u>	<u>Length</u>
Core 1 [†]	70 mm (2-3/4")	102 mm (4")
Core 2 [†]	70 mm (2-3/4")	108 mm (4-1/4")
Core 3 [†]	70 mm (2-3/4")	83 mm (3-1/4")
Core 4 [*]	70 mm (2-3/4")	76 mm (3")
Core 5 [*]	70 mm (2-3/4")	57 mm (2-1/4")
Core 6 [*]	70 mm (2-3/4")	51 mm (2")
Core 7 [†]	70 mm (2-3/4")	51 mm (2")
Core 8 [†]	70 mm (2-3/4")	102 mm (4")
Core 9 [†]	70 mm (2-3/4")	108 mm (4-1/4")
Core 10 [*]	70 mm (2-3/4")	102 mm (4")
Core 11 [*]	70 mm (2-3/4")	95 mm (3-3/4")
Core 12 [*]	70 mm (2-3/4")	108 mm (4-1/4")

* Inbound bore

† Outbound bore

Sample Type: Stainless Steel Rod

<u>Sample ID</u>	<u>Diameter</u>	<u>Length</u>
SS Rod	32 mm (1-1/4")	171 mm (6-3/4")

Sample Type: Powder

<u>Sample ID</u>	<u>Weight</u>
Dust from OB Rod 85	Approximately 55 grams

TEST RESULTS

Our complete petrographic analysis documentation appears on the attached sheets entitled 24-LAB-001 "Petrographic Examination of Hardened Concrete, ASTM C856." A brief summary of the general physical characteristics of the concrete is as follows:

1. The coarse aggregate in each of the samples was comprised of 19 mm (3/4") trap rock consisting of a porphyritic basalt that appeared well graded and exhibited fair overall distribution. The fine aggregate was a composite of natural carbonate sand and crushed basalt.
2. The paste color of the concretes was similar to medium gray. The paste hardness of the samples ranged from moderately soft to moderately hard with the paste/aggregate bond considered poor.
3. The outer surface condition of the concretes was smooth formed. Sample Core 1 was overlain by a thin, neat cement parge coat. The depth of carbonation ranged from negligible to 30 mm (1-3/16") depth from the outer surfaces and "spiked" up to 89 mm (3-1/2") along a macrocrack.
4. The w/cm of the concretes was estimated to be between 0.38 and 0.47 with approximately 4 to 11% residual portland cement clinker particles. No supplementary cementitious materials were observed in any of the concrete samples.

AIR CONTENT TESTING

Sample ID	Total Air Content (%)	"Entrained" Air (%) voids < 1 mm (0.040")	"Entrapped" Air (%) voids < 1 mm (0.040")	Spacing Factor, in.
Core 1	2.0	1.6	0.4	0.012
Core 3	1.3	1.1	0.2	0.019
Core 4	0.8	0.6	0.2	0.030
Core 6	0.8	0.4	0.4	0.030
Core 7	3.3	3.0	0.3	0.010
Core 9	3.1	1.9	1.2	0.019
Core 10	1.2	1.0	0.2	0.021
Core 12	1.0	0.8	0.2	0.024

TEST PROCEDURES

Laboratory testing was performed on April 22, 2022, and subsequent dates. Our procedures were as follows:

1.0 Petrographic Analysis

A petrographic analysis was performed in accordance with AET Standard Operating Procedure 24-LAB-001, "Petrographic Examination of Hardened Concrete," ASTM C856-latest revision. The petrographic analysis consisted of reviewing the cement paste and aggregate qualities on a whole basis on saw cut, lapped, and fractured sections. Reflected light microscopy was performed under an Olympus SZX-12 binocular stereozoom microscope at magnifications up to 160x. The depth of carbonation was documented using a phenolphthalein pH indicator solution applied on freshly saw cut

and lapped surfaces of the concrete sample. The paste-coarse aggregate bond quality was determined by fracturing a sound section of the concrete in the laboratory with a rock hammer.

The water/cementitious of the concrete was estimated by viewing a thin section of the concrete under a Nikon E600 polarizing light microscope at magnifications of up to 600x. Thin section analysis was performed in accordance with Standard Operating Procedure 24-LAB-009, "Determining the Water/Cement of Portland Cement Concrete, AET Method." An additional, smaller, saw cut subdivision of the concrete sample is epoxy impregnated, highly polished, and then attached to a glass slide using an optically clear epoxy. Excess sample is saw cut from the glass and the thin slice remaining on the slide is lapped and polished until the concrete reaches 25 microns or less in thickness. Thin section analysis allows for the observation of portland cement morphology, including: phase identification, an estimate of the amount of residual material, and spatial relationships. Also, the presence and relative amounts of supplementary cementitious materials and pozzolans may be identified and estimated.

2.0 Air Content Testing

Air content testing was performed using Standard Operating Procedure 24-LAB-003, "Microscopical Determination of Air Void Content and Parameters of the Air Void System in Hardened Concrete, ASTM C457-latest revision." The linear traverse method was used. The concrete core was saw cut parallel to the direction of coring and then lapped prior to testing.

3.0 X-ray Diffraction Testing

X-ray diffraction was performed on a Bruker D2 Phaser equipped with a Copper tube radiation source with a slit opening of 1 mm. Measurements were made with an operating voltage of 30 kV and amperage of 10 mA. Diffraction counts were gathered with a Lynxeye detector at an angle of 5 degrees. The sample was screened over a #200 sieve and passing material was then scanned from approximately 5 degrees to 65 degrees 2 theta. A grab sample of the overall material was pulverized and scanned under these same parameters. The data collected was compared to the PDF-4 International Center for Diffraction Data database for phase identification.

4.0 Scanning Electron Microscopy with EDS analysis

A Scanning electron microscopy and elemental microanalysis were performed using a JEOL JSM-IT500 Low Vacuum microscope and Peltier cooled dry Silicon Drift Detector with integrated software. Microscope and facilities allow up to 15,000x magnification. SEM is equipped with both secondary and backscatter electron detectors. Energy dispersive x-ray spectrometer (EDS) unit has an energy resolution (Mn Ka, FWHM) of 129eV or less and a 30mm² detection area. Analysis was performed on a both a polished cross-sectional surface and surface of the SS Rod as received. All images included with this report were gathered using the backscatter electron detector at various magnifications.

5.0 Laser Induced Breakdown Spectroscopy

SciAps Z300 LIBS and Alloy application were used to obtain a spectral analysis of the steel substrate (SS Rod sample) and compare to a calibration library for identification of the alloy.

REMARKS

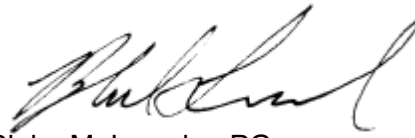
The test samples will be retained for a period of at least sixty days from the date of this report. Unless further instructions are received by that time, the samples may be discarded. Test results relate only to the items tested. No warranty, expressed or implied, is made.

We appreciate the opportunity to have been of service to you on this project. If you have any questions regarding the information presented in this report or if we can be of additional assistance, please contact us.

Report Prepared By
American Engineering Testing, Inc.



Christine A. Tillemma
Senior Petrographer
ctillemma@teamAET.com
Work: 651-659-1353



Blake M. Lemcke, PG
Senior Petrographer/Geologist
MN License #50337
blemcke@teamAET.com
Work: 651-659-1362

24-LAB-001 PETROGRAPHIC EXAMINATION OF HARDENED CONCRETE, ASTM C856

Project No. P-0012413 **Date:** 5/18/2022 **Date reviewed:** 5/23/2022
Sample ID: Core 1 **Performed by:** B. Jessen **Reviewed by:** C. Tillema

I. GENERAL OBSERVATIONS

1. **Sample Dimensions:** Our analysis was performed on both sides of a 98 mm (3-7/8") x 70 mm (2-3/4") x 28 mm (1-1/8") thick lapped profile section and a 76 mm (3") x 52 mm (2") thin section that were saw-cut and prepared from the original 70 mm (2-3/4") diameter x 102 mm (4") long core.
2. **Surface Conditions:**
Outer: Fairly smooth, flat, formed surface; placed in formwork
Inner: Rough, irregular, fractured surface
3. **Reinforcement:** None observed.
4. **General Physical Conditions:** The outer surface of the concrete was overlain by a very thin (<0.5mm) neat cement parge coating. A branching macrocrack was observed on both lapped surfaces. The macrocrack proceeded at high angle to the top surface through the length of the core, from the cored surface near the top of the core up to 23 mm (7/8") from that cored surface at the bottom of the sample. The cracking primarily proceeded around coarse aggregate particles. A few microcracks oriented mostly sub-parallel to the macrocrack branched off the macrocrack and reached a maximum length of 21 mm (13/16"). Several microcracks oriented mostly sub-perpendicular to the outer surface were observed at various depths throughout the concrete and reached maximum lengths of 15 mm (9/16"). The depth of carbonation ranged from negligible up to 10 mm (3/8") from the outer surface and spiked up to 89 mm (3-1/2") along the macrocrack. The concrete contained a small amount of spherical entrained sized air voids. The concrete was well consolidated but exhibited a poor paste/aggregate bond. A few weathered coarse aggregate particles, scattered throughout the concrete, displayed a rusty coloration of their phenocrysts. Soft paste was observed surrounding a few of the weathered aggregate particles. Darker colored, denser paste was observed within a recessed notches of a few of the coarse aggregate particles.

II. AGGREGATE

1. **Coarse:** 19 mm (3/4") nominal sized quarried and crushed porphyritic basalt. The particles were mostly sub-angular to angular in shape. The coarse aggregate appeared well graded and exhibited good overall distribution.
2. **Fine:** Combined natural carbonate sand and crushed basalt (fossiliferous carbonates, fossils/fossil fragments, with many basalt, and several olivine, pyroxene, and iron oxide particles). The grains were mostly rounded to sub-rounded with many sub-angular basalt particles. The fine aggregate appeared fairly graded and exhibited good overall uniform distribution.

III. CEMENTITIOUS PROPERTIES

1. Air Content: 2.0% total
2. Depth of carbonation: Ranged from negligible up to 10 mm (3/8") depth from the outer surface and spiked up to 89 mm (3-1/2") along the macrocrack.
3. Paste/aggregate bond: Poor.
4. Paste color: Medium light gray (Munsell® N6) overall, slightly lighter within the carbonated paste.
5. Paste hardness: Moderately hard (Mohs ≈3.5) overall, soft along a few paste-aggregate interfaces.
6. Microcracking: A macrocrack was observed that proceeded sub-perpendicularly from the outer surface through the full depth of the core. A few microcracks oriented sub-perpendicular to the outer surface branched off the macrocrack. Several microcracks oriented sub-perpendicular to the outer surface were observed at various depths.
7. Secondary deposits: None observed.
8. w/cm: Estimated at between 0.40 and 0.45 with approximately 5 to 7% residual portland cement clinker particles.
9. Cement hydration: Alites: Well to fully
Belites: Negligible to low

24-LAB-001 PETROGRAPHIC EXAMINATION OF HARDENED CONCRETE, ASTM C856

Project No. P-0012413 **Date:** 5/18/2022 **Date reviewed:** 5/23/2022
Sample ID: Core 3 **Performed by:** B. Jessen **Reviewed by:** C. Tillema

I. GENERAL OBSERVATIONS

1. Sample Dimensions: Our analysis was performed on both sides of an 81 mm (3-3/16") x 68 mm (2-11/16") x 30 mm (1-3/16") thick lapped profile section and a 76 mm (3") x 52 mm (2") thin section that were saw-cut and prepared from the original 70 mm (2-3/4") diameter x 83 mm (3-1/4") long core.
2. Surface Conditions:
Outer: Fairly smooth, flat, formed surface
Inner: Rough, irregular, fractured surface
3. Reinforcement: None observed.
4. General Physical Conditions: A microcrack oriented sub-perpendicular to the outer surface proceeded from that surface up to 2 mm depth. Carbonation ranged from negligible up to 1 mm (1/32") from the outer surface. A few microcracks observed at various depths and orientations occurred at paste aggregate interfaces and reached up to 17 mm (11/16") in length. The microcracks primarily proceeded around coarse aggregate particles. The concrete contained a small amount of spherical, entrained-sized air voids. The concrete was well consolidated but exhibited a poor paste/aggregate bond. A few weathered coarse aggregate particles observed at various depths displayed a rusty coloration of their phenocrysts. Soft paste was observed surrounding a few of the weathered aggregate particles. Darker colored, denser paste was observed within a recessed notches of a few of the coarse aggregate particles.

II. AGGREGATE

1. Coarse: 19 mm (3/4") nominal sized quarried and crushed porphyritic basalt. The particles were mostly sub-angular to angular in shape. The coarse aggregate appeared well graded and exhibited good overall distribution.
2. Fine: Combined natural carbonate sand and crushed basalt (fossiliferous carbonates, fossils/fossil fragments, with many basalt, and several olivine, pyroxene, and iron oxide particles). The grains were mostly rounded to sub-rounded with many sub-angular basalt particles. The fine aggregate appeared fairly graded and exhibited good overall uniform distribution.

III. CEMENTITIOUS PROPERTIES

1. Air Content: 1.3% total
2. Depth of carbonation: Ranged from negligible up to 1 mm (1/32") from the outer surface.
3. Paste/aggregate bond: Poor.
4. Paste color: Medium light gray (Munsell® N6).
5. Paste hardness: Moderately soft (Mohs ≈2.5-3).
6. Microcracking: A few randomly oriented microcracks, up to 17 mm (11/16") in length, were observed at various depths throughout the concrete.
7. Secondary deposits: None observed.

8. w/cm: Estimated at between 0.38 and 0.43 with approximately 9 to 11% residual portland cement clinker particles.
9. Cement hydration: Alites: Well to fully
Belites: Negligible to low

24-LAB-001 PETROGRAPHIC EXAMINATION OF HARDENED CONCRETE, ASTM C856

Project No. P-0012413 **Date:** 5/18/2022 **Date reviewed:** 5/23/2022
Sample ID: Core 4 **Performed by:** B. Jessen **Reviewed by:** C. Tillema

I. GENERAL OBSERVATIONS

1. Sample Dimensions: Our analysis was performed on both sides of a 72 mm (2-13/16") x 69 mm (2-11/16") x 27 mm (1-1/16") thick lapped profile section and a 76 mm (3") x 52 mm (2") thin section that were saw-cut and prepared from the original 70 mm (2-3/4") diameter x 76 mm (3") long core.
2. Surface Conditions:
Outer: Fairly smooth, flat, formed surface
Inner: Rough, irregular, fractured surface
3. Reinforcement: None observed.
4. General Physical Conditions: The sample was received with roughly 60% of the outer surface cleanly delaminated from the rest of the core sample. The sections of the core were reattached in-lab using strapping tape and cyanoacrylate adhesive to ensure stabilization during sample preparation.

Approximately 60% of the outer surface had spalled at a depth ranging from 1 mm (1/32") to 7 mm (1/4"). Up to 1 mm (1/32") An up to 25 mm (1") wide and up to 1 mm (1/32") deep section of the concrete surface, between the spalled and the intact surface was not received. The macrocrack of the delamination surface proceeded through several coarse and fine aggregate particles. The depth of carbonation ranged from 1 mm (1/32") up to 8 mm (5/16") from the original outer surface. The concrete contained a small amount of entrained-sized air voids. The concrete was well consolidated but exhibited a poor paste/aggregate bond. A few weathered coarse aggregate particles at various depths throughout the concrete displayed a rusty coloration of their phenocrysts. Soft paste was observed surrounding a few of the weathered aggregate particles. Darker colored, denser paste was observed within a recessed notches of a few of the coarse aggregate particles.

II. AGGREGATE

1. Coarse: 19 mm (3/4") nominal sized quarried and crushed porphyritic basalt. The particles were mostly sub-angular to angular in shape. The coarse aggregate appeared well graded and exhibited good overall distribution.
2. Fine: Combined natural carbonate sand and crushed basalt (fossiliferous carbonates, fossils/fossil fragments, with many basalt, and several olivine, pyroxene, and iron oxide particles). The grains were mostly sub-rounded with many smaller sub-angular particles. The fine aggregate appeared fairly graded and exhibited good overall uniform distribution.

III. CEMENTITIOUS PROPERTIES

1. Air Content: 0.8% total
2. Depth of carbonation: Ranged from 1 mm (1/32") up to 8 mm (5/16") depth from the outer surface.

3. Paste/aggregate bond: Poor.
4. Paste color: Darker than medium light gray (Munsell® N6) overall, slightly lighter within the carbonated paste.
5. Paste hardness: Moderately hard (Mohs ≈3.5).
6. Microcracking: An up to 34 mm (1-5/16") long macrocrack occurred at low angle to the outer surface and was observed between 1 mm (1/32") and 7 mm (1/4") depth.
7. Secondary deposits: None observed.
8. w/cm: Estimated at between 0.40 and 0.45 with approximately 6 to 8% residual portland cement clinker particles.
9. Cement hydration:
Alites: Well to fully
Belites: Negligible to low

24-LAB-001 PETROGRAPHIC EXAMINATION OF HARDENED CONCRETE, ASTM C856

Project No. P-0012413 **Date:** 5/18/2022 **Date reviewed:** 5/23/2022
Sample ID: Core 6 **Performed by:** B. Jessen **Reviewed by:** C. Tillema

I. GENERAL OBSERVATIONS

1. **Sample Dimensions:** Our analysis was performed on a 70 mm (2-3/4") x 43 mm (1-11/16") x 27 mm (1-1/16") thick lapped profile section and a 76 mm (3") x 52 mm (2") thin section that were saw-cut and prepared from the original 70 mm (2-3/4") diameter x 51 mm (2") long core.
2. **Surface Conditions:**
Outer: Fairly smooth, flat, formed surface
Inner: Rough, irregular, fractured surface
3. **Reinforcement:** None observed.
4. **General Physical Conditions:** The sample was received with roughly 50% of the outer surface cleanly spalled from the rest of the core sample. The sections of the core were reattached in-lab using strapping tape and cyanoacrylate adhesive to ensure stabilization during sample preparation.

Approximately 50% of the outer surface had spalled at a depth ranging from 2 mm (1/16") to 14 mm (9/16"). An up to 35 mm (1-3/8") wide and up to 2 mm (1/16") deep section of concrete between the spalled and the intact surface was not received with the sample. The depth of carbonation ranged from 12 mm (1/2") up to 18 mm (11/16") from the original outer surface. The concrete was not air entrained but contained a few spherical air voids. The concrete contained a small amount of entrained-sized air voids. A few weathered coarse aggregate particles at various depths throughout the concrete displayed a rusty coloration of their phenocrysts. Soft paste was observed surrounding a few of the weathered aggregate particles. Darker colored, denser paste was observed within a recessed notches of a few of the coarse aggregate particles.

II. AGGREGATE

1. **Coarse:** 19 mm (3/4") nominal sized quarried and crushed porphyritic basalt. The particles were mostly sub-angular to angular in shape. The coarse aggregate appeared well graded and exhibited fair overall distribution.
2. **Fine:** Combined natural carbonate sand and crushed basalt (fossiliferous carbonates, fossils/fossil fragments, with many basalt, and several olivine, pyroxene, and iron oxide particles). The grains were mostly sub-rounded with many smaller sub-angular particles. The fine aggregate appeared fairly graded and exhibited good overall uniform distribution.

III. CEMENTITIOUS PROPERTIES

1. Air Content: 0.8% total
2. Depth of carbonation: Ranged from 12 mm (1/2") up to 18 mm (11/16") depth from the outer surface.
3. Paste/aggregate bond: Poor to fair.
4. Paste color: Medium light gray (Munsell® N6) overall, slightly lighter within the carbonated paste.
5. Paste hardness: Moderate (Mohs ≈3).
6. Microcracking: An up to 37 mm (1-7/16") long macrocrack occurred at low angle to the outer surface and was observed between 2 mm (1/16") and 14 mm (9/16") depth
7. Secondary deposits: None observed.
8. w/cm: Estimated at between 0.40 and 0.45 with approximately 5 to 7% residual portland cement clinker particles.
9. Cement hydration: Alites: Well to fully
Belites: Negligible to low

24-LAB-001 PETROGRAPHIC EXAMINATION OF HARDENED CONCRETE, ASTM C856

Project No. P-0012413 **Date:** 5/18/2022 **Date reviewed:** 5/23/2022
Sample ID: Core 7 **Performed by:** B. Jessen **Reviewed by:** C. Tillema

I. GENERAL OBSERVATIONS

1. **Sample Dimensions:** Our analysis was performed on a 69 mm (2-13/16") x 48 mm (1-7/8") x 27 mm (1-1/16") thick lapped profile section and a 76 mm (3") x 52 mm (2") thin section that were saw-cut and prepared from the original 70 mm (2-3/4") diameter x 51 mm (2") long core.
2. **Surface Conditions:**
Outer: Fairly smooth, flat, formed surface
Inner: Rough, irregular, fractured surface
3. **Reinforcement:** None observed.
4. **General Physical Conditions:** A few microcracks oriented sub-perpendicular to the outer surface proceeded from that surface up to 2 mm (1/16") depth. The depth of carbonation ranged from 9 mm (3/8") up to 17 mm (11/16") from the outer surface. The concrete contained a small amount of spherical entrained-sized air voids. The concrete was well consolidated but exhibited a poor paste/aggregate bond. A few weathered coarse aggregate particles at various depths throughout the concrete displayed a rusty coloration of their phenocrysts. Soft paste was observed surrounding a few of the weathered aggregate particles.

II. AGGREGATE

1. **Coarse:** 19 mm (3/4") nominal sized quarried and crushed porphyritic basalt. The particles were mostly sub-angular to angular in shape. The coarse aggregate appeared well graded and exhibited good overall distribution.
2. **Fine:** Combined natural carbonate sand and crushed basalt (fossiliferous carbonates, fossils/fossil fragments, with many basalt, and several olivine, pyroxene, and iron oxide particles). The grains were mostly sub-rounded with many smaller sub-angular particles. The fine aggregate appeared fairly graded and exhibited good overall uniform distribution.

III. CEMENTITIOUS PROPERTIES

1. **Air Content:** 3.3% total
2. **Depth of carbonation:** Ranged from 9 mm (3/8") up to 17 mm (11/16") depth from the top surface.
3. **Paste/aggregate bond:** Poor.
4. **Paste color:** Medium light gray (Munsell® N6) overall, slightly lighter within the carbonated paste.
5. **Paste hardness:** Moderately hard (Mohs ≈3.5).

6. Microcracking: A few microcracks oriented sub-perpendicular to the outer surface proceeded from that surface up to 2 mm (1/16") depth.
7. Secondary deposits: None observed.
8. w/cm: Estimated at between 0.42 and 0.47 with approximately 4 to 6% residual portland cement clinker particles.
9. Cement hydration: Alites: Well to fully
Belites: Negligible to low

24-LAB-001 PETROGRAPHIC EXAMINATION OF HARDENED CONCRETE, ASTM C856

Project No. P-0012413 **Date:** 5/18/2022 **Date reviewed:** 5/23/2022
Sample ID: Core 9 **Performed by:** B. Jessen **Reviewed by:** C. Tillema

I. GENERAL OBSERVATIONS

1. Sample Dimensions: Our analysis was performed on a 105 mm (1-1/8") x 70 mm (2-3/4") x 28 mm (1-1/8") thick lapped profile section and a 76 mm (3") x 52 mm (2") thin section that were saw-cut and prepared from the original 70 mm (2-3/4") diameter x 108 mm (4-1/4") long core.
2. Surface Conditions:
Outer: Fairly smooth, flat, formed surface
Inner: Rough, irregular, fractured surface
3. Reinforcement: None observed.
4. General Physical Conditions: A few microcracks oriented sub-perpendicular to the outer surface proceeded from that surface up to 5 mm (3/16") depth and one proceeded to 32 mm (1-1/4"). The depth of carbonation ranged from 27 mm (1-1/16") up to 30 mm (1-3/16") from the outer surface. Several microcracks, up to 34 mm (1-5/16") in length, were observed in various orientations within the outer 67 mm (2-5/8") of the concrete, with some concentration within the outer 39 mm (9/16"). The microcracks primarily proceeded around coarse aggregate particles. The concrete contained a small amount of spherical, entrained-sized air voids. The concrete was well consolidated but exhibited a poor paste/aggregate bond. A few weathered coarse aggregate particles at various depths throughout the concrete displayed a rusty coloration of their phenocrysts. Soft paste was observed surrounding a few of the weathered aggregate particles.

II. AGGREGATE

1. Coarse: 19 mm (3/4") nominal sized quarried and crushed porphyritic basalt. The particles were mostly sub-angular to angular in shape. The coarse aggregate appeared well graded and exhibited good overall distribution.
2. Fine: Combined natural carbonate sand and crushed basalt (fossiliferous carbonates, fossils/fossil fragments, with many basalt, and several olivine, pyroxene, and iron oxide particles). The grains were mostly sub-rounded with many smaller sub-angular particles. The fine aggregate appeared fairly graded and exhibited good overall uniform distribution.

III. CEMENTITIOUS PROPERTIES

1. Air Content: 3.1% total
2. Depth of carbonation: Ranged from 27 mm (1-1/16") to 30 mm (1-3/16") depth from the outer surface.
3. Paste/aggregate bond: Poor.
4. Paste color: Medium light gray (Munsell® N6) overall, slightly lighter within the carbonated paste.
5. Paste hardness: Moderately soft (Mohs ≈2.5-3).

6. Microcracking: A few microcracks oriented sub-perpendicular to the outer surface proceeded from that surface up to 5 mm (3/16") depth and one proceeded to 32 mm (1-1/4"). Many randomly oriented microcracks were observed within the outer 67 mm (2-5/8") of the concrete, with some concentration within the outer 39 mm (9/16").
7. Secondary deposits: None observed.
8. w/cm: Estimated at between 0.45 and 0.47 with approximately 4 to 6% residual portland cement clinker particles.
9. Cement hydration: Alites: Well to fully
Belites: Negligible to low

24-LAB-001 PETROGRAPHIC EXAMINATION OF HARDENED CONCRETE, ASTM C856

Project No. P-0012413 **Date:** 5/18/2022 **Date reviewed:** 5/24/2022
Sample ID: Core 10 **Performed by:** B. Jessen **Reviewed by:** C. Tillema

I. GENERAL OBSERVATIONS

1. Sample Dimensions: Our analysis was performed on both sides of a 91 mm (3-9/16") x 69 mm (2-13/16") x 25 mm (1") thick lapped profile section and a 76 mm (3") x 52 mm (2") thin section that were saw-cut and prepared from the original 70 mm (2-3/4") diameter x 102 mm (4") long core.
2. Surface Conditions:
Outer: Fairly smooth, flat, formed surface
Inner: Rough, irregular, fractured surface
3. Reinforcement: None observed.
4. General Physical Conditions: A few microcracks oriented sub-perpendicular to the outer surface proceeded from that surface up to 1 mm (1/32") depth, one proceeded up to 11 mm (7/16") depth. The depth of carbonation ranged from 1 mm (1/32") up to 10 mm (3/8") from the outer surface. The concrete was not air entrained but contained a few spherical air voids. The concrete was well consolidated but exhibited a poor paste/aggregate bond. A few weathered coarse aggregate particles at various depths throughout the concrete displayed a rusty coloration of their phenocrysts. Soft paste was observed surrounding a few of the weathered aggregate particles. Darker colored, denser paste was observed within the recessed notches of a few of the coarse aggregate particles.

II. AGGREGATE

1. Coarse: 19 mm (3/4") nominal sized quarried and crushed porphyritic basalt. The particles were mostly sub-angular to angular in shape. The coarse aggregate appeared well graded and exhibited good overall distribution.
2. Fine: Combined natural carbonate sand and crushed basalt (fossiliferous carbonates, fossils/fossil fragments, with many basalt, and several olivine, pyroxene, and iron oxide particles). The grains were mostly sub-rounded with many smaller sub-angular particles. The fine aggregate appeared fairly graded and exhibited good overall uniform distribution.

III. CEMENTITIOUS PROPERTIES

1. Air Content: 1.2% total
2. Depth of carbonation: Ranged from 1 mm (1/32") up to 10 mm (3/8") depth from the outer surface.
3. Paste/aggregate bond: Poor.
4. Paste color: Similar to but lighter than medium light gray (Munsell® N6).
5. Paste hardness: Moderately soft (Mohs ≈2.5-3).
6. Microcracking: A few microcracks oriented sub-perpendicular to the outer surface proceeded from that surface up to 1 mm (1/32") depth, one proceeded up to 11 mm (7/16") depth.

- | | |
|------------------------|---|
| 7. Secondary deposits: | None observed. |
| 8. w/cm: | Estimated at between 0.40 and 0.45 with approximately 7 to 9% residual portland cement clinker particles. |
| 9. Cement hydration: | Alites: Well to fully
Belites: Negligible to low |

24-LAB-001 PETROGRAPHIC EXAMINATION OF HARDENED CONCRETE, ASTM C856

Project No. P-0012413 **Date:** 5/18/2022 **Date reviewed:** 5/24/2022
Sample ID: Core 12 **Performed by:** B. Jessen **Reviewed by:** C. Tillema

I. GENERAL OBSERVATIONS

1. Sample Dimensions: Our analysis was performed on a 108 mm (4-1/4") x 70 mm (2-3/4") x 28 mm (1-1/8") thick lapped profile section and a 76 mm (3") x 52 mm (2") thin section that were saw-cut and prepared from the original 70 mm (2-3/4") diameter x 108 mm (4-1/4") long core.
2. Surface Conditions:
Outer: Fairly smooth, flat, formed surface
Inner: Rough, irregular, fractured surface
3. Reinforcement: None observed.
4. General Physical Conditions: A few microcracks oriented sub-perpendicular to the outer surface proceeded from that surface up to 2 mm (1/16") depth. The depth of carbonation ranged from negligible up to 5 mm (3/16") from the outer surface. The concrete was not air entrained but contained several spherical air voids. The concrete was well consolidated but exhibited a poor paste/aggregate bond. A few weathered coarse aggregate particles at various depths throughout the concrete displayed a rusty coloration of their phenocrysts. Soft paste was observed surrounding a few of the weathered aggregate particles.

II. AGGREGATE

1. Coarse: 19 mm (3/4") nominal sized quarried and crushed porphyritic basalt. The particles were mostly sub-angular to angular in shape. The coarse aggregate appeared well graded and exhibited good overall distribution.
2. Fine: Combined natural carbonate sand and crushed basalt (fossiliferous carbonates, fossils/fossil fragments, with many basalt, and several olivine, pyroxene, and iron oxide particles). The grains were mostly sub-rounded with many smaller sub-angular particles. The fine aggregate appeared fairly graded and exhibited good overall uniform distribution.

III. CEMENTITIOUS PROPERTIES

1. Air Content: 1.0% total
2. Depth of carbonation: Ranged from negligible up to 5 mm (3/16") depth from the outer surface.
3. Paste/aggregate bond: Poor.
4. Paste color: Medium light gray (Munsell® N6)
5. Paste hardness: Moderately soft (Mohs ≈2.5-3).

- | | |
|------------------------|---|
| 6. Microcracking: | A few microcracks oriented sub-perpendicular to the outer surface proceeded from that surface up to 2 mm (1/16") depth. |
| 7. Secondary deposits: | None observed. |
| 8. w/cm: | Estimated at between 0.40 and 0.45 with approximately 5 to 7% residual portland cement clinker particles. |
| 9. Cement hydration: | Alites: Well to fully
Belites: Negligible to low |



AIR VOID ANALYSIS

Project:
Wilson Tunnel Plenum Inspection

Reported To:
Conzor Engineers, LLC
737 Bishop Street, Suite 2530
Honolulu, HI 96813

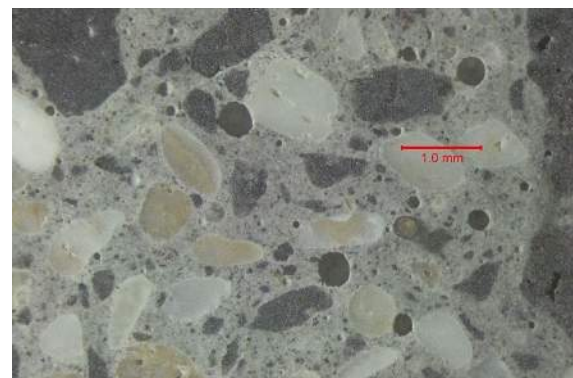
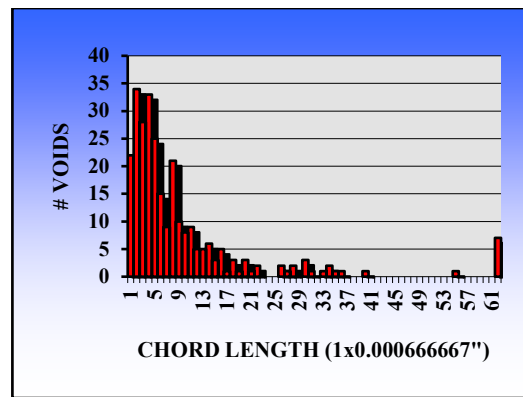
AET Project No.: P-0012413

Attn: Joshua Steiner
Date: May 27, 2022

Sample: Core 1
Conformance: The sample contains an air void system which is not consistent with current American Concrete Institute (ACI) recommendations for freeze-thaw resistance.

Sample Data
Description: Hardened Concrete Core
Dimensions: 70 mm (2-3/4") diameter by 102 mm (4") long
Test Data: By ASTM C457, Procedure A

Air Void Content %	2.0
Entrained, % < 0.040" (1mm)	1.6
Entrapped, % > 0.040" (1mm)	0.4
Air Voids/inch	3.0
Specific Surface, in ² /in ³	600
Spacing Factor, inches	0.012
Paste Content, % estimated	26
Magnification	75x
Traverse Length, inches	90
Test Date	5/16/2022
Technician	B. Jessen



Magnification: 20x
Description: Hardened air void system



AIR VOID ANALYSIS

Project:
Wilson Tunnel Plenum Inspection

Reported To:
Conzor Engineers, LLC
737 Bishop Street, Suite 2530
Honolulu, HI 96813

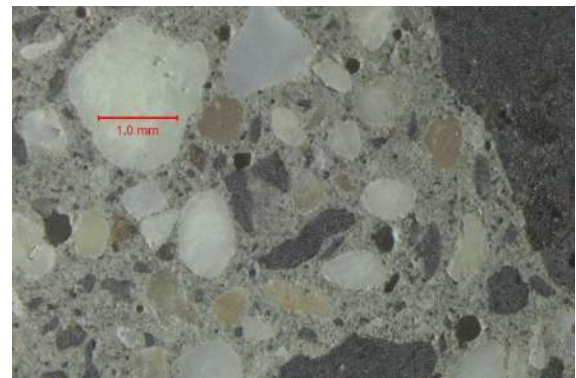
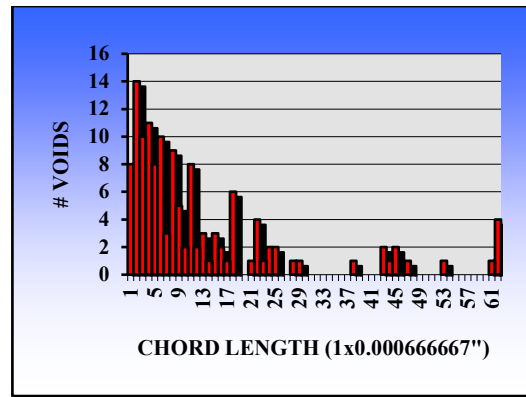
AET Project No.: P-0012413

Attn: Joshua Steiner
Date: May 27, 2022

Sample: Core 3
Conformance: The sample contains an air void system which is not consistent with current American Concrete Institute (ACI) recommendations for freeze-thaw resistance.

Sample Data
Description: Hardened Concrete Core
Dimensions: 70 mm (2-3/4") diameter by 83 mm (3-1/4") long
Test Data: By ASTM C457, Procedure A

Air Void Content %	1.3
Entrained, % < 0.040" (1mm)	1.1
Entrapped, % > 0.040" (1mm)	0.2
Air Voids/inch	1.5
Specific Surface, in ² /in ³	460
Spacing Factor, inches	0.019
Paste Content, % estimated	26
Magnification	75x
Traverse Length, inches	90
Test Date	5/17/2022
Technician	B. Jessen



Magnification: 20x
Description: Hardened air void system



AIR VOID ANALYSIS

Project:
Wilson Tunnel Plenum Inspection

Reported To:
Conzor Engineers, LLC
737 Bishop Street, Suite 2530
Honolulu, HI 96813

AET Project No.: P-0012413

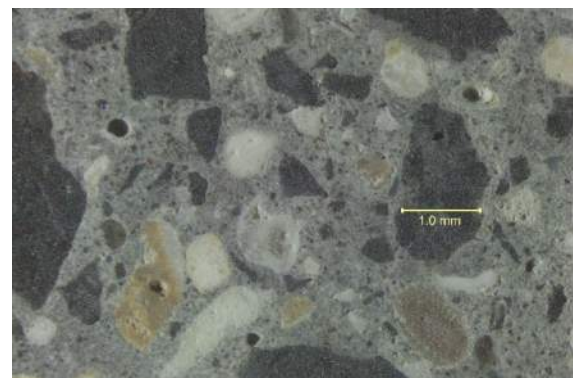
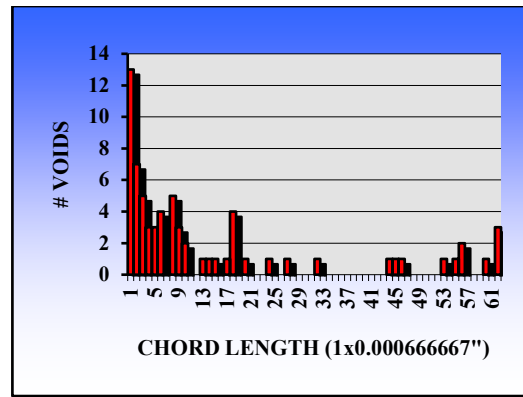
Attn: Joshua Steiner
Date: May 27, 2022

Sample: Core 4
Conformance: The sample contains an air void system which is not consistent with current American Concrete Institute (ACI) recommendations for freeze-thaw resistance.

Sample Data
Description: Hardened Concrete Core
Dimensions: 70 mm (2-3/4") diameter by 76 mm (3") long

Test Data: By ASTM C457, Procedure A

Air Void Content %	0.8
Entrained, % < 0.040" (1mm)	0.6
Entrapped, % > 0.040" (1mm)	0.2
Air Voids/inch	0.8
Specific Surface, in ² /in ³	350
Spacing Factor, inches	0.030
Paste Content, % estimated	30
Magnification	75x
Traverse Length, inches	90
Test Date	5/16/2022
Technician	B. Jessen



Magnification: 20x
Description: Hardened air void system



AIR VOID ANALYSIS

Project:
Wilson Tunnel Plenum Inspection

Reported To:
Conzor Engineers, LLC
737 Bishop Street, Suite 2530
Honolulu, HI 96813

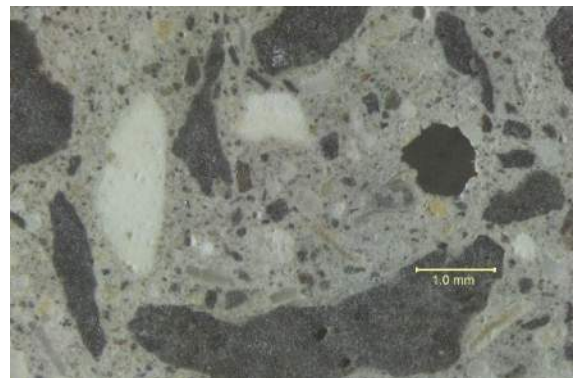
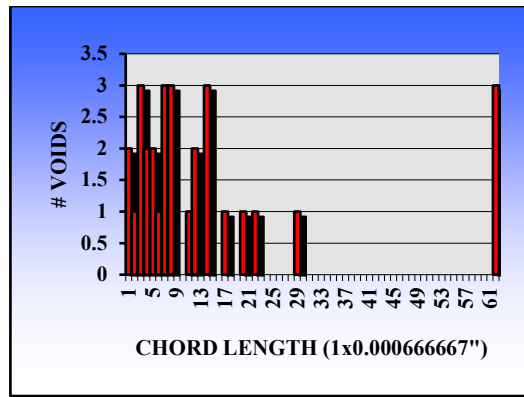
AET Project No.: P-0012413

Attn: Joshua Steiner
Date: May 27, 2022

Sample: Core 6
Conformance: The sample contains an air void system which is not consistent with current American Concrete Institute (ACI) recommendations for freeze-thaw resistance.

Sample Data
Description: Hardened Concrete Core
Dimensions: 70 mm (2-3/4") diameter by 51 mm (2") long

Test Data: By ASTM C457, Procedure A
Air Void Content % 0.8
Entrained, % < 0.040" (1mm) 0.4
Entrapped, % > 0.040" (1mm) 0.4
Air Voids/inch 0.8
Specific Surface, in²/in³ 370
Spacing Factor, inches 0.030
Paste Content, % estimated 30
Magnification 75x
Traverse Length, inches 40
Test Date 5/17/2022
Technician B. Jessen



Magnification: 20x
Description: Hardened air void system



AIR VOID ANALYSIS

Project:
Wilson Tunnel Plenum Inspection

Reported To:
Conzor Engineers, LLC
737 Bishop Street, Suite 2530
Honolulu, HI 96813

AET Project No.: P-0012413

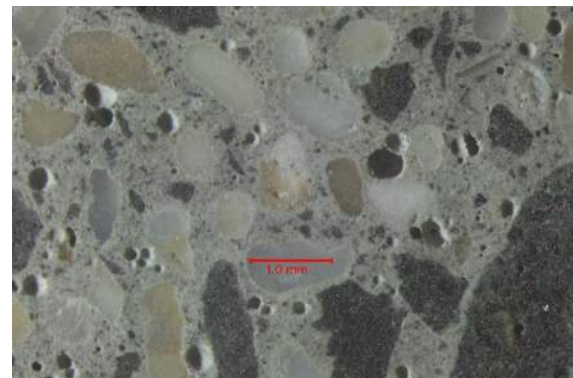
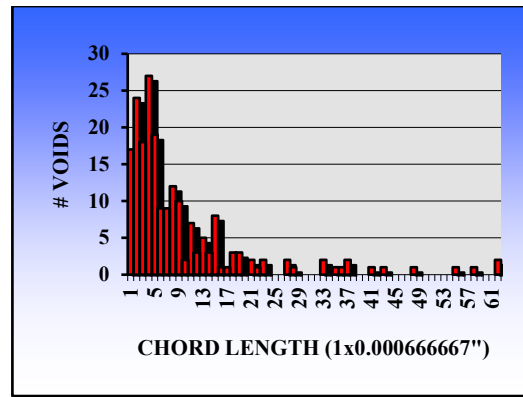
Attn: Joshua Steiner
Date: May 27, 2022

Sample: Core 7
Conformance: The sample contains an air void system which is not consistent with current American Concrete Institute (ACI) recommendations for freeze-thaw resistance.

Sample Data
Description: Hardened Concrete Core
Dimensions: 70 mm (2-3/4") diameter by 51 mm (2") long

Test Data: By ASTM C457, Procedure A

Air Void Content %	3.3
Entrained, % < 0.040" (1mm)	3.0
Entrapped, % > 0.040" (1mm)	0.3
Air Voids/inch	5.1
Specific Surface, in ² /in ³	620
Spacing Factor, inches	0.010
Paste Content, % estimated	32
Magnification	75x
Traverse Length, inches	40
Test Date	5/17/2022
Technician	B. Jessen



Magnification: 20x
Description: Hardened air void system



AIR VOID ANALYSIS

Project:
Wilson Tunnel Plenum Inspection

Reported To:
Conzor Engineers, LLC
737 Bishop Street, Suite 2530
Honolulu, HI 96813

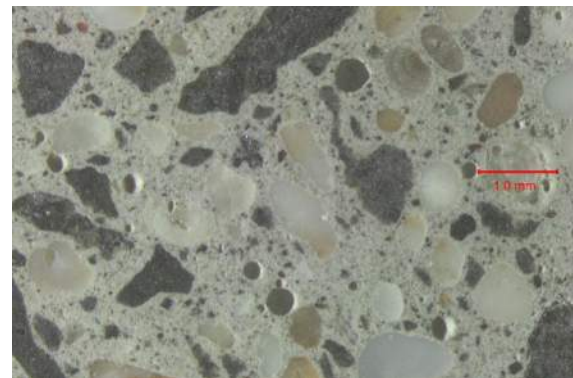
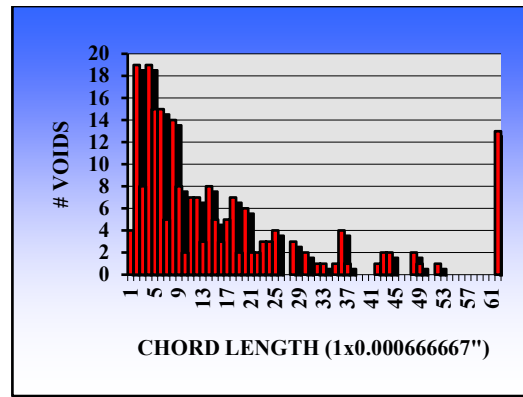
AET Project No.: P-0012413

Attn: Joshua Steiner
Date: May 27, 2022

Sample: Core 9
Conformance: The sample contains an air void system which is not consistent with current American Concrete Institute (ACI) recommendations for freeze-thaw resistance.

Sample Data
Description: Hardened Concrete Core
Dimensions: 70 mm (2-3/4") diameter by 108 mm (4-1/4") long
Test Data: By ASTM C457, Procedure A

Air Void Content %	3.1
Entrained, % < 0.040" (1mm)	1.9
Entrapped, % > 0.040" (1mm)	1.2
Air Voids/inch	2.3
Specific Surface, in ² /in ³	310
Spacing Factor, inches	0.019
Paste Content, % estimated	25
Magnification	75x
Traverse Length, inches	90
Test Date	5/16/2022
Technician	B. Jessen



Magnification: 20x
Description: Hardened air void system



AIR VOID ANALYSIS

Project:
Wilson Tunnel Plenum Inspection

Reported To:
Conzor Engineers, LLC
737 Bishop Street, Suite 2530
Honolulu, HI 96813

AET Project No.: P-0012413

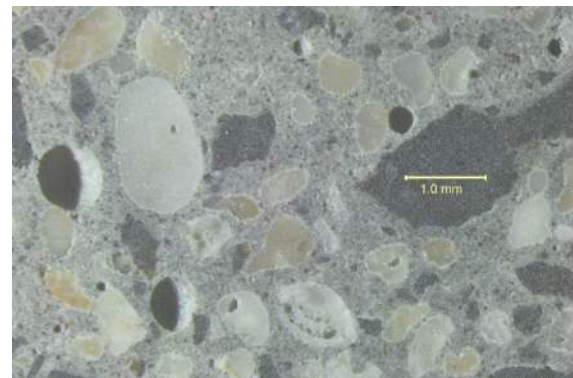
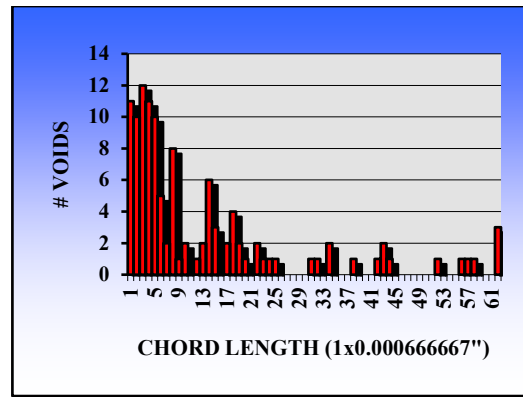
Attn: Joshua Steiner
Date: May 27, 2022

Sample: Core 10
Conformance: The sample contains an air void system which is not consistent with current American Concrete Institute (ACI) recommendations for freeze-thaw resistance.

Sample Data
Description: Hardened Concrete Core
Dimensions: 70 mm (2-3/4") diameter by 102 mm (4") long

Test Data: By ASTM C457, Procedure A

Air Void Content %	1.2
Entrained, % < 0.040" (1mm)	1.0
Entrapped, % > 0.040" (1mm)	0.2
Air Voids/inch	1.3
Specific Surface, in ² /in ³	440
Spacing Factor, inches	0.021
Paste Content, % estimated	28
Magnification	75x
Traverse Length, inches	90
Test Date	5/16/2022
Technician	B. Jessen



Magnification: 20x
Description: Hardened air void system



AIR VOID ANALYSIS

Project:
Wilson Tunnel Plenum Inspection

Reported To:
Conzor Engineers, LLC
737 Bishop Street, Suite 2530
Honolulu, HI 96813

AET Project No.: P-0012413

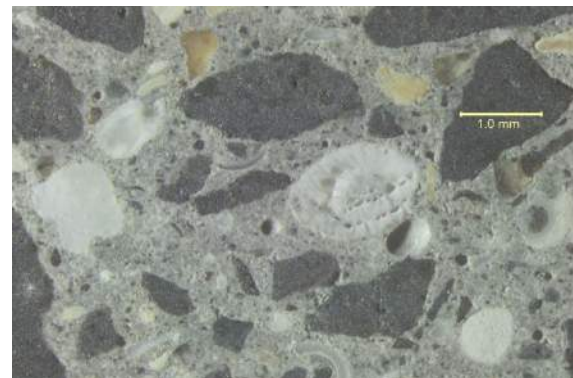
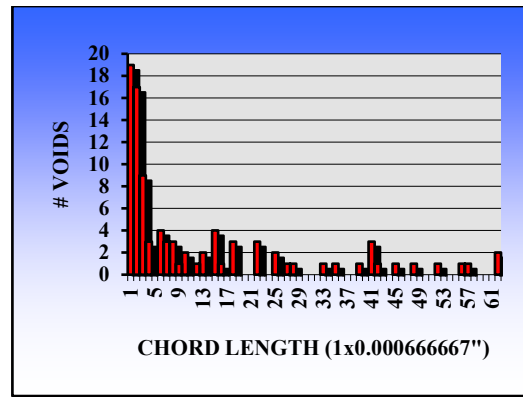
Attn: Joshua Steiner
Date: May 27, 2022

Sample: Core 12
Conformance: The sample contains an air void system which is not consistent with current American Concrete Institute (ACI) recommendations for freeze-thaw resistance.

Sample Data
Description: Hardened Concrete Core
Dimensions: 70 mm (2-3/4") diameter by 108 mm (4-1/4") long

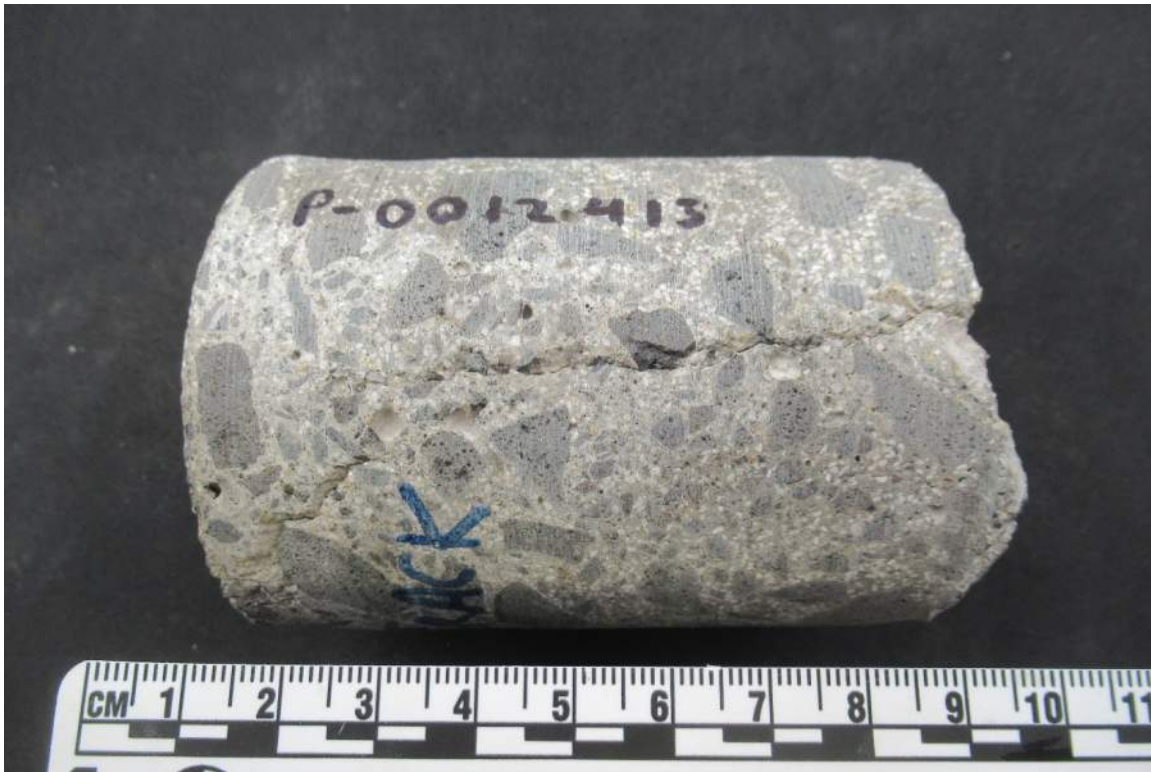
Test Data: By ASTM C457, Procedure A

Air Void Content %	1.0
Entrained, % < 0.040" (1mm)	0.8
Entrapped, % > 0.040" (1mm)	0.2
Air Voids/inch	1.0
Specific Surface, in ² /in ³	420
Spacing Factor, inches	0.024
Paste Content, % estimated	29
Magnification	75x
Traverse Length, inches	90
Test Date	5/16/2022
Technician	B. Jessen



Magnification: 20x
Description: Hardened air void system

Photo: 1



Sample ID:

Core 1

Description: Profile of the core sample as received with the outer surface to the left. This core was submitted for petrographic analysis and chloride ion content testing.

Photo: 2

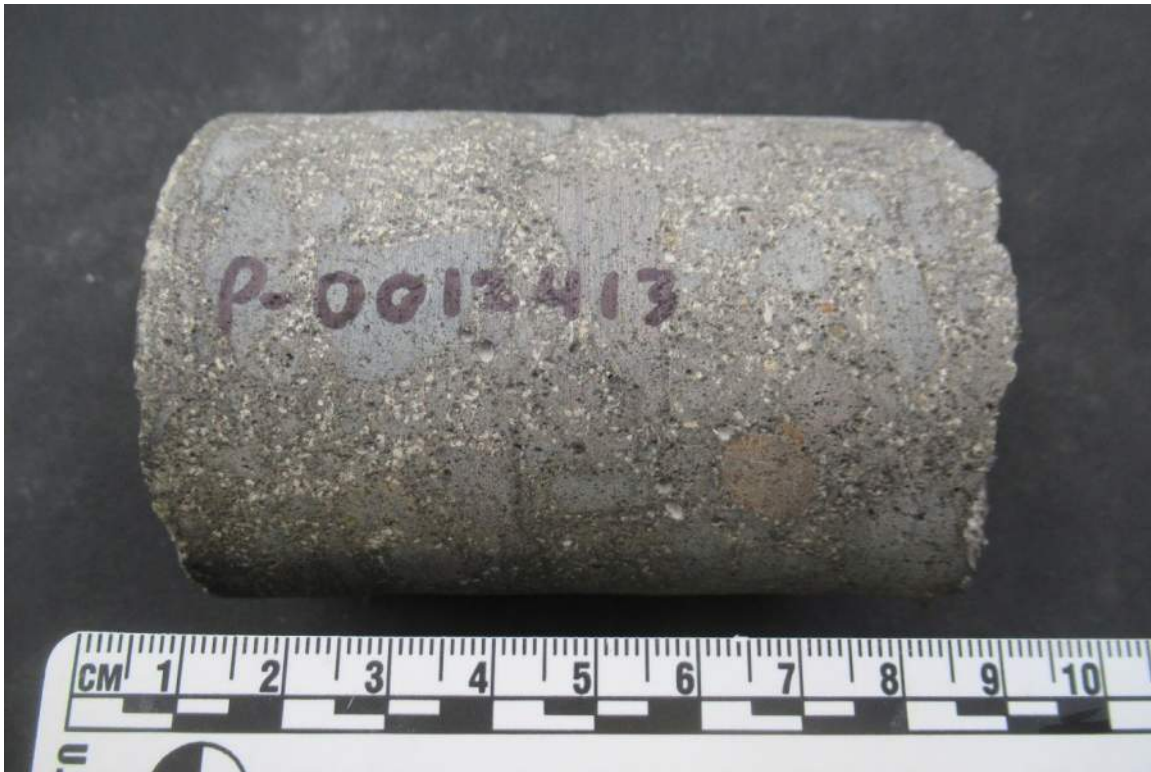


Sample ID:

Core 1

Description: The formed outer surface of the sample as received. The red line shows the approximate location of the macrocrack.

Photo: 3



Sample ID:

Core 2

Description: Profile of the core sample as received with the outer surface to the left. This sample was submitted for chloride ion content testing.

Photo: 4



Sample ID:

Core 2

Description: The formed outer surface of the sample as received.

Photo: 5



Sample ID:

Core 3

Description: Profile of the core sample as received with the outer surface to the left. This sample was submitted for petrographic analysis and chloride ion content testing.

Photo: 6

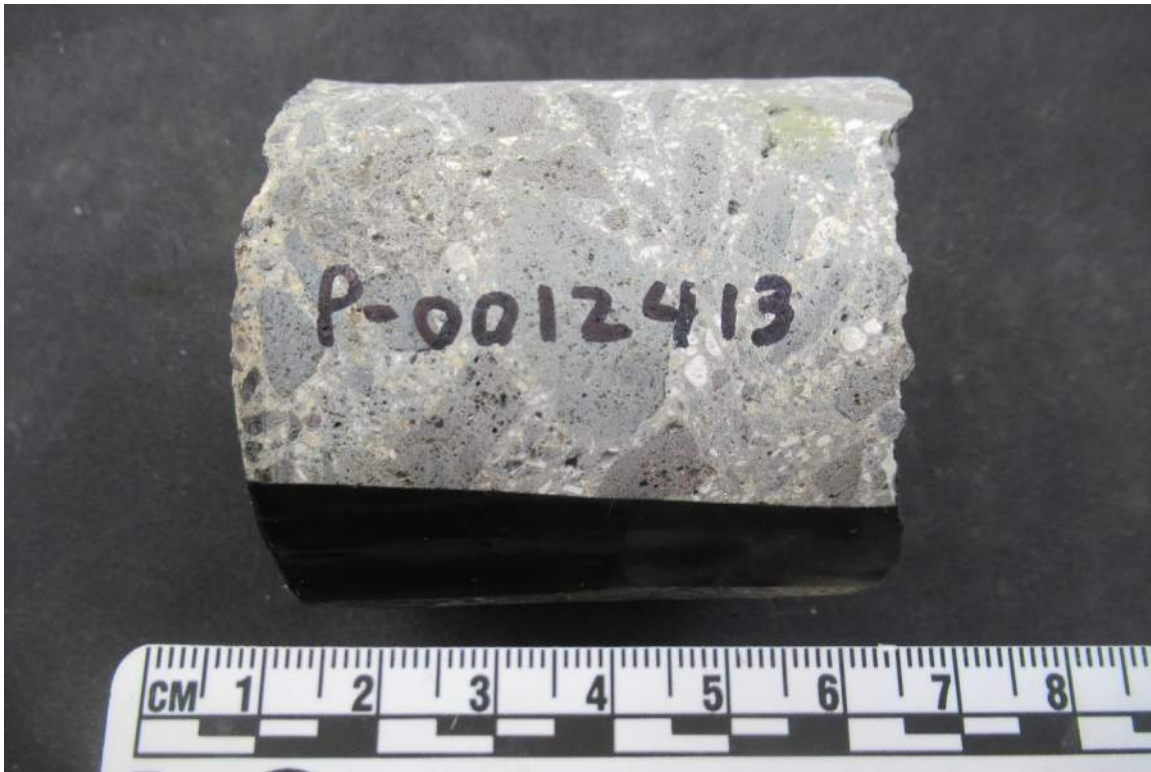


Sample ID:

Core 3

Description: The formed outer surface of the sample as received.

Photo: 7



Sample ID:

Core 4

Description: Profile of the core sample as received with the outer surface to the left. This sample was submitted for petrographic analysis and chloride ion content testing.

Photo: 8

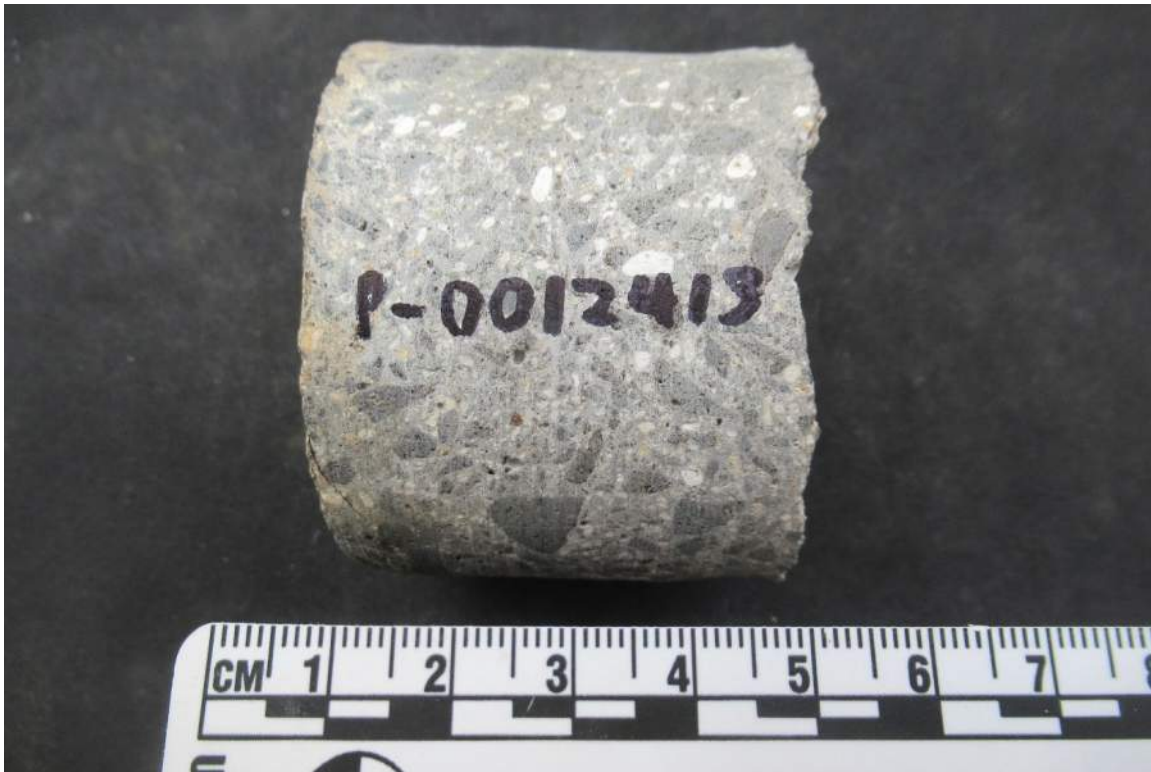


Sample ID:

Core 4

Description: The formed outer surface of the sample as received.

Photo: 9



Sample ID:

Core 5

Description: Profile of the core sample as received with the outer surface to the left. This sample was submitted for chloride ion content testing.

Photo: 10



Sample ID:

Core 5

Description: The formed outer surface of the sample as received.

Photo: 11

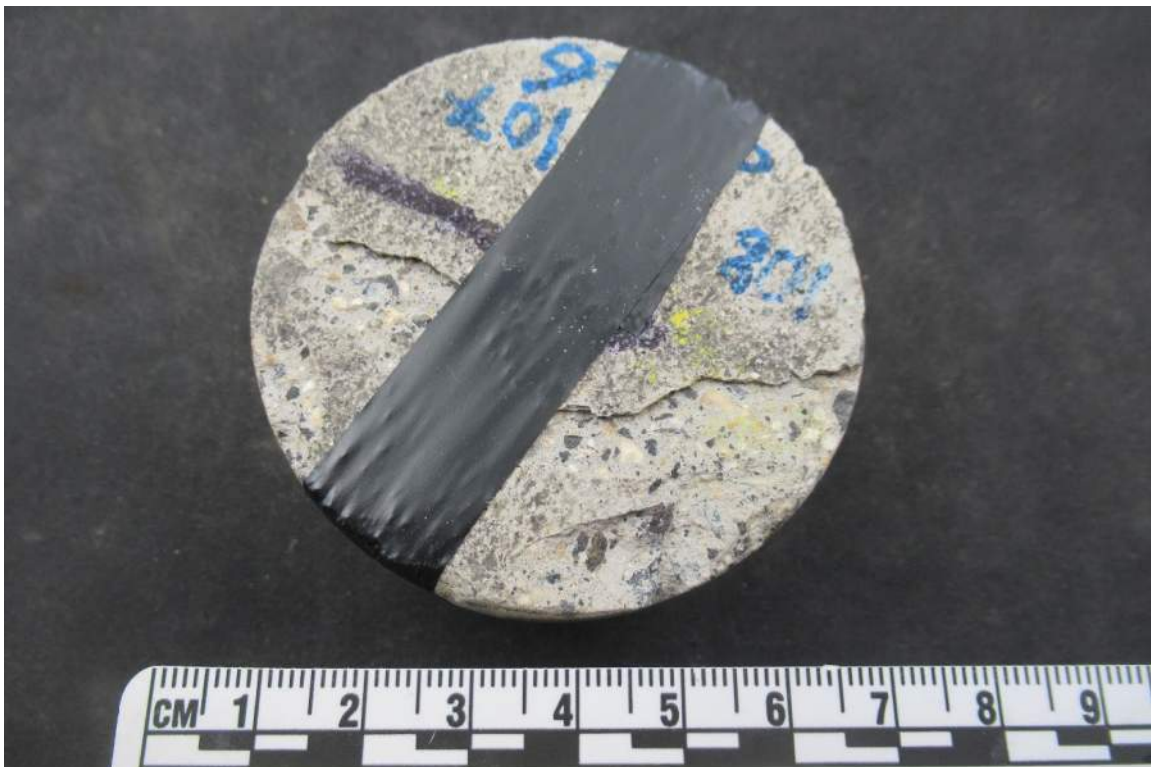


Sample ID:

Core 6

Description: Profile of the core sample as received with the outer surface to the left. This sample was submitted for petrographic analysis and chloride ion content testing.

Photo: 12



Sample ID:

Core 6

Description: The formed outer surface of the sample as received.

Photo: 13



Sample ID:

Core 7

Description: Profile of the core sample as received with the outer surface to the left. This sample was submitted for petrographic analysis and chloride ion content testing.

Photo: 14

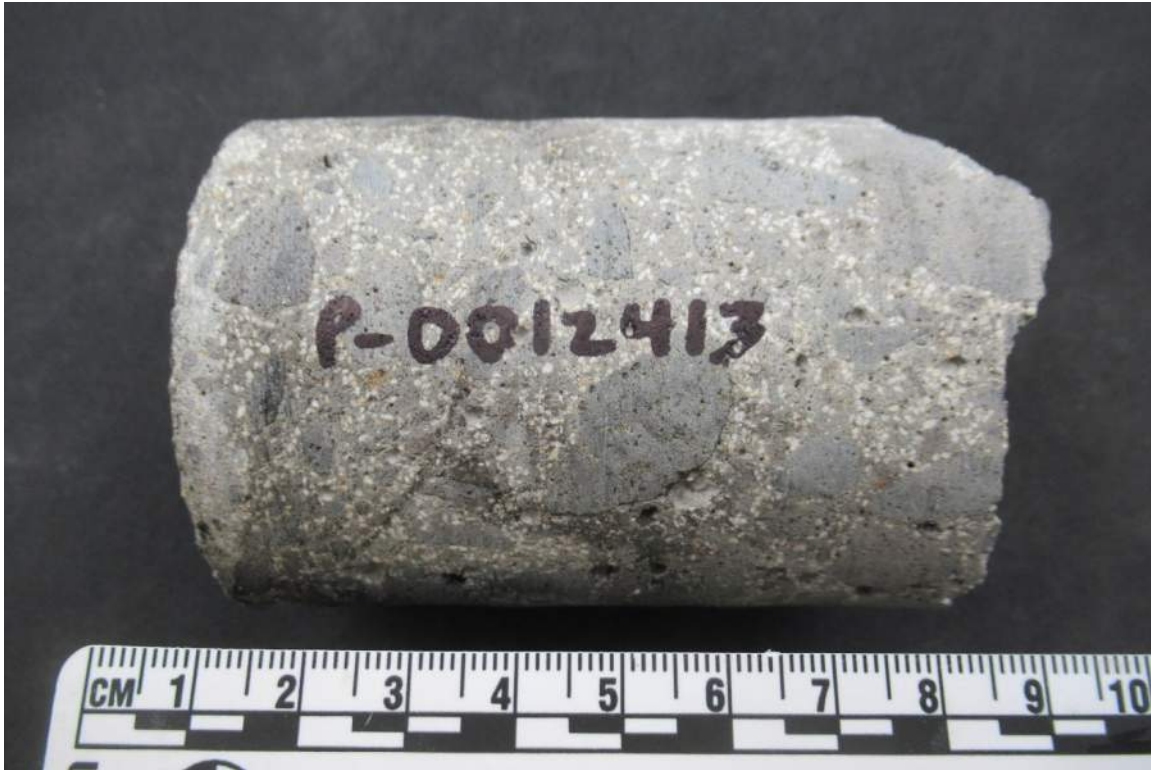


Sample ID:

Core 7

Description: The formed outer surface of the sample as received.

Photo: 15



Sample ID:

Core 8

Description: Profile of the core sample as received with the outer surface to the left. This sample was submitted for chloride ion content testing.

Photo: 16

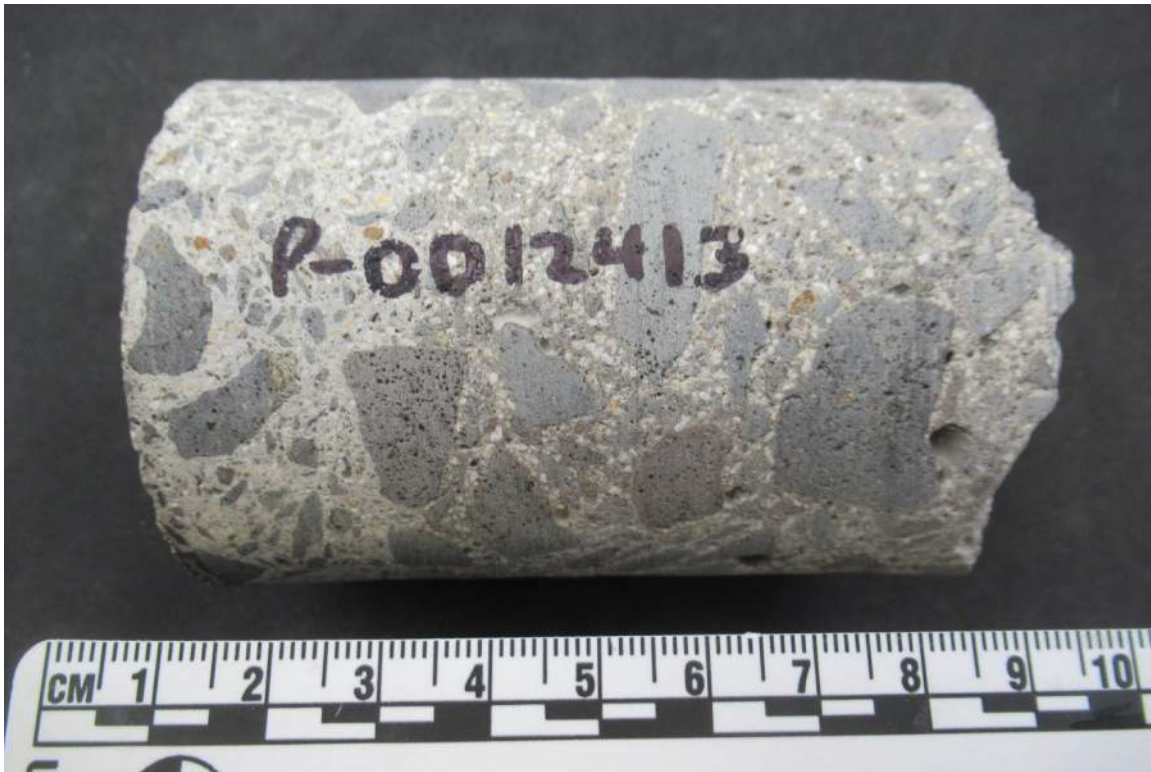


Sample ID:

Core 8

Description: The formed outer surface of the sample as received.

Photo: 17



Sample ID:

Core 9

Description: Profile of the core sample as received with the outer surface to the left. This sample was submitted for petrographic analysis and chloride ion content testing.

Photo: 18

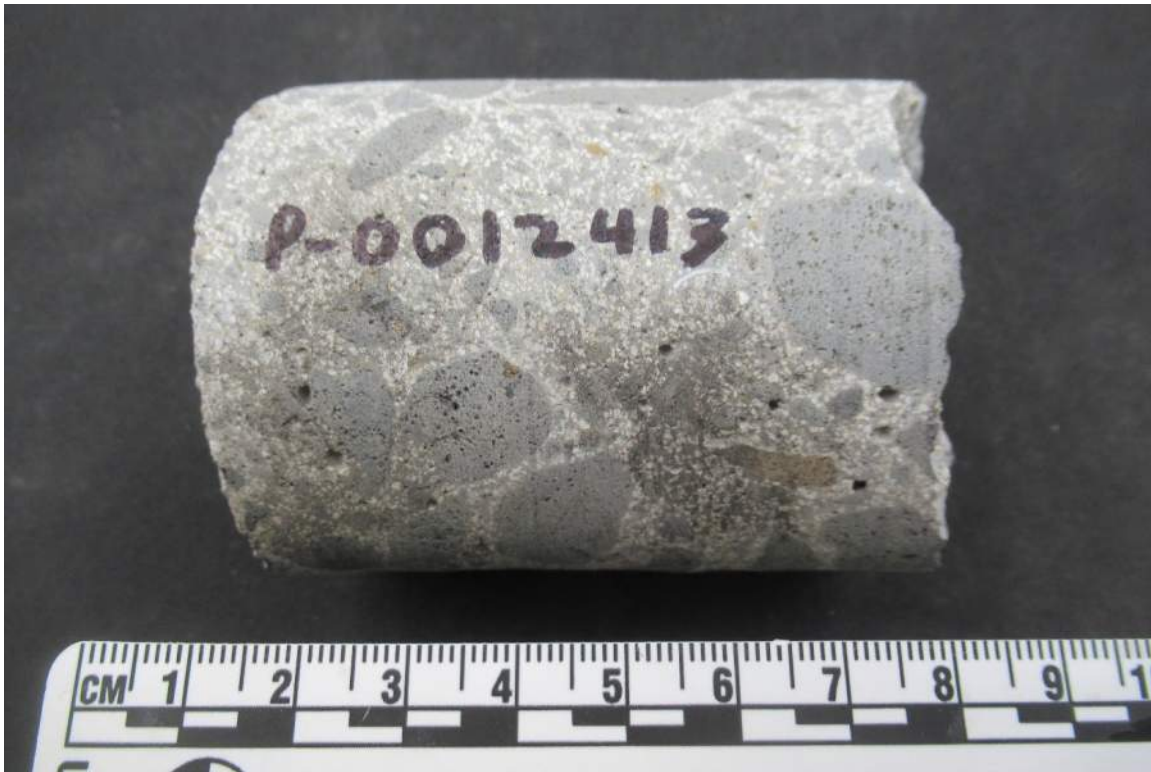


Sample ID:

Core 9

Description: The formed outer surface of the sample as received.

Photo: 19



Sample ID:

Core 10

Description: Profile of the core sample as received with the outer surface to the left. This sample was submitted for petrographic analysis and chloride ion content testing.

Photo: 20



Sample ID:

Core 10

Description: The formed outer surface of the sample as received.

Photo: 21



Sample ID:

Core 11

Description: Profile of the core sample as received with the outer surface to the left. This sample was submitted for chloride ion content testing.

Photo: 22

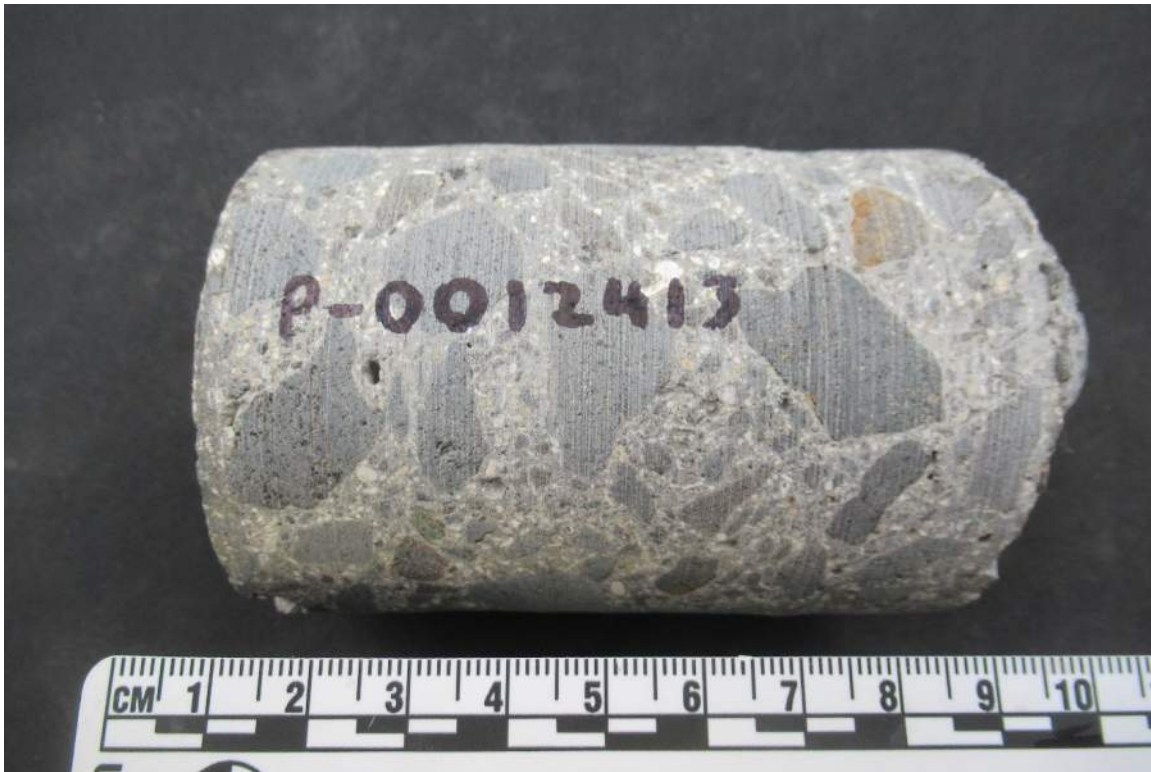


Sample ID:

Core 11

Description: The formed outer surface of the sample as received.

Photo: 23



Sample ID:

Core 12

Description: Profile of the core sample as received with the outer surface to the left. This sample was submitted for petrographic analysis and chloride ion content testing.

Photo: 24

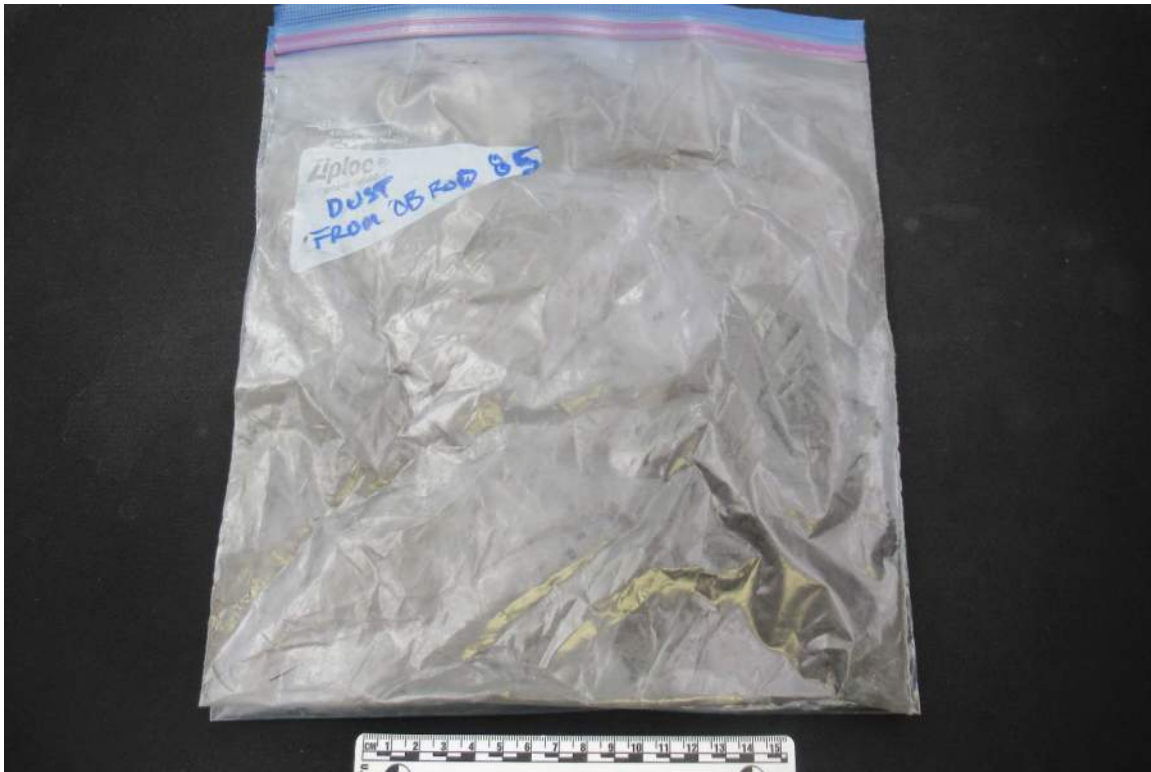


Sample ID:

Core 12

Description: The formed outer surface of the sample as received.

Photo: 25



Sample ID: Dust From OB Rod 85 **Description:** The sample as received.

Photo: 26



Sample ID: SS Rod **Description:** Profile of the sample as received.

Photo: 27

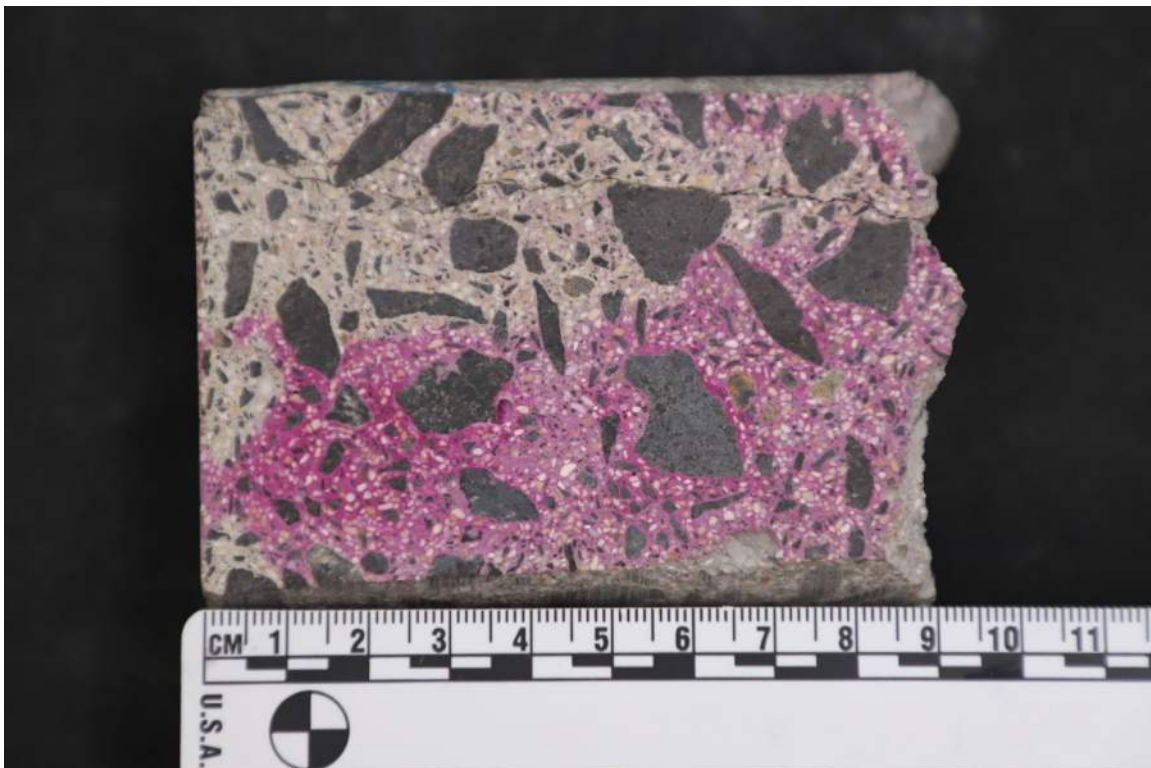


Sample ID:

Core 1

Description: Saw cut and lapped cross section of the sample with the outer surface oriented to the left. Cracking was mapped in red ink. Yellow arrows indicate the macrocrack.

Photo: 28



Sample ID:

Core 1

Description: Saw cut and lapped cross section of the sample with the outer surface oriented to the left. Phenolphthalein pH indicator was applied to the entire lapped cross section. Carbonation "spikes" along the length of the macrocrack.

Photo: 29

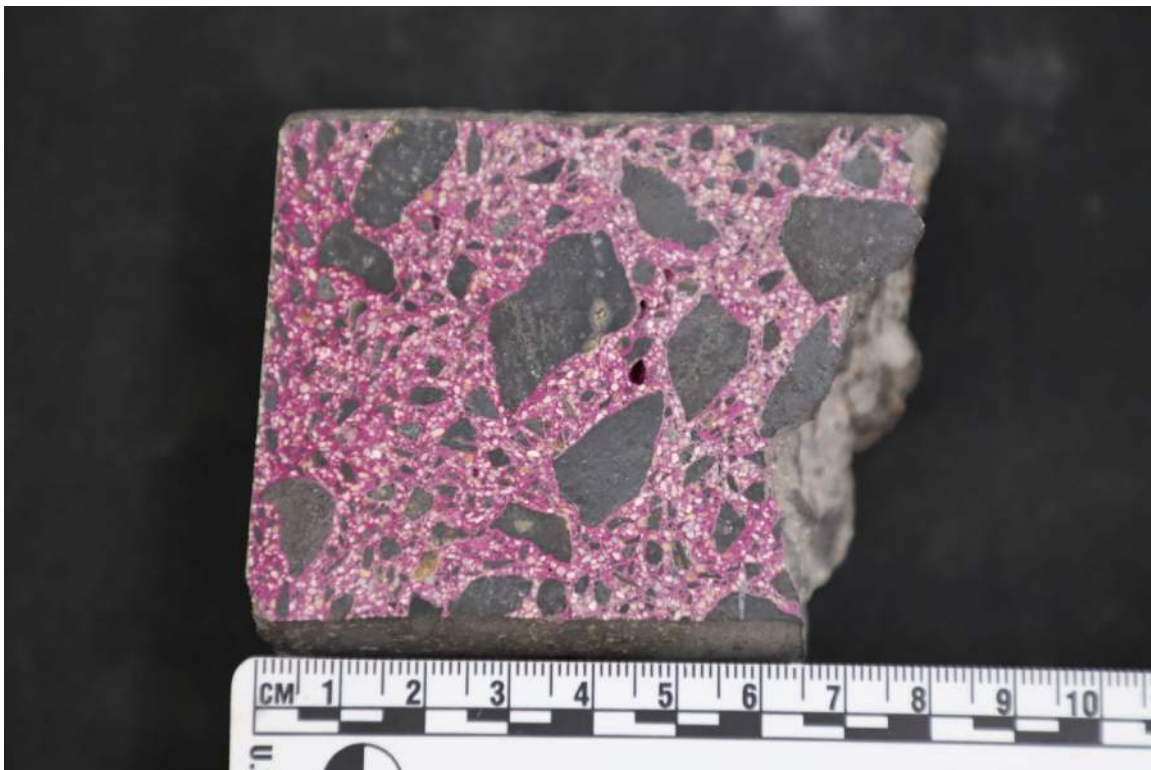


Sample ID:

Core 3

Description: Saw cut and lapped cross section of the sample with the outer surface oriented to the left. Cracking was mapped in red ink.

Photo: 30

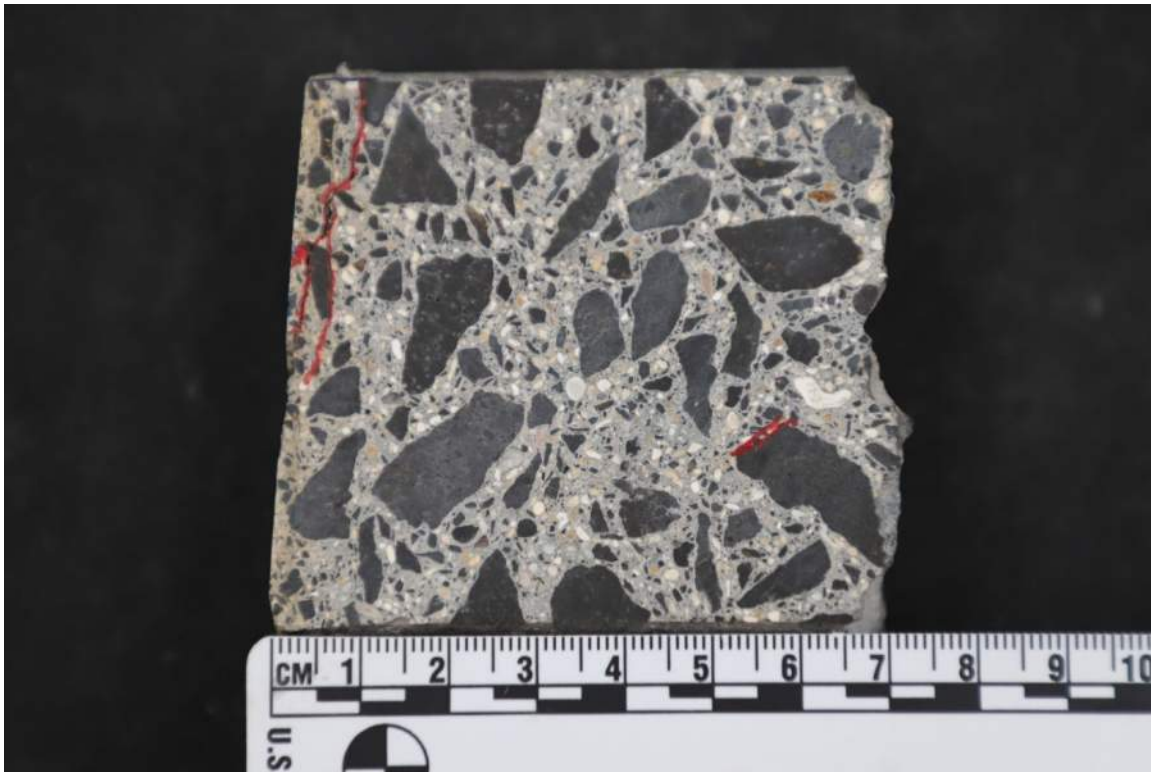


Sample ID:

Core 3

Description: Saw cut and lapped cross section of the sample with the outer surface oriented to the left. Phenolphthalein pH indicator was applied to the entire lapped cross section.

Photo: 31

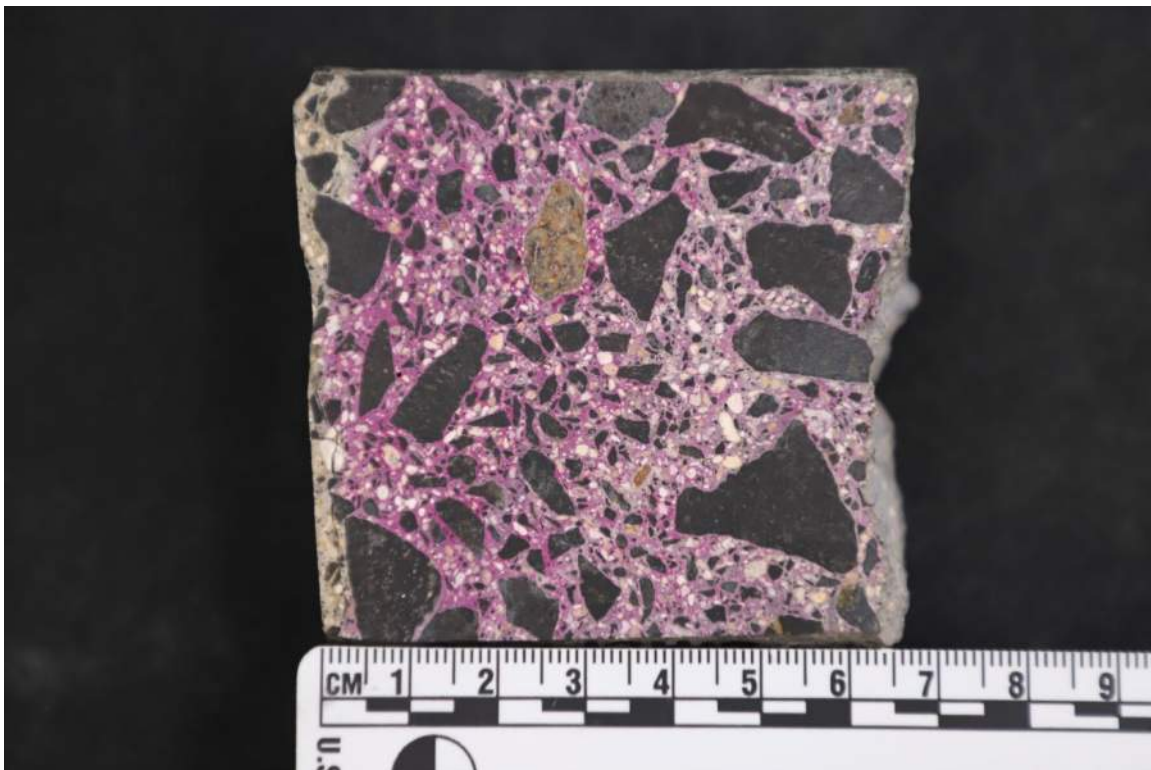


Sample ID:

Core 4

Description: Saw cut and lapped cross section of the sample with the outer surface oriented to the left. Cracking was mapped in red ink.

Photo: 32



Sample ID:

Core 4

Description: Saw cut and lapped cross section of the sample with the outer surface oriented to the left. Phenolphthalein pH indicator was applied to the entire lapped cross section.

Photo: 33

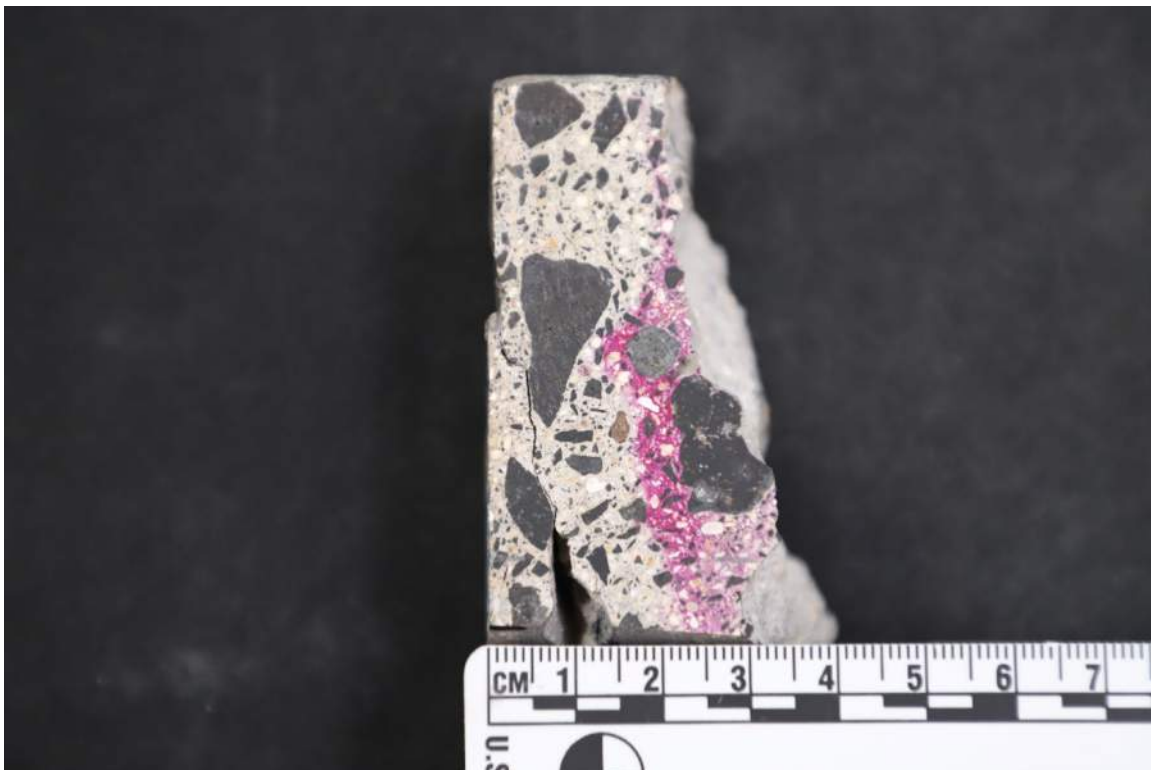


Sample ID:

Core 6

Description: Saw cut and lapped cross section of the sample with the outer surface oriented to the left. Cracking was mapped in red ink.

Photo: 34

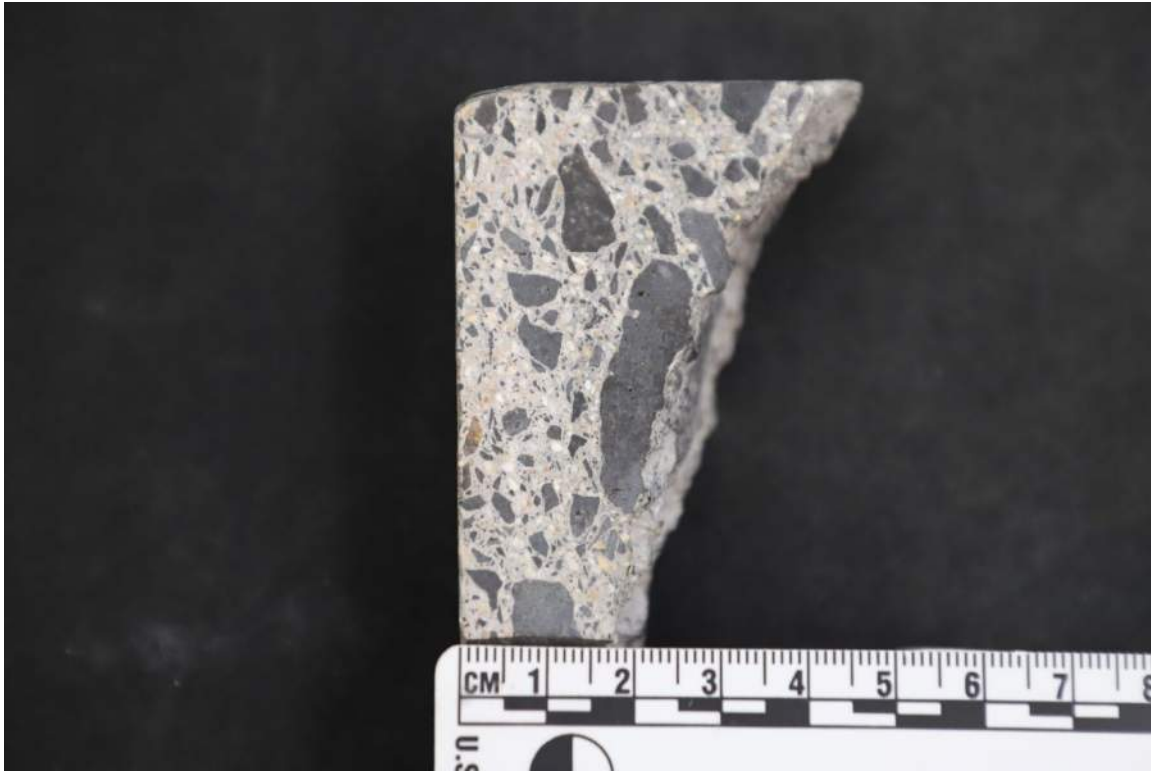


Sample ID:

Core 6

Description: Saw cut and lapped cross section of the sample with the outer surface oriented to the left. Phenolphthalein pH indicator was applied to the entire lapped cross section.

Photo: 35

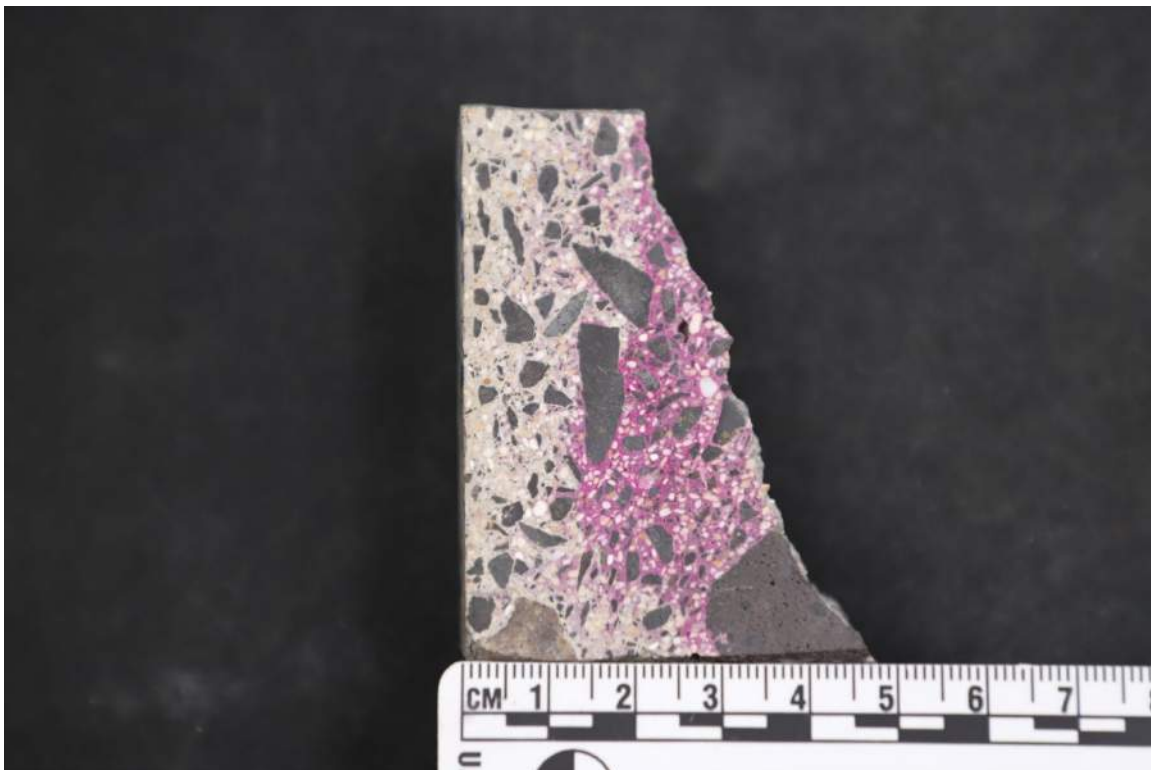


Sample ID:

Core 7

Description: Saw cut and lapped cross section of the sample with the outer surface oriented to the left.

Photo: 36



Sample ID:

Core 7

Description: Saw cut and lapped cross section of the sample with the outer surface oriented to the left. Phenolphthalein pH indicator was applied to the entire lapped cross section.

Photo: 37



Sample ID:

Core 9

Description: Saw cut and lapped cross section of the sample with the outer surface oriented to the left. Cracking was mapped in red ink.

Photo: 38



Sample ID:

Core 9

Description: Saw cut and lapped cross section of the sample with the outer surface oriented to the left. Phenolphthalein pH indicator was applied to the entire lapped cross section.

Photo: 39



Sample ID:

Core 10

Description: Saw cut and lapped cross section of the sample with the outer surface oriented to the left.

Photo: 40



Sample ID:

Core 10

Description: Saw cut and lapped cross section of the sample with the outer surface oriented to the left. Phenolphthalein pH indicator was applied to the entire lapped cross section.

Photo: 41

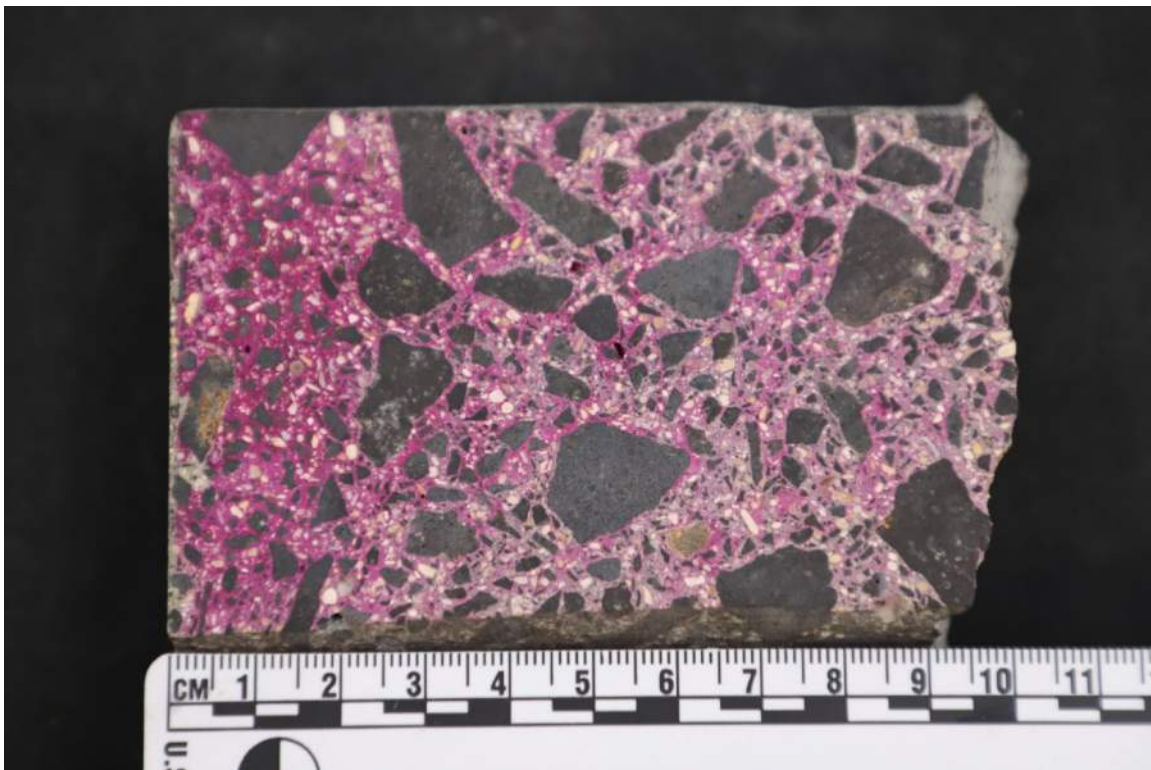


Sample ID:

Core 12

Description: Saw cut and lapped cross section of the sample with the outer surface oriented to the left.

Photo: 42

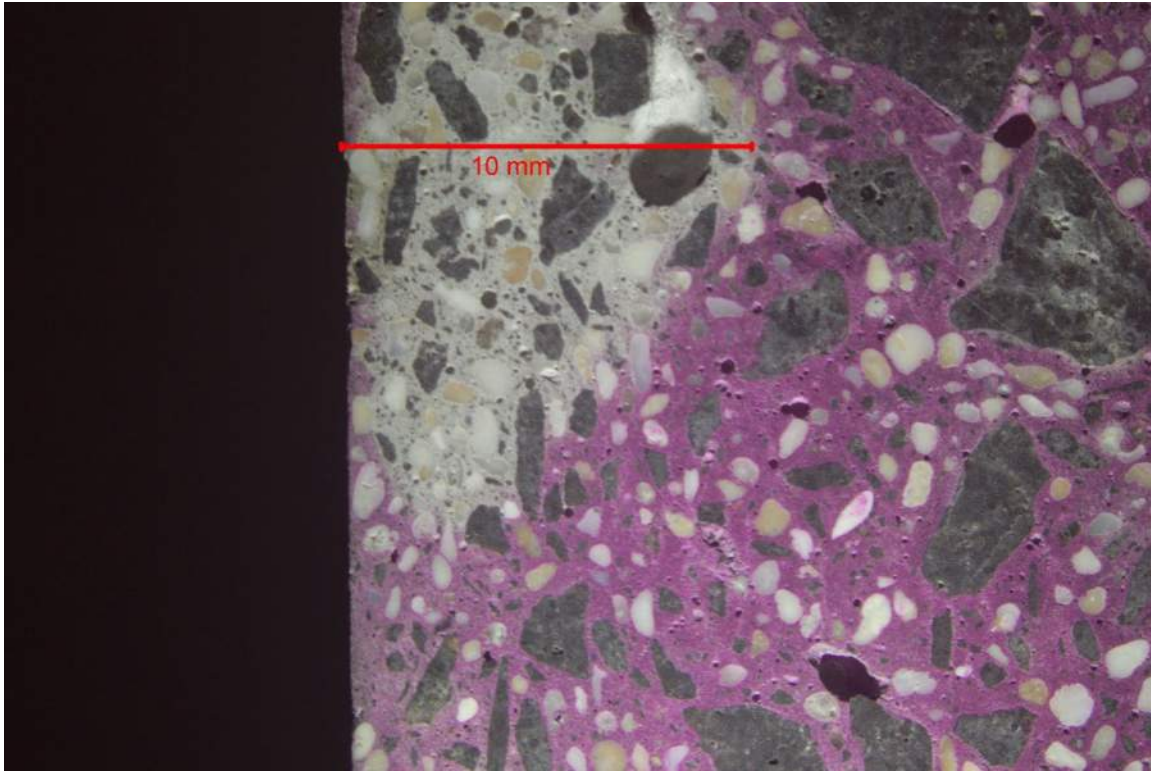


Sample ID:

Core 12

Description: Saw cut and lapped cross section of the sample with the outer surface oriented to the left. Phenolphthalein pH indicator was applied to the entire lapped cross section.

Photo: 43

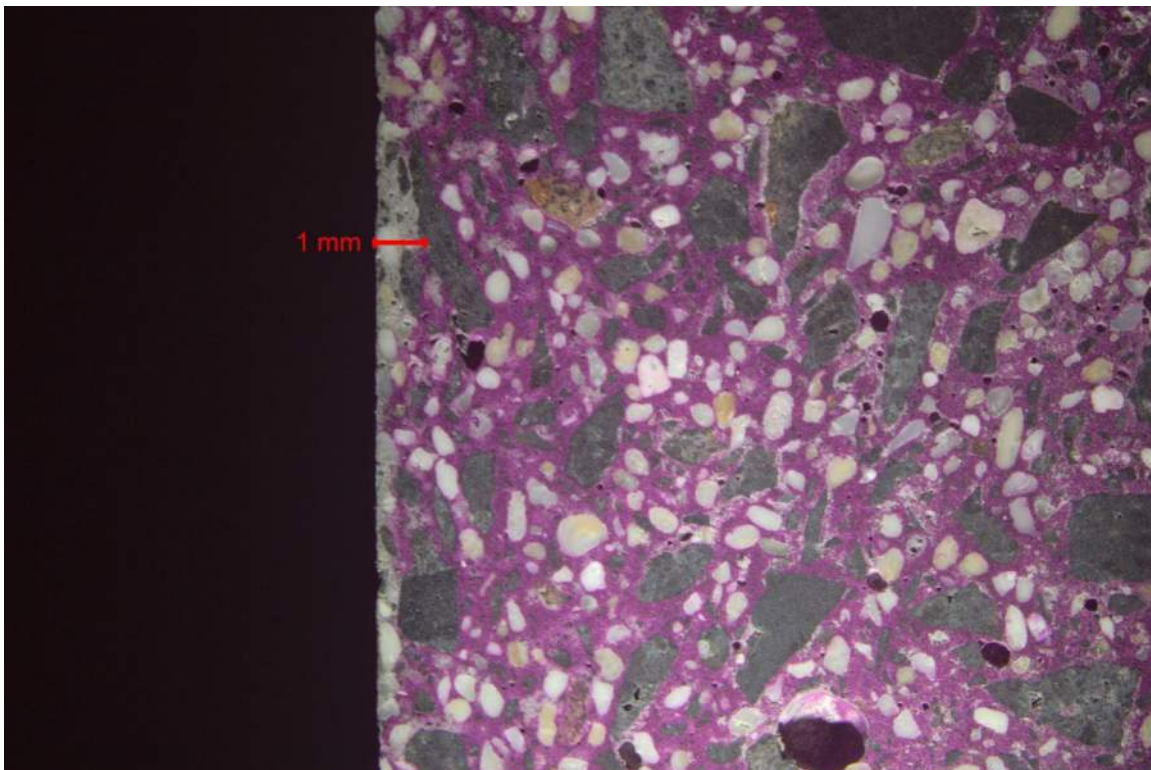


Sample ID:
Mag:

Core 1
5x

Description: Carbonation (unstained paste, pH <8.5) ranged from negligible up to 10 mm (3/8") from the outer surface, as viewed on saw cut and lapped cross section at low magnification.

Photo: 44

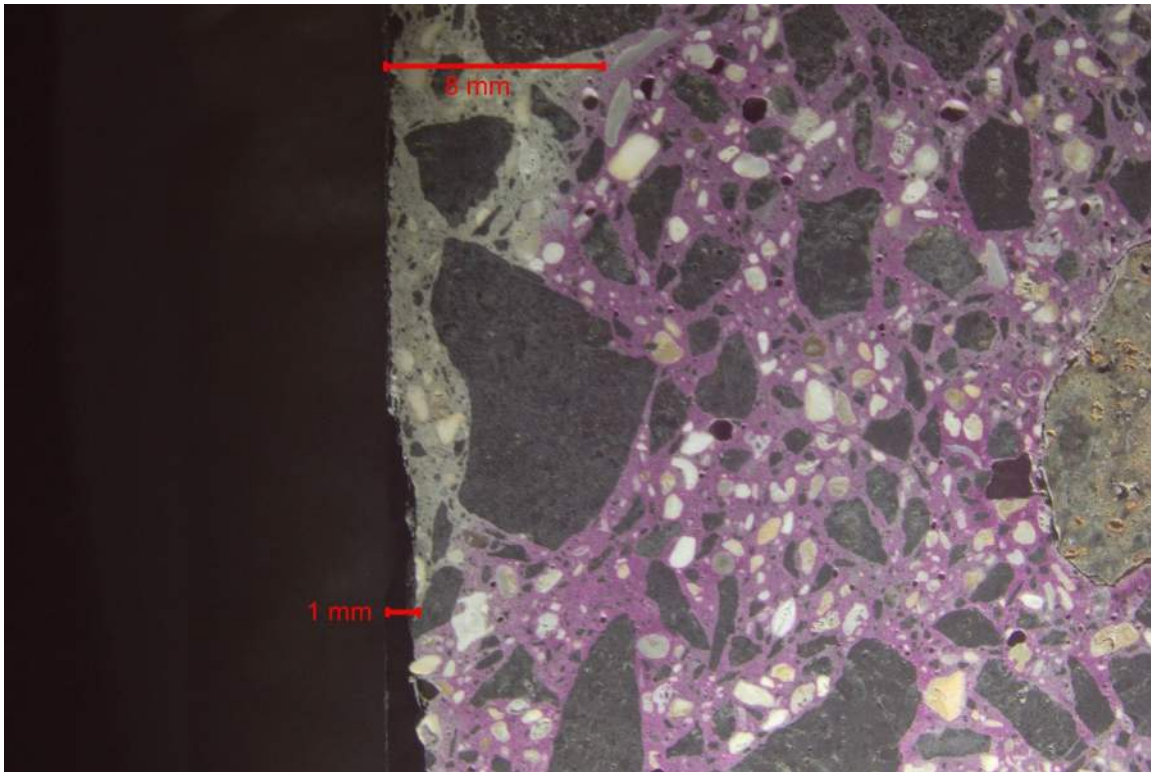


Sample ID:
Mag:

Core 3
5x

Description: Carbonation (unstained paste, pH <8.5) ranged from negligible up to 1 mm (1/32") from the outer surface, as viewed on saw cut and lapped cross section at low magnification.

Photo: 45

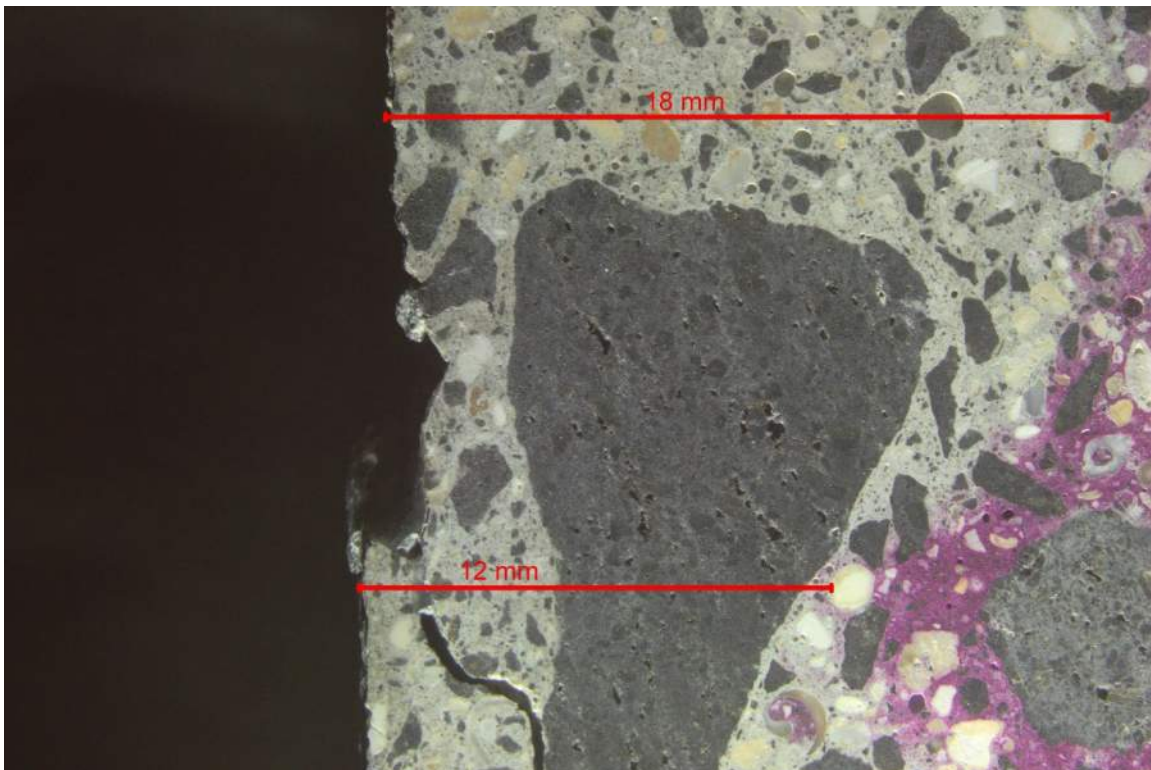


Sample ID:
Mag:

Core 4
3.5x

Description: Carbonation (unstained paste, PH <8.5) ranged from 1 mm (1/32") up to 8 mm (5/16") from the outer surface, as viewed on saw cut and lapped cross section at low magnification.

Photo: 46

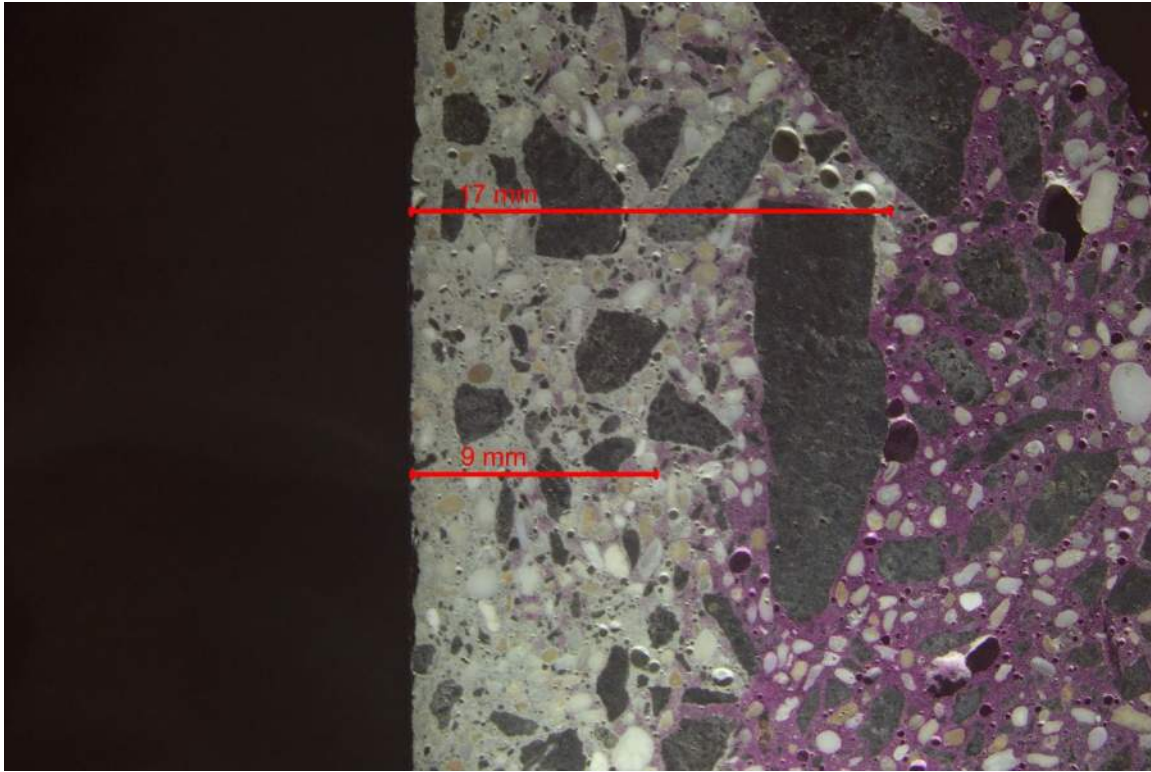


Sample ID:
Mag:

Core 6
5x

Description: Carbonation (unstained paste, pH,8.5) ranged from 12 mm (1/2") up to 18 mm (11/16") from the outer surface, as viewed on saw cut and lapped cross section at low magnification.

Photo: 47

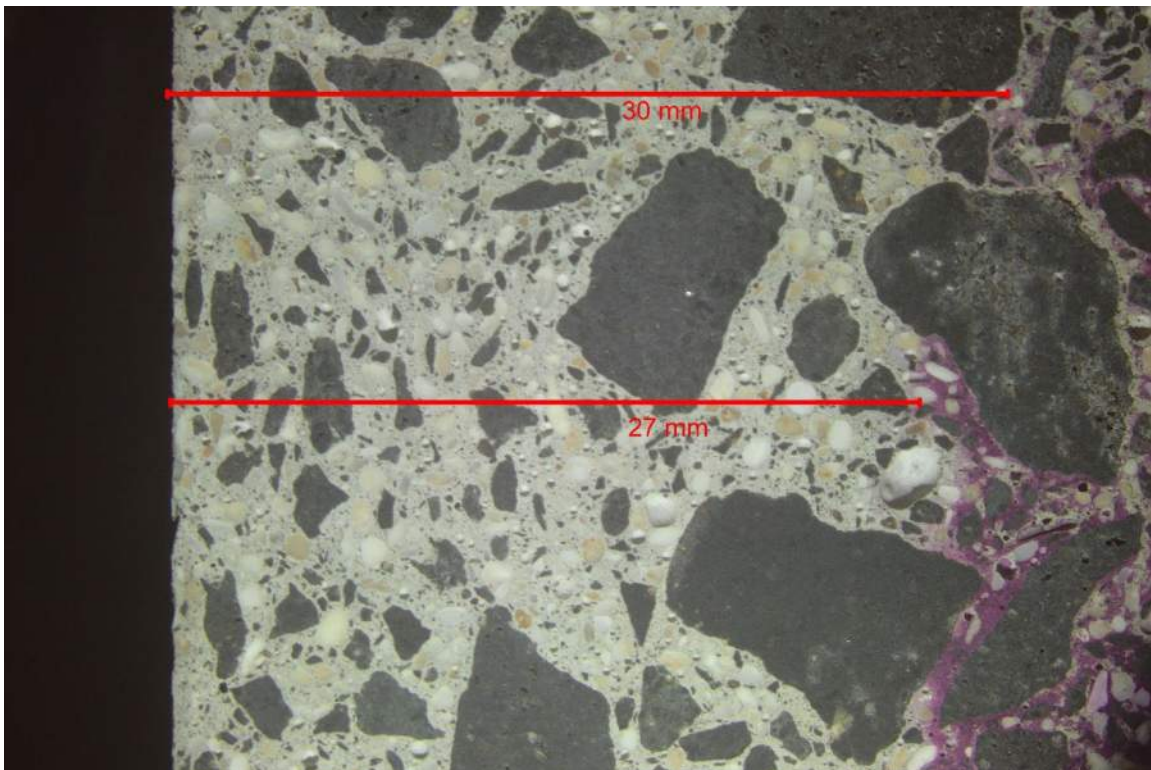


Sample ID:
Mag:

Core 7
3.5x

Description: Carbonation (unstained paste, pH <8.5) ranged from 9 mm (3/8") up to 17 mm (11/16") from the outer surface, as viewed on saw cut and lapped cross section at low magnification.

Photo: 48

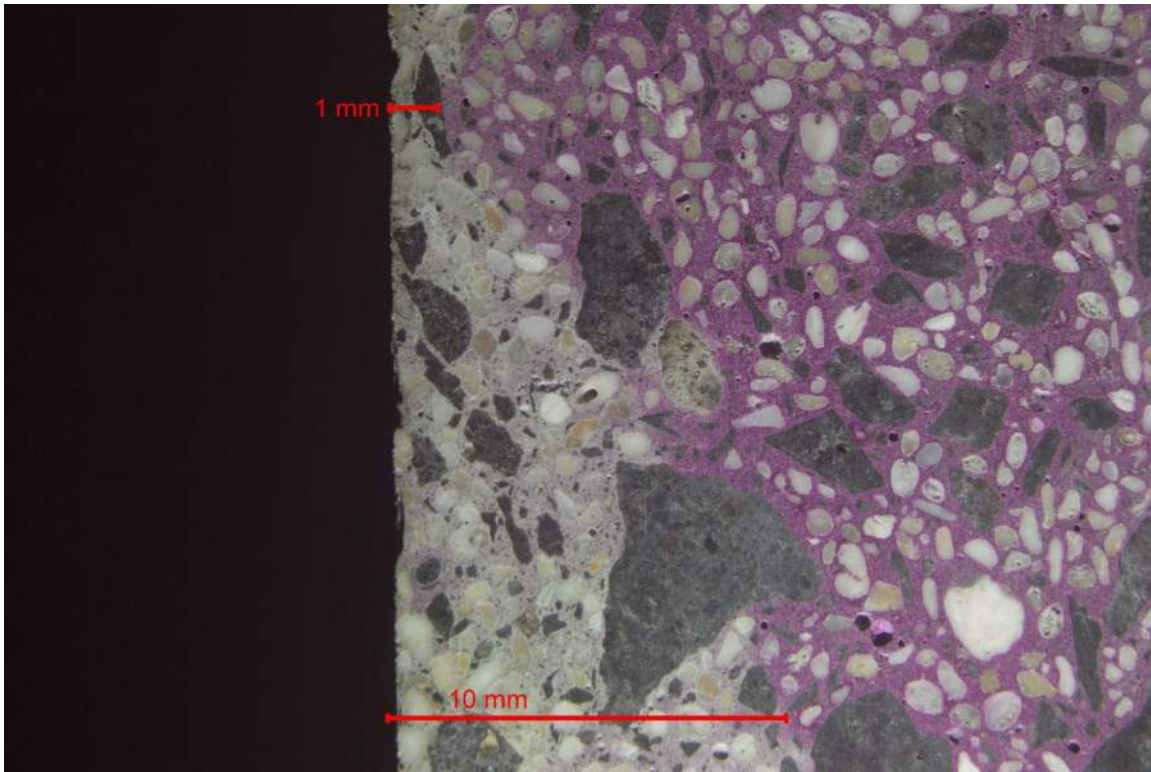


Sample ID:
Mag:

Core 9
3.5x

Description: Carbonation (unstained paste, pH <8.5) ranged from 27 mm (1-1/16") up to 30 mm (1-3/16") from the outer surface, as viewed on saw cut and lapped cross section at low magnification.

Photo: 49

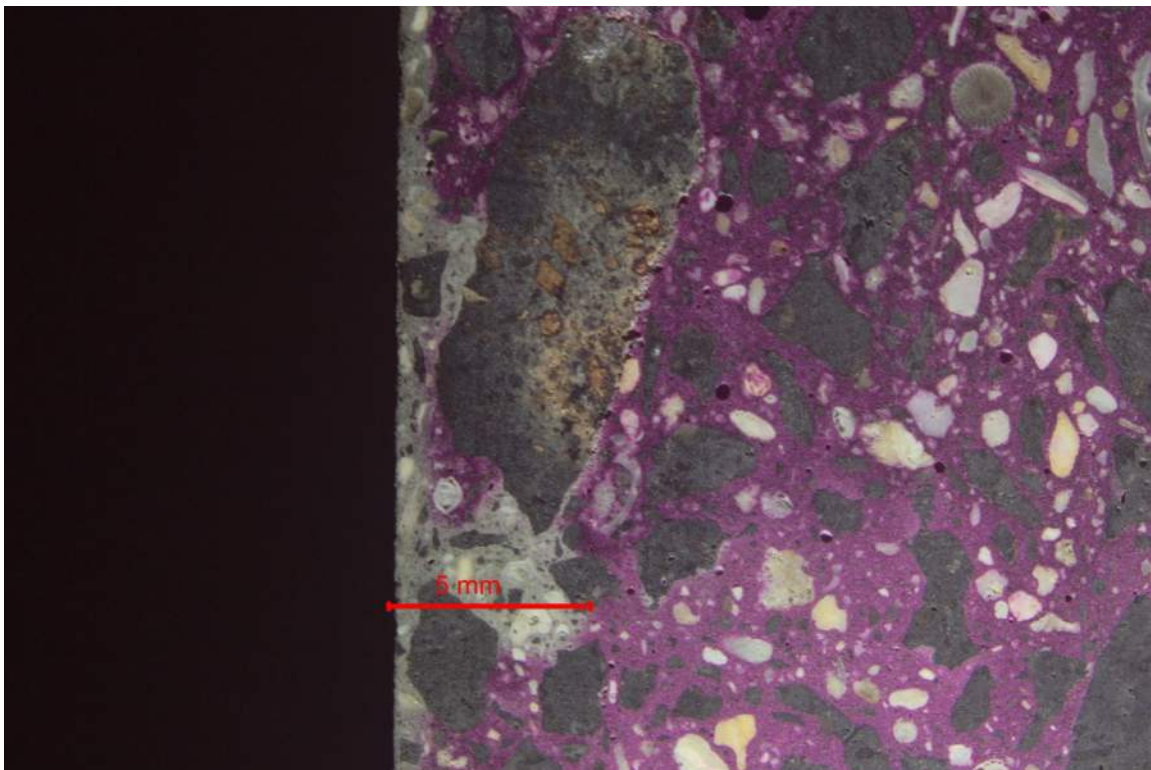


Sample ID:
Mag:

Core 10
5x

Description: Carbonation (unstained paste, pH <8.5) ranged from 1 mm (1/32") up to 10 mm (3/8") from the outer surface, as viewed on saw cut and lapped cross section at low magnification.

Photo: 50

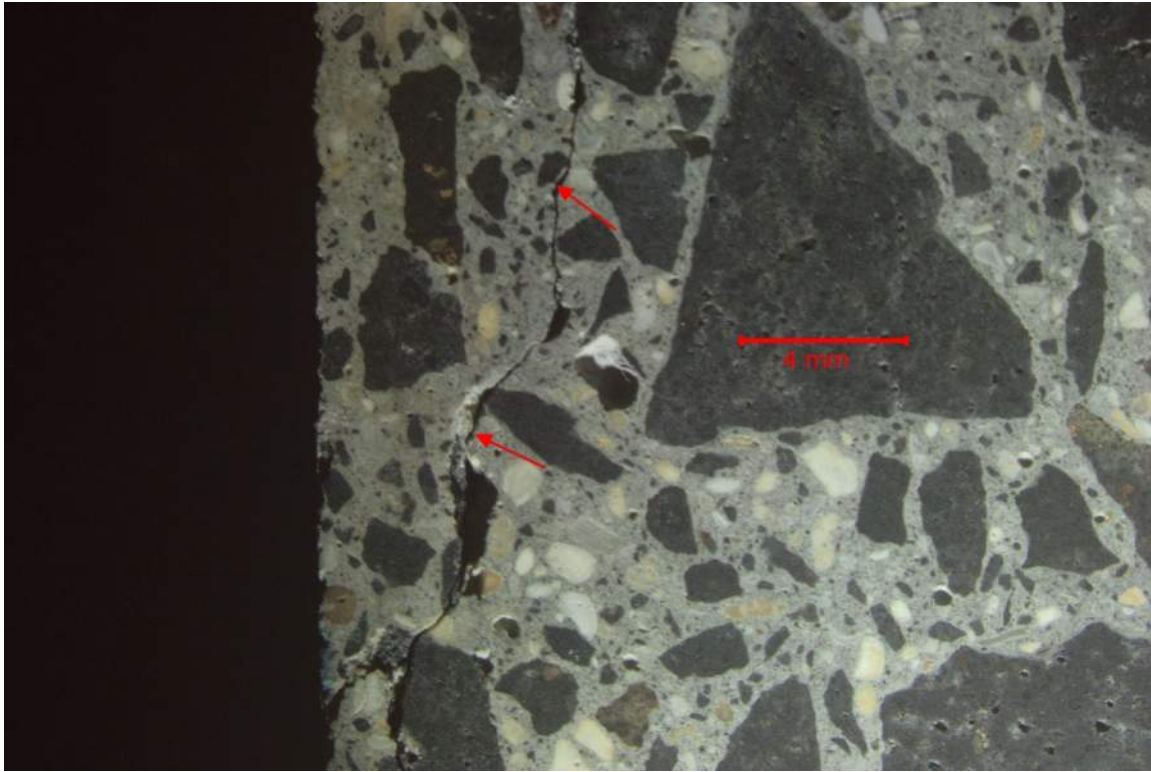


Sample ID:
Mag:

Core 12
5x

Description: Carbonation (unstained paste, pH <8.5) ranged from negligible up to 5 mm (3/16") from the outer surface, as viewed on saw cut and lapped cross section at low magnification.

Photo: 51

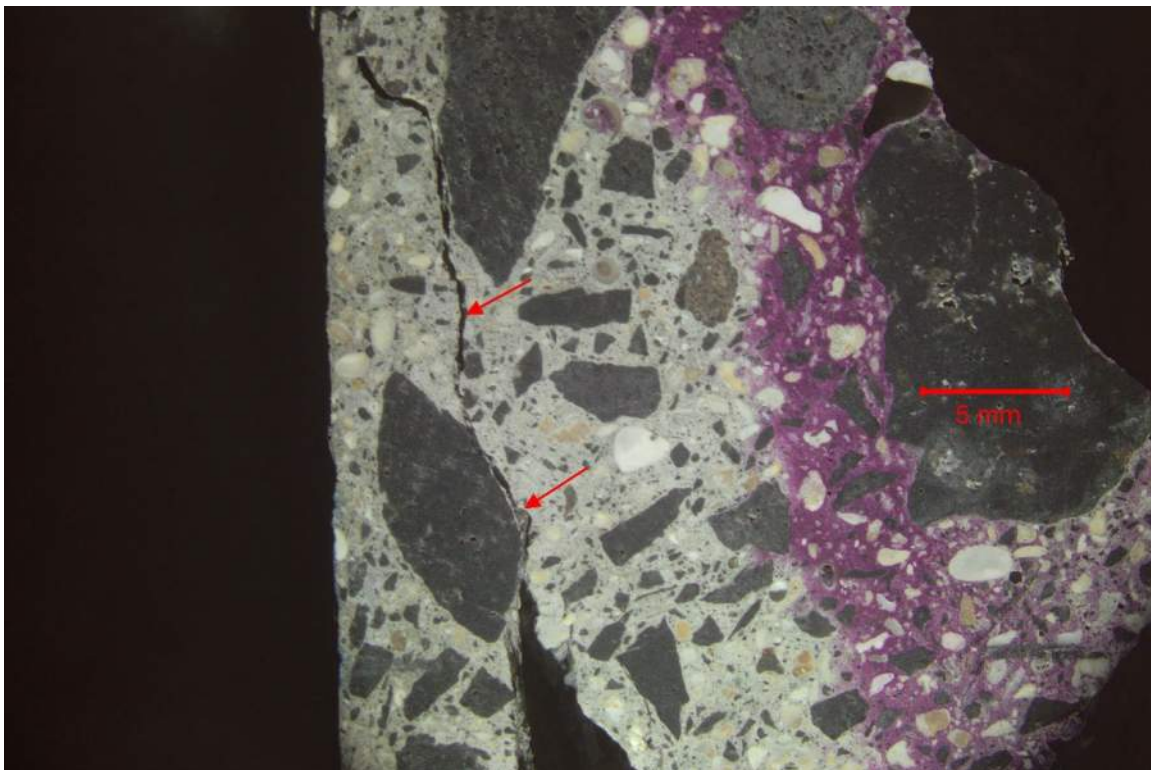


Sample ID:
Mag:

Core 4
5x

Description: Spalling of the outer surface of the core sample, after the two sections of the sample were reattached, viewed on saw cut and lapped cross section at low magnification.

Photo: 52

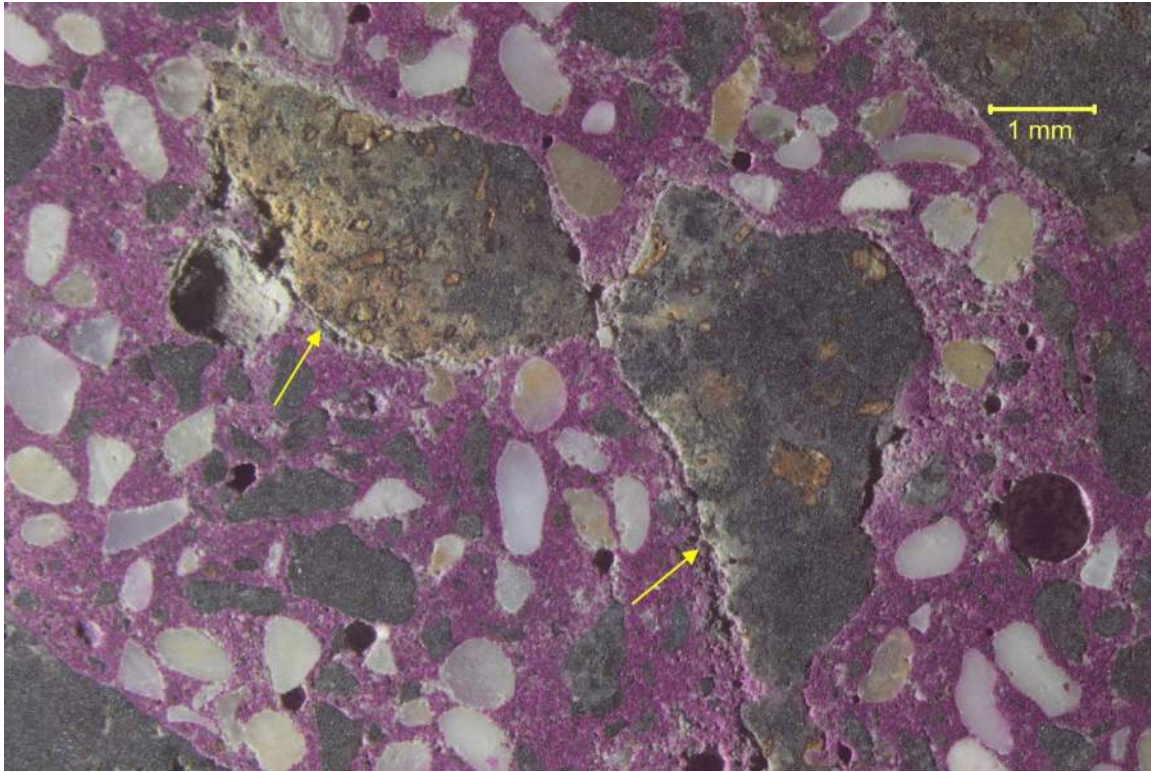


Sample ID:
Mag:

Core 6
5x

Description: Spalling of the outer surface of the core sample, after the two sections of the sample were reattached, viewed on saw cut and lapped cross section at low magnification.

Photo: 53

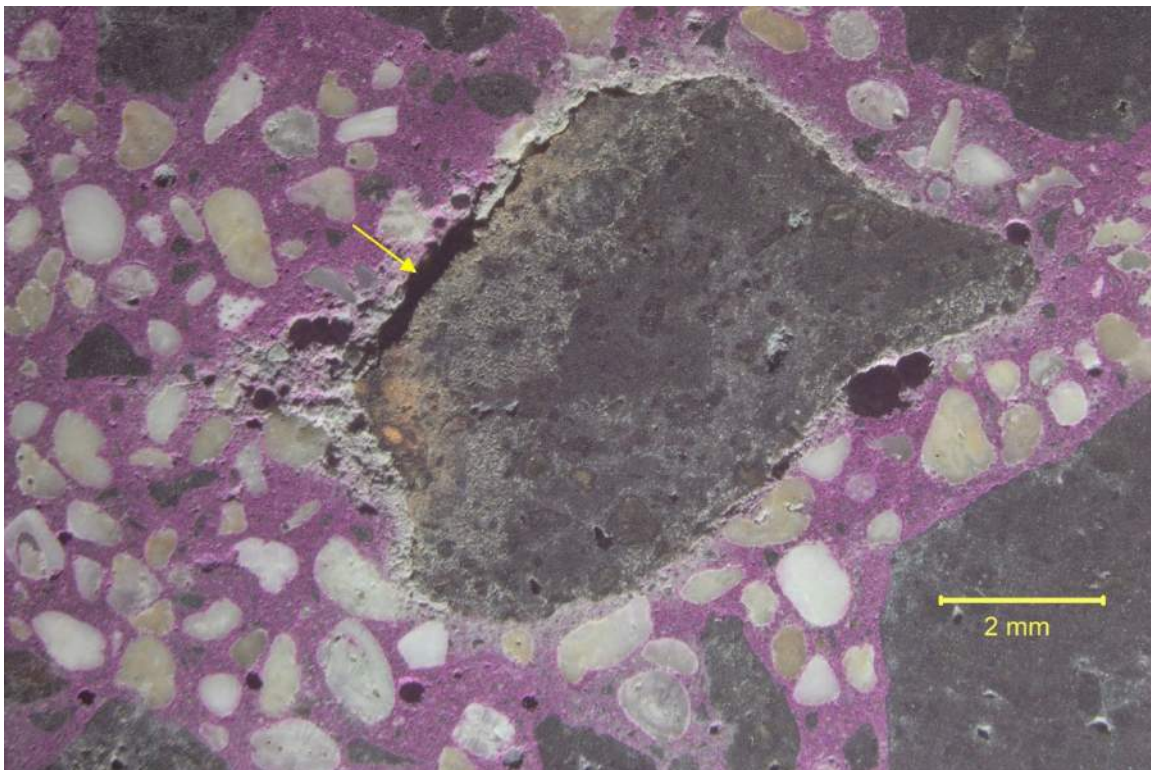


Sample ID:
Mag:

Core 3
12.5x

Description: Weathered basalt coarse aggregate particles surrounded by soft paste which eroded during sample preparation, viewed on saw cut and lapped cross section at magnification.

Photo: 54

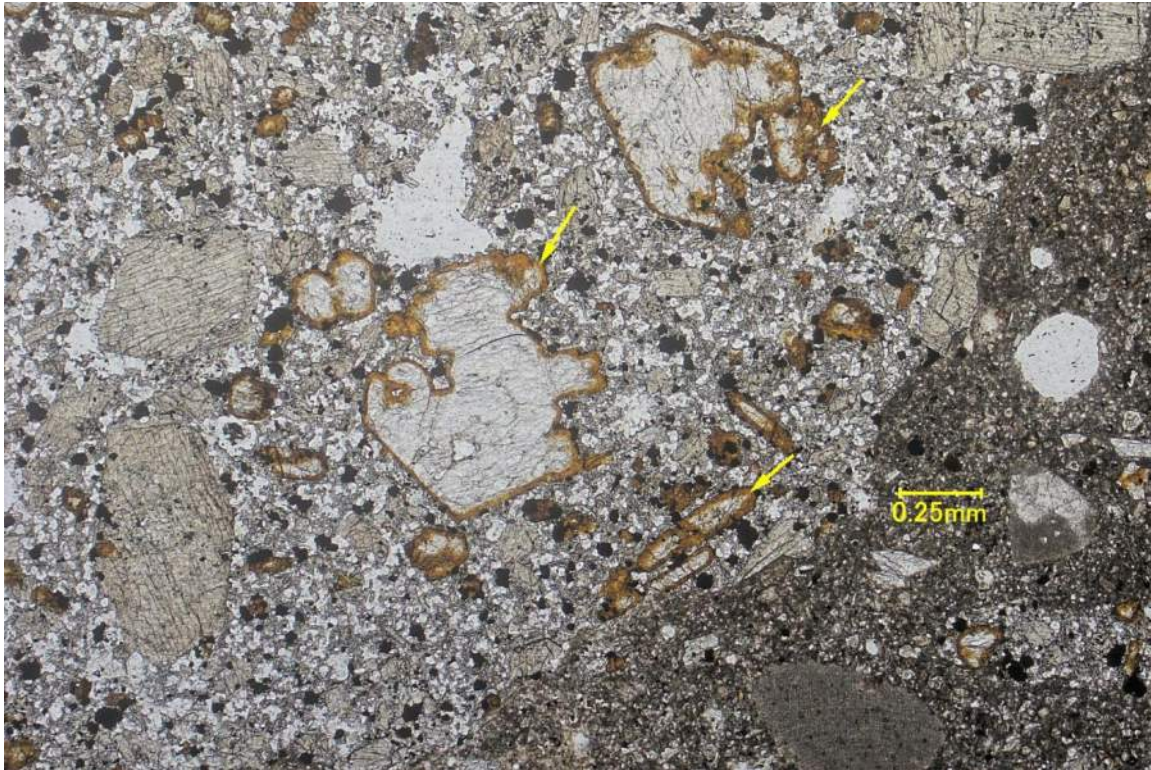


Sample ID:
Mag:

Core 10
10x

Description: A weathered basalt coarse aggregate particle particles surrounded by soft paste which eroded during sample preparation, viewed on saw cut and lapped cross section at magnification.

Photo: 55

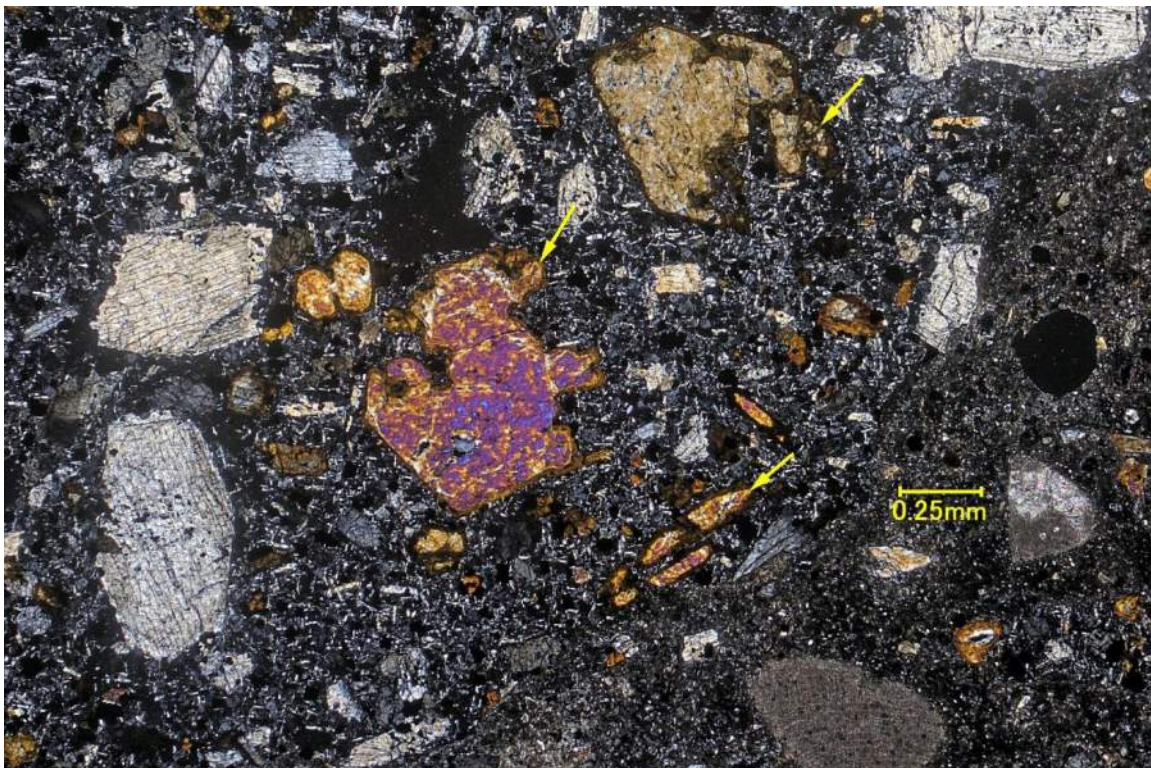


Sample ID:
Mag:

Core 1
40x

Description: Olivine phenocrysts within a basaltic coarse aggregate particle altering to iddingsite, viewed in thin section of concrete paste with transmitted plane polarized light.

Photo: 56

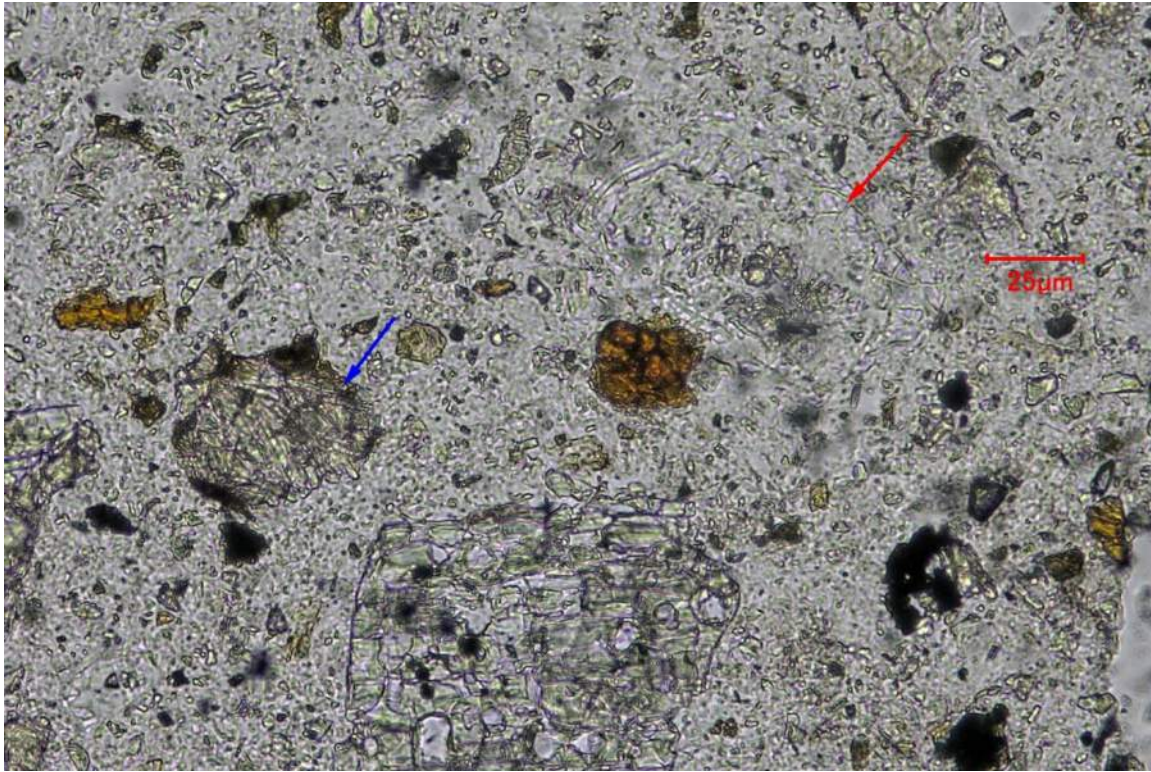


Sample ID:
Mag:

Core 1
40x

Description: Same view as above, as seen in thin section of concrete paste with transmitted plane polarized light.

Photo: 57

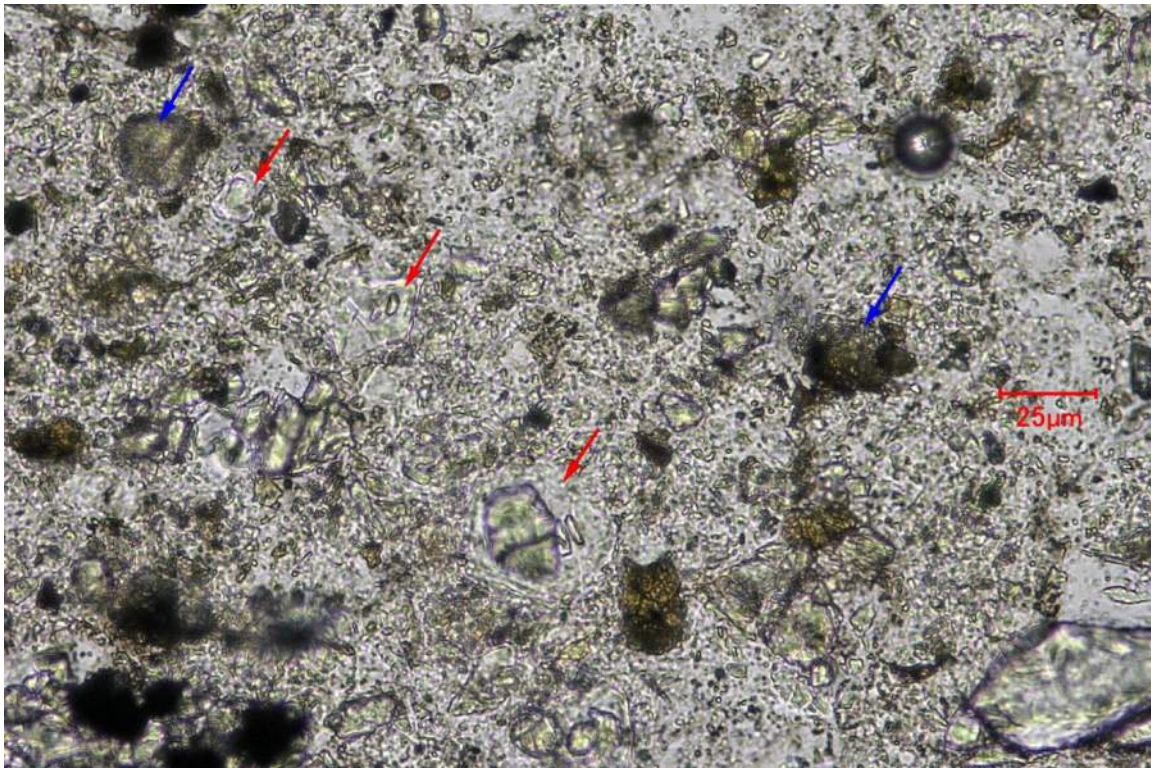


Sample ID:
Mag:

Core 1
400x

Description: Fully hydrated relict alite (red arrow) and unhydrated residual belite (blue arrow) portland cement particles, as viewed in thin section of concrete paste with transmitted plane polarized light.

Photo: 58

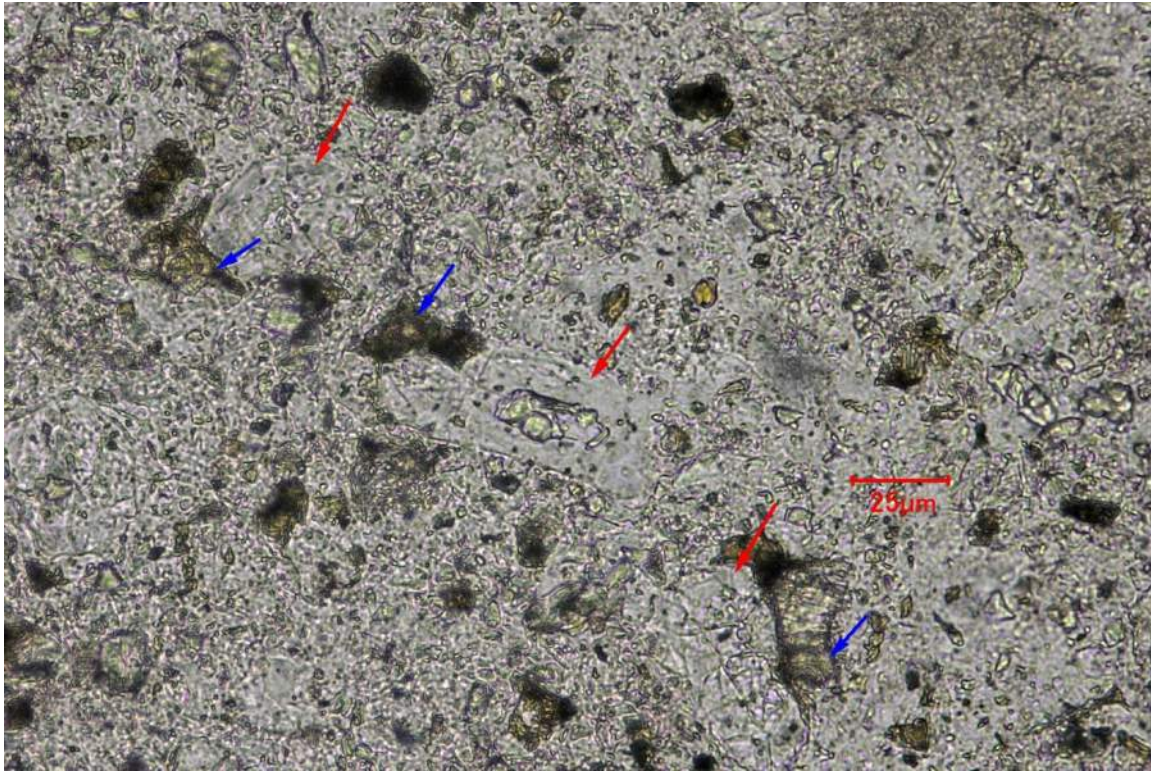


Sample ID:
Mag:

Core 3
400x

Description: Partially to fully hydrated relict alite (red arrows) and unhydrated residual belite (blue arrows) portland cement particles, as viewed in thin section of concrete paste with transmitted plane polarized light.

Photo: 59

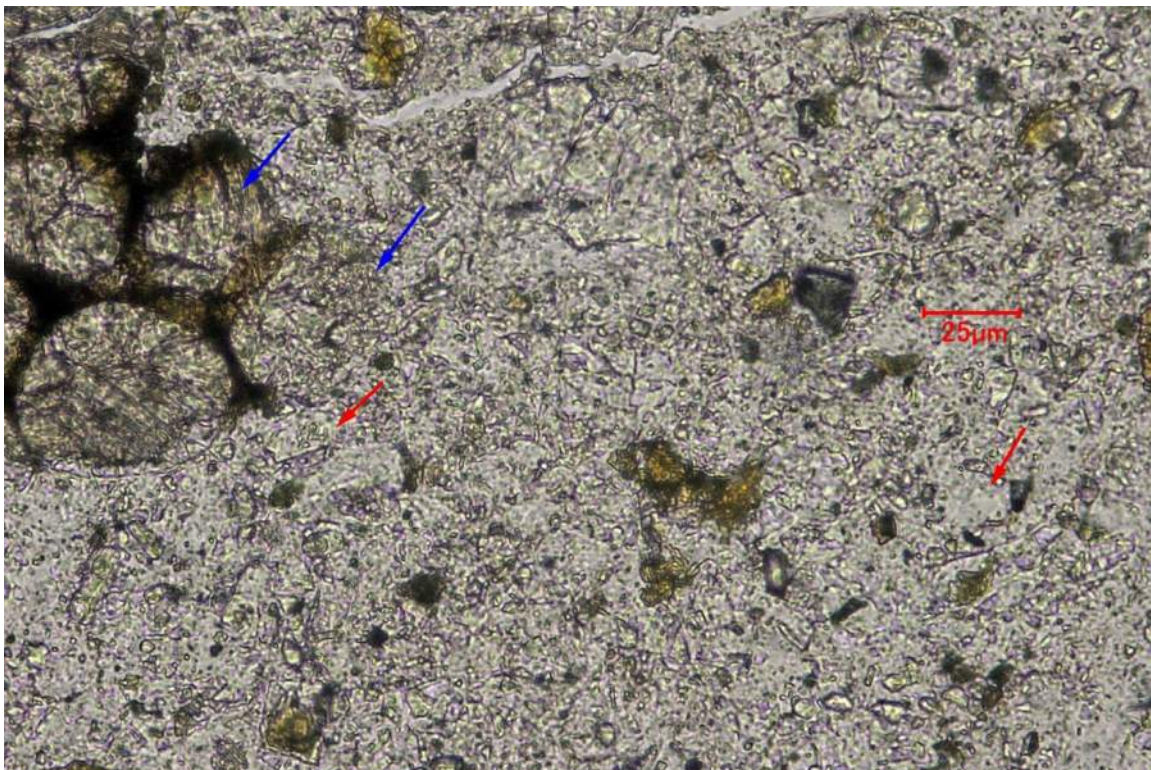


Sample ID:
Mag:

Core 4
400x

Description: Fully hydrated relict alite (red arrows) and unhydrated residual belite (blue arrows) portland cement particles, as viewed in thin section of concrete paste with transmitted plane polarized light.

Photo: 60

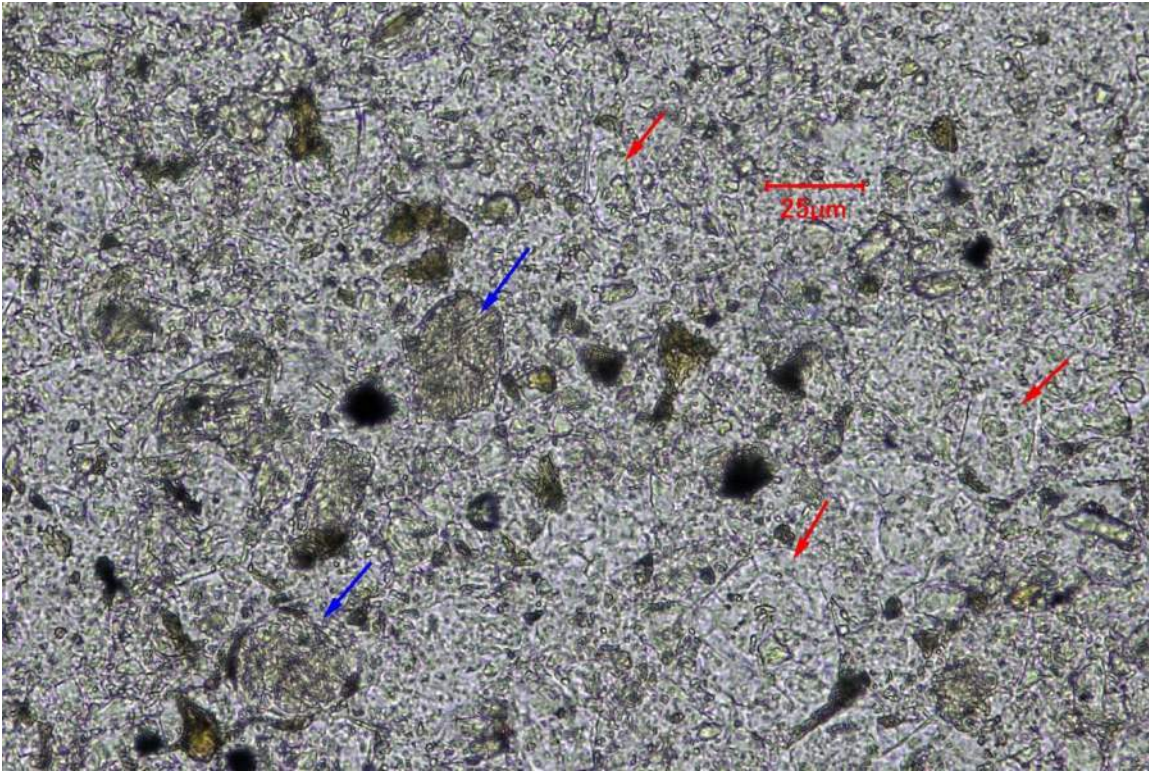


Sample ID:
Mag:

Core 6
400x

Description: Fully hydrated relict alite (red arrows) and unhydrated residual belite (blue arrows) portland cement particles, as viewed in thin section of concrete paste with transmitted plane polarized light.

Photo: 61

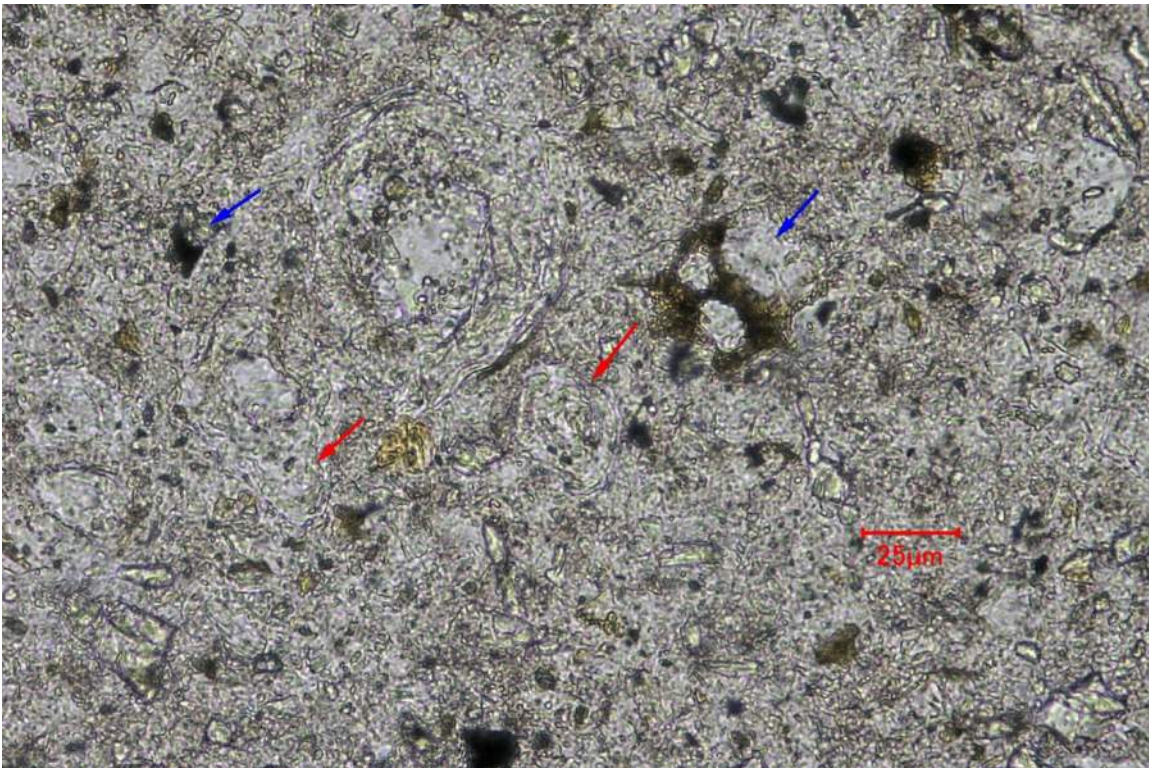


Sample ID:
Mag:

Core 7
400x

Description: Fully hydrated relict alite (red arrows) and unhydrated residual belite (blue arrows) portland cement particles, as viewed in thin section of concrete paste with transmitted plane polarized light.

Photo: 62

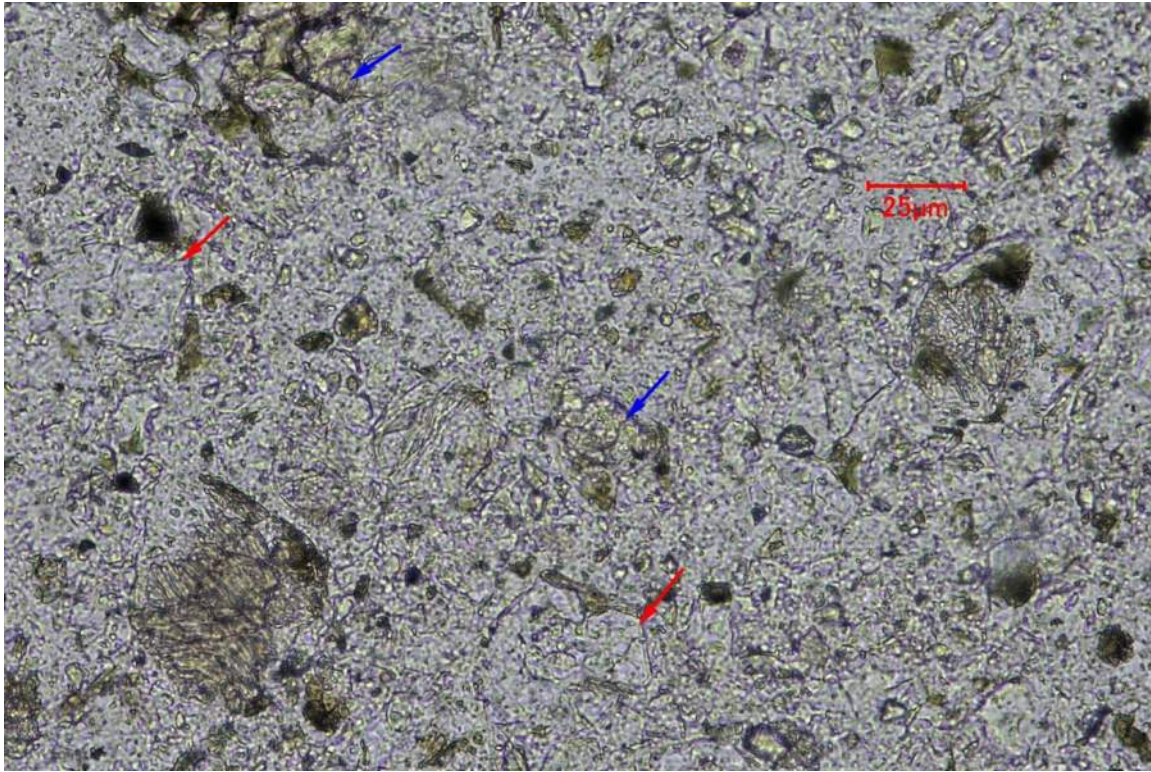


Sample ID:
Mag:

Core 9
400x

Description: Fully hydrated relict alite (red arrows) and unhydrated to partially hydrated residual belite (blue arrows) portland cement particles, as viewed in thin section of concrete paste with transmitted plane polarized light.

Photo: 63

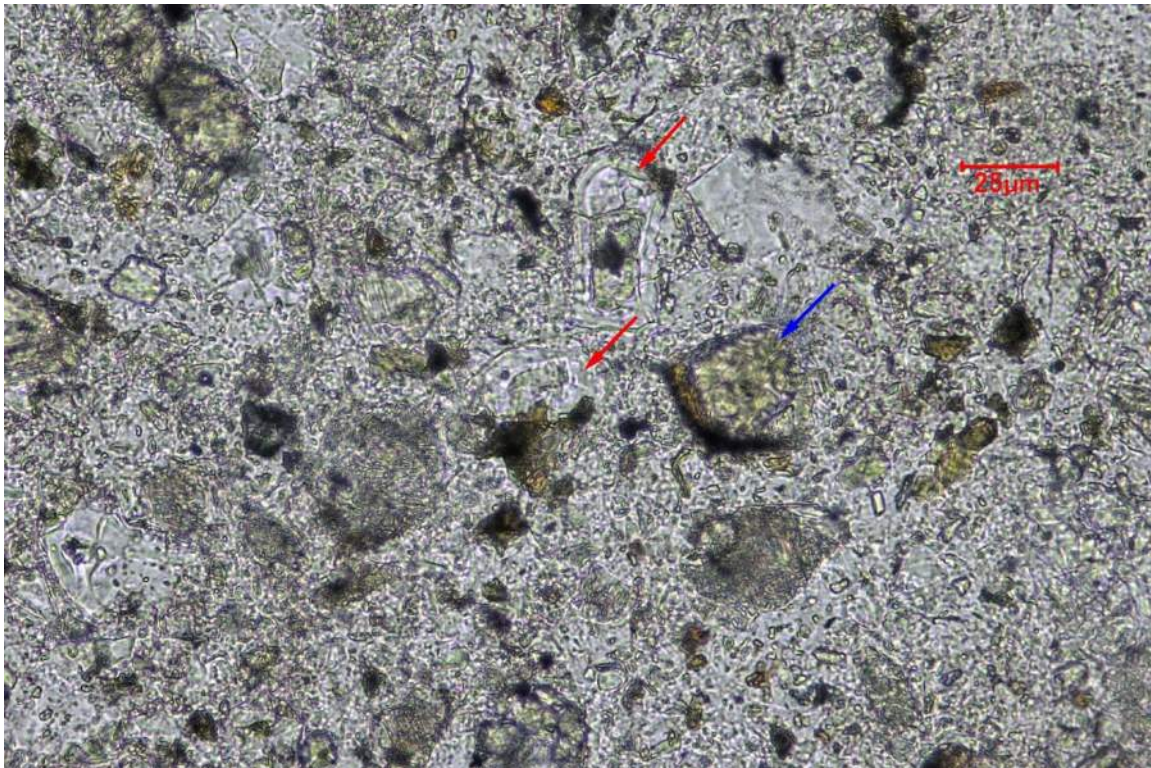


Sample ID:
Mag:

Core 10
400x

Description: Fully hydrated relict alite (red arrows) and unhydrated residual belite (blue arrows) portland cement particles, as viewed in thin section of concrete paste with transmitted plane polarized light.

Photo: 64

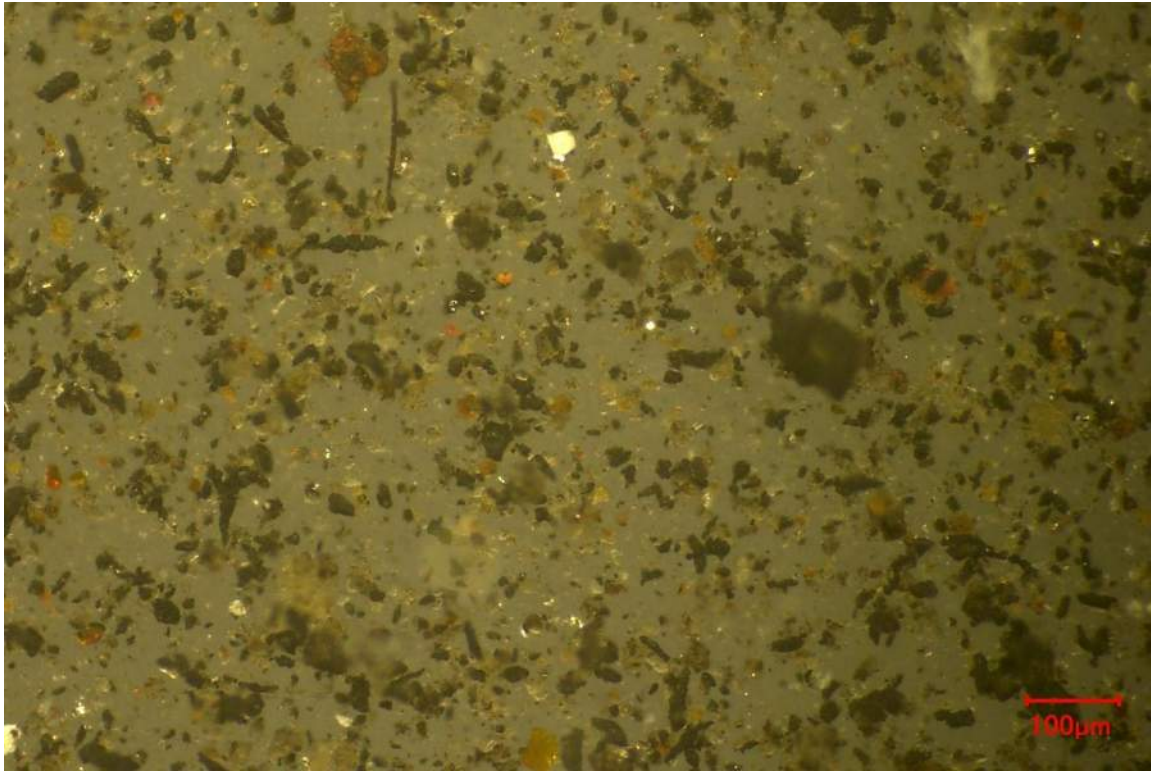


Sample ID:
Mag:

Core 12
400x

Description: Fully hydrated relict alite (red arrows) and unhydrated to partially hydrated residual belite (blue arrow) portland cement particle, as viewed in thin section of concrete paste with transmitted plane polarized light.

Photo: 65

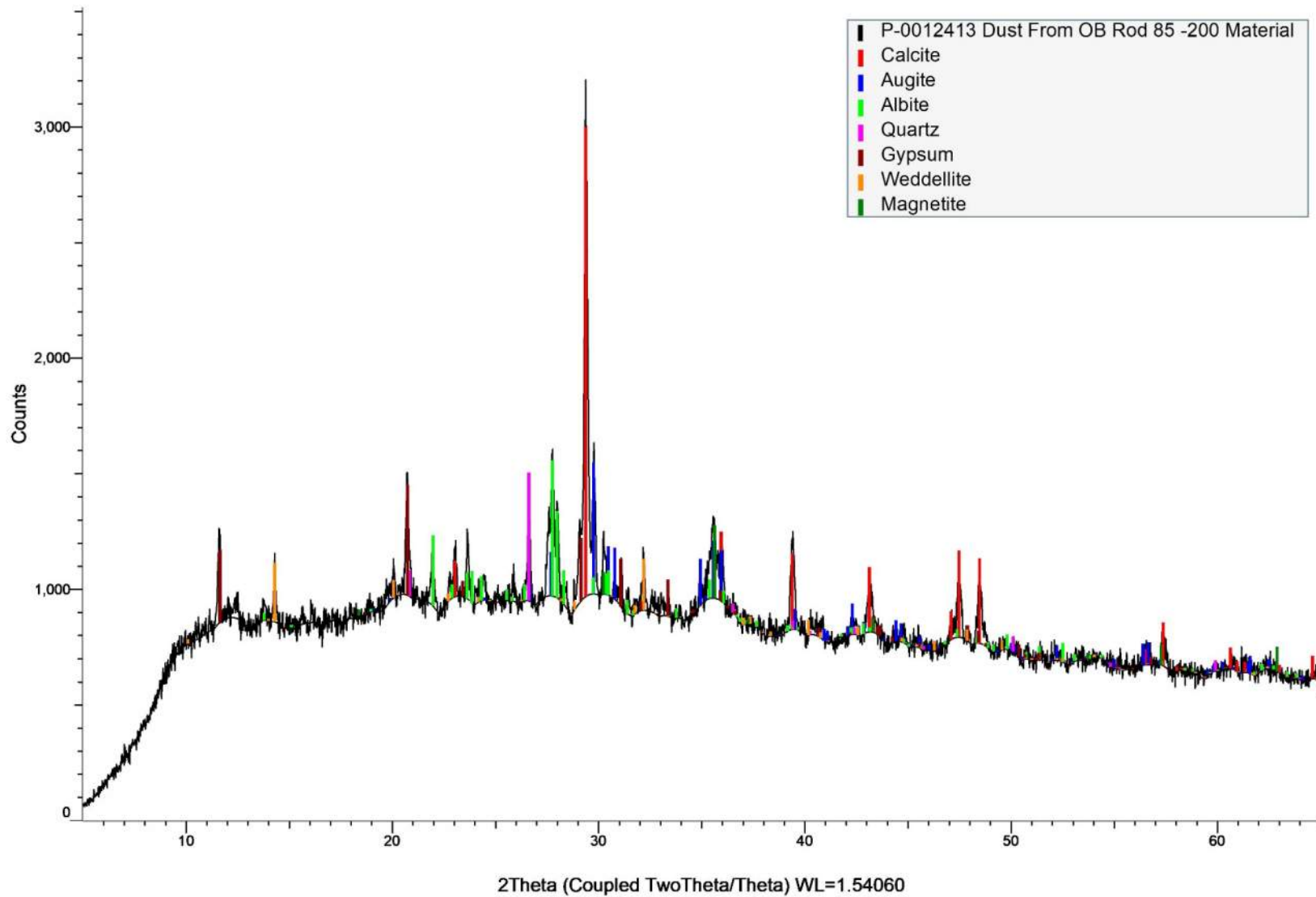


Sample ID:
Mag:

Dust
100x

Description: Powder mount of the bulk sample observed with reflected light.

P-0012413 Dust From OB Rod 85 -200 Material Powder X-Ray Diffraction



Sample ID: Dust from OB Rod 85
Photo: 66

Description: X-ray diffraction pattern of -200 material from the dust sample.

Photo: 67



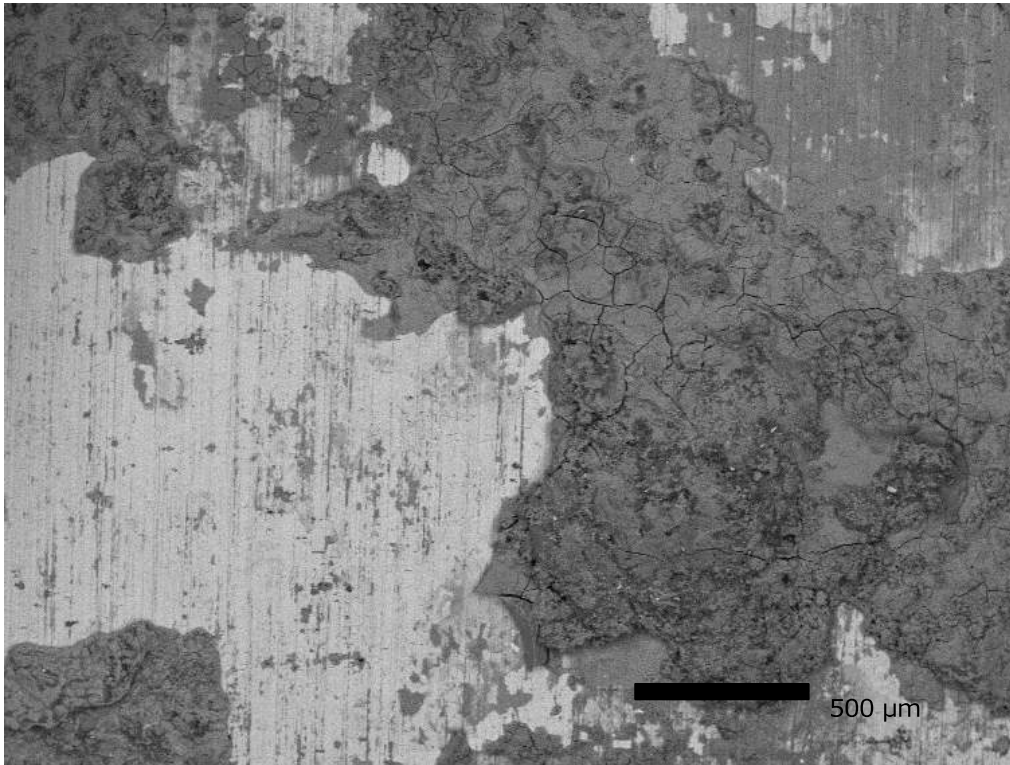
Sample ID: SS Rod **Description:** Steel rod as received. Cut end to the left and fractured to the right.

Photo: 68



Sample ID: SS Rod **Description:** Fractured end and SEM billet removed from bar (image left). UV illumination indicates presence of an epoxy type material.

Photo: 69

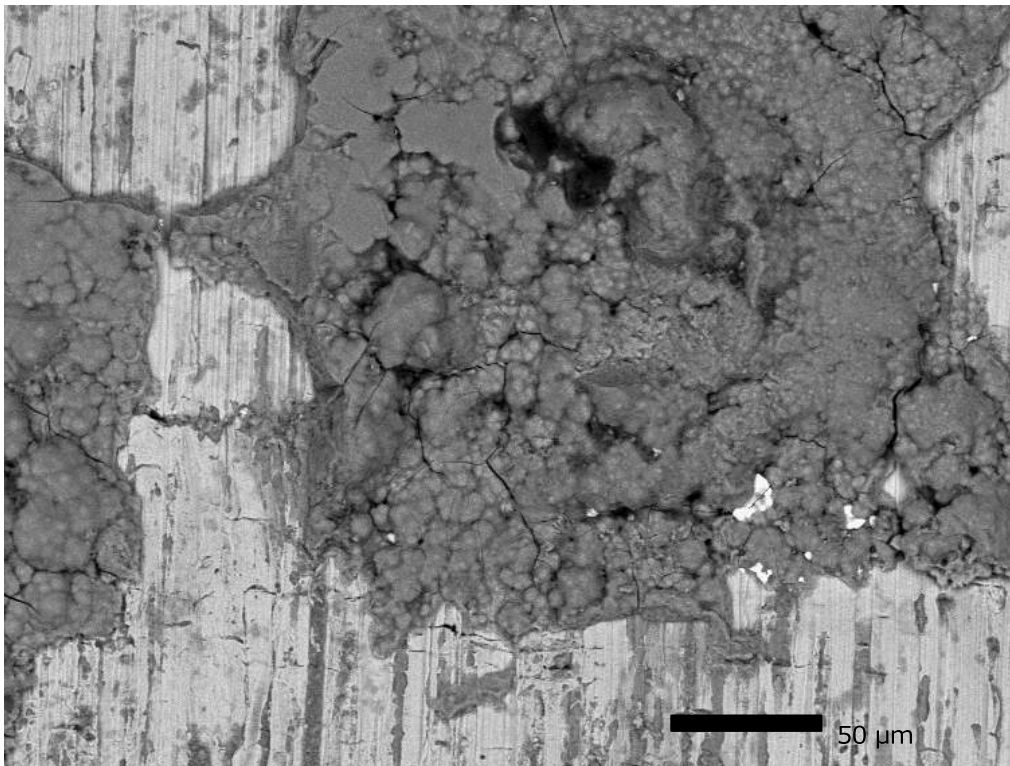


Sample ID:
Mag:

SS Rod
50x

Description: Low magnification view of corrosion product on the surface of the 304 SS steel substrate.

Photo: 70

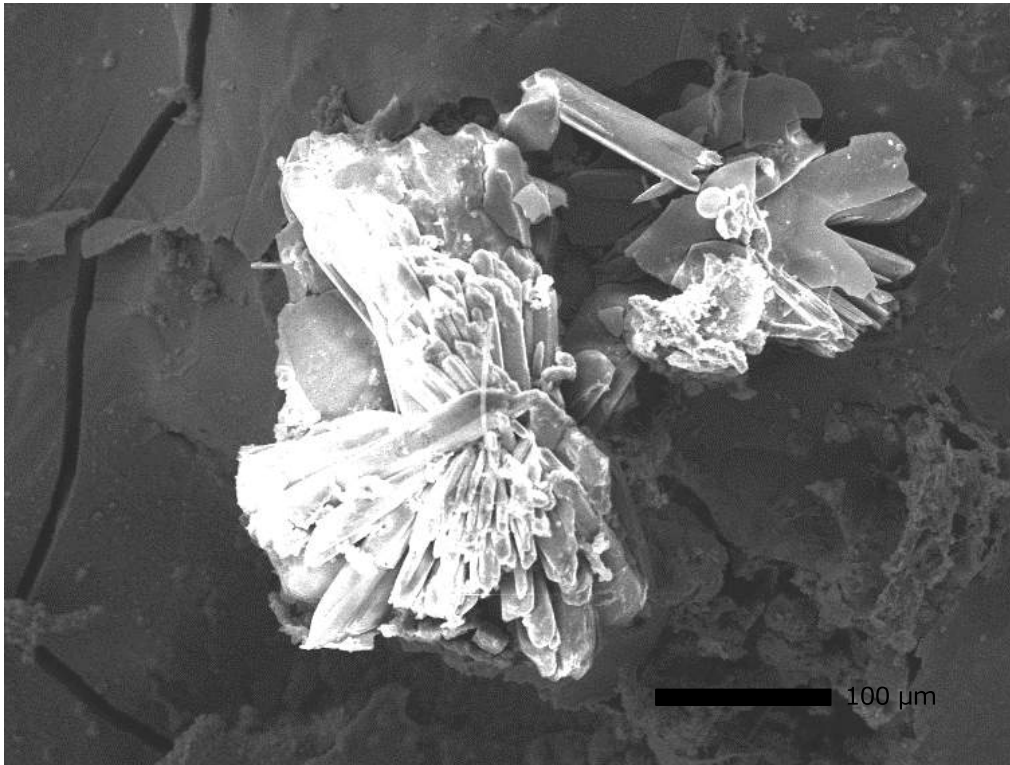


Sample ID:
Mag:

SS Rod
330x

Description: Chemical analysis of this region in following photo section (71). Botryoidal texture can be seen under slightly higher magnification.

Photo: 71

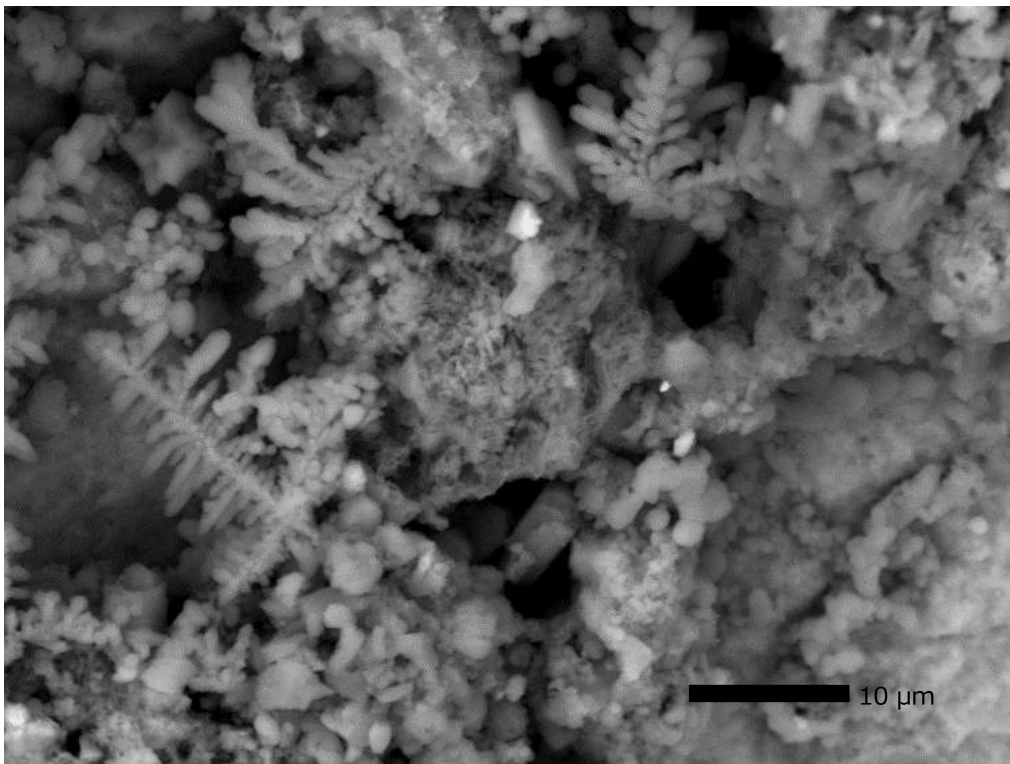


Sample ID:
Mag:

SS Rod
220x

Description: Crystal cluster on fractured bar surface. Chemical constituents reflect the 304 SS substrate with the addition of chlorine.

Photo: 72

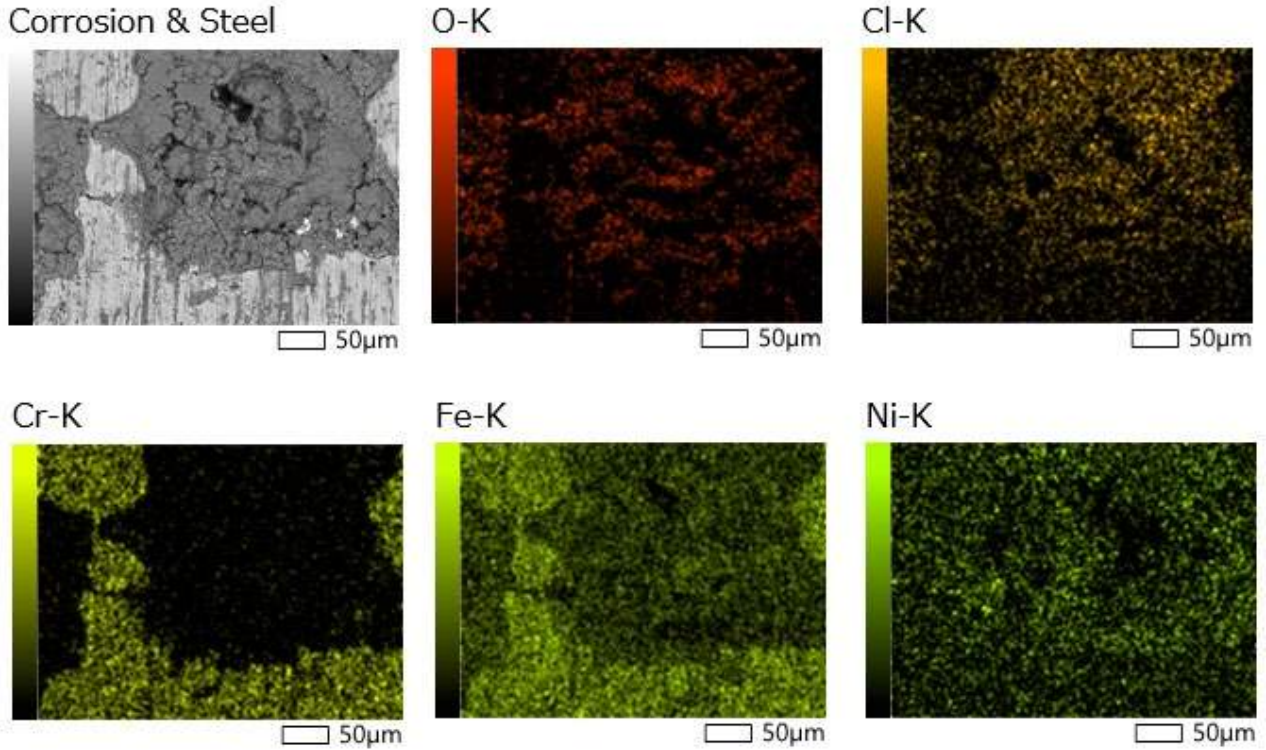


Sample ID:
Mag:

SS Rod
2000x

Description: Very fine crystalline component (tree-like structures) to the corrosion product. Crystals are primarily comprised of chlorine, sodium, potassium.

Photo: 73

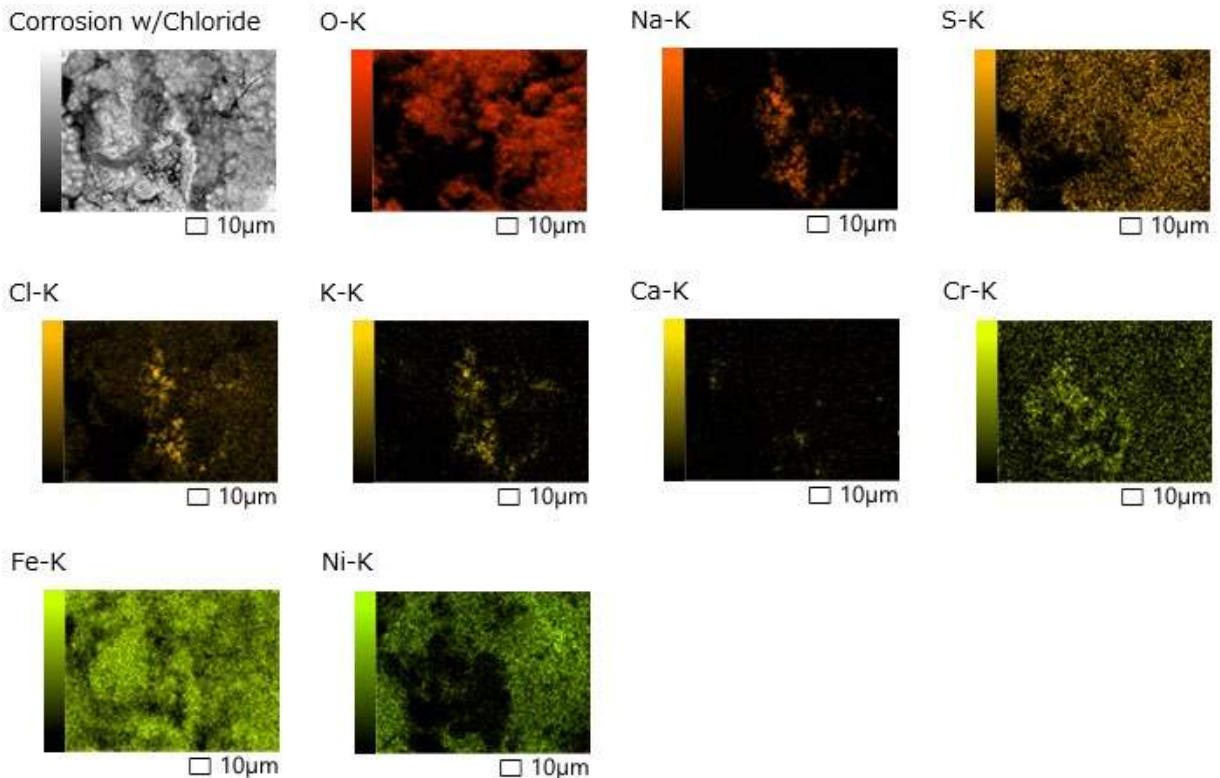


Sample ID:
Mag:

SS Rod
 See Scale

Description: EDS Chemical mapping and Backscatter Detector images. Upper left BED image shows 304 SS substrate (light grey), and corrosion product consisting of oxidized substrate and chloride (dark grey). Individual analytes represented in remaining images.

Photo: 74



Sample ID:
Mag:

SS Rod
 See Scale

Description: Similar to above image set, but entire field of view is of corrosion product. Crystals similar to those in photo 72 occupy the areas highlighted with Cl.

Appendix C

2016 TFHRC Laboratory Test Results



**WILSON TUNNEL
CEILING SUPPORT ROD INSPECTION
APRIL 2022**

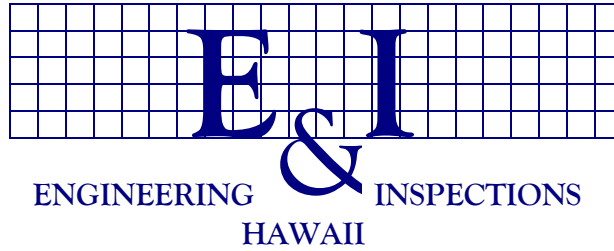


**CONSOR Engineers
737 Bishop Street Suite 2350
Honolulu, HI 96813**



**91-515 Nukuawa St.
Kapolei, HI. 96707**

**“Providing Excellence in NDE and Quality
Inspection Services to Industries Worldwide”**



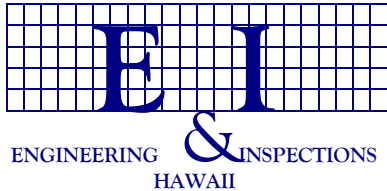
Inspection Dates: March 21st through April 1st, 2022



Inspection of stainless steel hanger rods in Hawaii's Wilson Tunnel

Introduction

Engineering & Inspections Hawaii (E&I Hawaii) was contracted to perform a visual evaluation of the stainless steel hanger rods in Hawaii's Wilson Tunnel. This inspection included visually inspecting the rods for external conditions indicating stress corrosion cracking (SCC) such as pitting, cracking, and complete fractures, as well as random penetrant testing (PT) for confirmation. Specific emphasis was made at each of the rod to concrete floor panel interfaces where fracture is likely to occur. Sections of the rods were mechanically cleaned using wire wheels until it could be determined if corrosion or cracking was visibly present. Photos were taken of each rod showing its condition at time of inspection.



04/14/22
Page 2 of 33

Summary of Findings

The overall condition of the support rods was poor with visible signs of corrosion and cracking present. Some rods were completely fractured radially at the bottom interface while others exhibited axial cracks between areas of pitting. This report addresses the areas by reference to their respective rod number.

Rod conditions were defined into three categories of severity.

- 1 – Least severe; visible signs of early stages of mild corrosion and / or pitting is present
- 2 – Moderate; visible signs of moderate corrosion and / or pitting is present, but no visible signs of cracking detected
- 3 – Severe; visible signs of cracking detected (complete fractures noted when present)

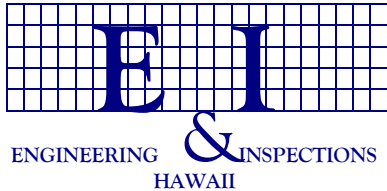
The attached spreadsheet identifies each of the pipe supports and the following conditions:

- Rod number
- Cracks present? Y/N
- Corrosion rating; Numerical severity of rod condition 1 – representing the least severe (mild corrosion) and 3 – representing the most severe (cracking)
- Dye penetrant performed? Y/N
- Pictures taken? Y/N
- Additional comments or notes during the inspection (complete fractures noted here)

Recommendations

The repair recommendation criteria are as follows:

- Rods receiving a corrosion rating 1; Monitor periodically for visible signs of cracking.
- Rods receiving a corrosion rating 2; Monitor periodically for visible signs of cracking, consider replacing.
- Rods receiving a corrosion rating of 3; Replace existing rod.



04/14/22
Page 3 of 33

Summary

Note: During mechanical wire wheel cleaning, small pieces of rod material were breaking off in heavily pitted areas indicating structural fragility.

In-bound (Kaneohe side)

- 228 of 228 rod locations were inspected.
- 21 rods were radially fractured at or near the bottom concrete interface (level 3).
- 195 non-fractured rods show signs of severe pitting and visible cracking (level 3).
- 0 rods show signs of moderate corrosion (level 2).
- New rods show signs of mild corrosion (level 1).

In-bound (Town side)

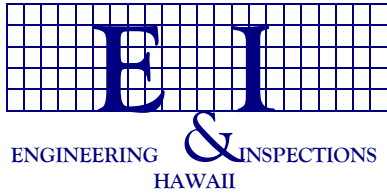
- 112 of 112 rod locations were inspected.
- 1 rod was radially fractured at or near the bottom concrete interface (level 3).
- 108 non-fractured rods show signs of severe pitting and visible cracking (level 3).
- 0 rods show signs of moderate corrosion (level 2).
- New rods show signs of mild corrosion (level 1).

Out-bound (Town side)

- 124 of 124 rod locations were inspected.
- 0 rods were radially fractured at or near the bottom concrete interface (level 3).
- 12 rods show signs of severe pitting and visible cracking (level 3).
- 13 rods show signs of moderate corrosion (level 2).
- All other rods show signs of mild corrosion (level 1).

Out-bound (Kaneohe side)

- 250 of 250 rod locations were inspected.
- 0 rods were radially fractured at or near the bottom concrete interface (level 3).
- 210 rods show signs of severe pitting and visible cracking (level 3).
- 31 rods show signs of moderate corrosion (level 2).
- All other rods show signs of mild corrosion (level 1).



04/14/22
Page 4 of 33

If you have any questions or concerns regarding this proposal, please feel free to contact me at (808) 630-8636.

Respectfully,

Jacob Blaylock
ACCP UT Level III
API-QUTE
PAUT PCN Level 2D
AWS CWI
API-570

Karrie Snyder
AWS CWI
NDE Level II

Randy Hill
VT Level II
NDE Level II

Engineering & Inspections Hawaii, Inc.

“Providing Excellence in NDE and Inspection Services to Industries Worldwide”

04/14/22
Page 5 of 33

The following is a small sample of photographs showing typical rod conditions by severity level.

(Note: a complete photo log of all 714 rods inspected will also be provided via USB drive)



Severity level 3, interface fracture

04/14/22
Page 6 of 33



Severity level 3, interface fracture and severe corrosion

04/14/22
Page 7 of 33



Severity level 3, visible cracking, and severe pitting

04/14/22
Page 8 of 33



Severity level 3, visible cracking, and severe pitting

04/14/22
Page 9 of 33



Severity level 3, visible cracking, and severe pitting

04/14/22
Page 10 of 33



Severity level 3, visible cracking, and severe pitting

04/14/22
Page 11 of 33



Severity level 3, visible cracking, and severe pitting

04/14/22
Page 12 of 33



Severity level 3, visible cracking, and severe pitting

04/14/22
Page 13 of 33



Severity level 2, moderate pitting

04/14/22
Page 14 of 33



Severity level 1, mild pitting (new rod)

WILSON TUNNEL CEILING SUPPORT RODS

Kaneohe Side (In-bound)

ROD #	CRACKS	CORROSION	DYE	PICTURES	COMMENTS
1	X	3	X	X	
2	X	3	X	X	
3	X	3	X	X	
4	X	3		X	
5	X	3		X	
6	X	3		X	
7	X	3		X	
8	X	3		X	
9	X	3		X	
10	X	3		X	
11	X	3		X	
12	X	3		X	
13	X	3		X	
14	X	3		X	
15	X	3		X	
16	X	3		X	
17	X	3		X	
18	X	3		X	
19	X	3		X	
20	X	3		X	
21	X	3		X	
22	X	3		X	
23	X	3		X	
24	X	3		X	
25	X	3		X	
26	X	3		X	
27	X	3		X	
28	X	3		X	
29	X	3		X	
30	X	3		X	
31		1		X	New supports; early signs of corrosion
32	X	3		X	
33	X	3		X	Fractured at interface
34		1		X	New supports; early signs of corrosion
35	X	3		X	
36	X	3		X	
37	X	3		X	
38	X	3		X	
39	X	3		X	
40		1		X	New supports; early signs of corrosion
41	X	3		X	
42	X	3		X	

* Corrosion Ratings: 1- Minor Corrosion 2- Moderate Corrosion 3- Severe Corrosion

WILSON TUNNEL CEILING SUPPORT RODS

Kaneohe Side (In-bound)

ROD #	CRACKS	CORROSION	DYE	PICTURES	COMMENTS
43	X	3		X	
44	X	3		X	
45	X	3		X	
46	X	3		X	
47	X	3		X	Fractured at interface
48	X	3		X	Fractured at interface
49		0		X	New supports; appears temporary
50	X	3		X	
51	X	3		X	
52	X	3		X	
53	X	3		X	
54	X	3		X	
55	X	3		X	
56	X	3		X	
57	X	3		X	Fractured at interface
58	X	3		X	Large areas of metal chunks eroded
59	X	3		X	Fractured at interface
60	X	3		X	
61	X	3		X	Fractured at interface
62	X	3		X	Fractured at interface
63	X	3		X	
64	X	3		X	
65	X	3		X	
66	X	3		X	
67	X	3		X	
68	X	3		X	
69	X	3		X	
70	X	3		X	
71	X	3		X	
72	X	3		X	
73	X	3		X	
74	X	3		X	
75	X	3		X	
76	X	3		X	
77	X	3		X	
78		1		X	New supports; early signs of corrosion
79	X	3		X	
80	X	3		X	
81		1		X	New supports; early signs of corrosion
82	X	3		X	
83	X	3		X	Fractured at interface
84	X	3		X	

* Corrosion Ratings: 1- Minor Corrosion 2- Moderate Corrosion 3- Severe Corrosion

WILSON TUNNEL CEILING SUPPORT RODS

Kaneohe Side (In-bound)

ROD #	CRACKS	CORROSION	DYE	PICTURES	COMMENTS
85	X	3		X	
86	X	3		X	
87	X	3		X	
88		1		X	New supports; early signs of corrosion
89	X	3		X	
90	X	3		X	
91	X	3		X	
92	X	3		X	
93	X	3		X	
94	X	3		X	
95		1		X	New supports; appears temporary
96	X	3		X	Fractured at interface
97	X	3		X	
98		1		X	New supports; appears temporary
99	X	3		X	
100	X	3		X	
101	X	3		X	
102	X	3		X	Fractured at interface
103	X	3		X	
104	X	3		X	
105	X	3		X	
106	X	3		X	Fractured at interface
107	X	3		X	
108		1		X	New supports; early signs of corrosion
109		1		X	New supports; early signs of corrosion
110		1		X	New supports; early signs of corrosion
111		1		X	New supports; early signs of corrosion
112		1		X	New supports; early signs of corrosion
113		1		X	New supports; early signs of corrosion
114		1		X	New supports; early signs of corrosion
115		1		X	New supports; early signs of corrosion
116		1		X	New supports; early signs of corrosion
117		1		X	New supports; early signs of corrosion
118		1		X	New supports; early signs of corrosion
119		1		X	New supports; early signs of corrosion
120		1		X	New supports; early signs of corrosion
121	X	3		X	
122	X	3		X	
123	X	3		X	Fractured at interface
124	X	3		X	Fractured at interface
125	X	3		X	Fractured at interface
126	X	3		X	Fractured at interface

* Corrosion Ratings: 1- Minor Corrosion 2- Moderate Corrosion 3- Severe Corrosion

WILSON TUNNEL CEILING SUPPORT RODS

Kaneohe Side (In-bound)

ROD #	CRACKS	CORROSION	DYE	PICTURES	COMMENTS
127		1		X	New supports; early signs of corrosion
128	X	3		X	
129	X	3		X	
130	X	3		X	
131	X	3		X	
132	X	3		X	
133	X	3		X	
134	X	3		X	Fractured at interface
135	X	3		X	
136		0		X	New supports; appear temporary
137	X	3		X	
138	X	3		X	Large areas of metal chunks eroded
139	X	3		X	Fractured at interface
140	X	3		X	
141	X	3		X	
142	X	3		X	
143	X	3		X	
144	X	3		X	
145		1		X	New supports; early signs of corrosion
146	X	3		X	
147	X	3		X	
148	X	3		X	
149	X	3		X	
150	X	3		X	
151	X	3		X	
152	X	3		X	
153	X	3		X	
154	X	3		X	
155	X	3		X	
156		1		X	New supports; early signs of corrosion
157		1		X	New supports; early signs of corrosion
158	X	3		X	
159	X	3		X	
160	X	3		X	Fractured at interface
161	X	3		X	
162	X	3		X	
163	X	3		X	
164	X	3		X	
165	X	3		X	
166	X	3		X	
167		1		X	New supports; early signs of corrosion
168	X	3		X	

* Corrosion Ratings: 1- Minor Corrosion 2- Moderate Corrosion 3- Severe Corrosion

WILSON TUNNEL CEILING SUPPORT RODS

Kaneohe Side (In-bound)

ROD #	CRACKS	CORROSION	DYE	PICTURES	COMMENTS
169	X	3		X	
170	X	3		X	
171	X	3		X	
172	X	3		X	
173	X	3		X	
174	X	3		X	
175	X	3		X	
176	X	3		X	
177	X	3		X	Fractured at interface
178	X	3		X	
179	X	3		X	
180		1		X	New supports; early signs of corrosion
181	X	3		X	
182	X	3		X	
183	X	3		X	
184	X	3		X	
185	X	3		X	
186	X	3		X	
187	X	3		X	
188	X	3		X	
189		0		X	New supports; appears temporary
190	X	3		X	
191	X	3		X	
192	X	3		X	
193	X	3		X	Fractured at interface
194	X	3		X	
195	X	3		X	
196	X	3		X	
197	X	3		X	
198	X	3		X	
199	X	3		X	
200	X	3		X	
201	X	3		X	
202	X	3		X	
203	X	3		X	
204	X	3		X	
205		0		X	New supports; appears temporary
206	X	3		X	
207	X	3		X	
208	X	3		X	
209	X	3		X	Fractured at interface
210	X	3		X	

* Corrosion Ratings: 1- Minor Corrosion 2- Moderate Corrosion 3- Severe Corrosion

WILSON TUNNEL CEILING SUPPORT RODS

Honolulu Side (In-bound)

ROD #	CRACKS	CORROSION	DYE	PICTURES	COMMENTS
1	X	3		X	
2	X	3		X	
3	X	3		X	
4	X	3		X	
5	X	3		X	
6	X	3		X	
7	X	3		X	
8	X	3		X	
9	X	3		X	
10	X	3		X	
11	X	3		X	
12	X	3		X	
13	X	3		X	
14	X	3		X	
15	X	3		X	
16		1		X	New supports; early signs of corrosion
17	X	3		X	
18	X	3		X	
19	X	3		X	
20	X	3		X	
21		1		X	New supports; early signs of corrosion
22	X	3		X	
23	X	3		X	
24	X	3		X	
25	X	3		X	
26	X	3		X	
27	X	3		X	
28	X	3		X	
29	X	3		X	
30	X	3		X	
31	X	3		X	
32	X	3		X	
33	X	3		X	
34	X	3		X	
35	X	3		X	
36	X	3		X	
37	X	3		X	
38	X	3		X	
39	X	3		X	
40	X	3		X	
41	X	3		X	
42	X	3		X	

* Corrosion Ratings: 1- Minor Corrosion 2- Moderate Corrosion 3- Severe Corrosion

WILSON TUNNEL CEILING SUPPORT RODS

Honolulu Side (In-bound)

ROD #	CRACKS	CORROSION	DYE	PICTURES	COMMENTS
43	X	3		X	
44		1		X	New supports; early signs of corrosion
45	X	3		X	
46	X	3		X	
47	X	3		X	
48	X	3		X	
49	X	3		X	
50	X	3		X	
51	X	3		X	
52	X	3		X	
53	X	3		X	
54	X	3		X	
55	X	3		X	
56	X	3		X	
57	X	3		X	
58	X	3		X	
59	X	3		X	
60	X	3		X	
61	X	3		X	
62	X	3		X	
63	X	3		X	
64	X	3		X	
65	X	3		X	
66	X	3		X	
67	X	3		X	
68		0		X	New supports; appear temporary
69	X	3		X	
70	X	3		X	
71	X	3		X	
72	X	3		X	
73	X	3		X	
74	X	3		X	
75	X	3		X	
76	X	3		X	
77	X	3		X	
78	X	3		X	
79	X	3		X	
80	X	3		X	
81	X	3		X	
82	X	3		X	
83	X	3		X	
84	X	3		X	

* Corrosion Ratings: 1- Minor Corrosion 2- Moderate Corrosion 3- Severe Corrosion

WILSON TUNNEL CEILING SUPPORT RODS

Honolulu Side (Outbound)

ROD #	CRACKS	CORROSION	DYE	PICTURES	COMMENTS
1		1	X	X	
2		1	X	X	
3		1		X	
4		1		X	
5		1		X	
6		1		X	
7		1		X	
8		1		X	
9		1		X	
10		1		X	
11		1		X	
12		1		X	
13		1		X	
14		1		X	
15		1		X	
16		1		X	
17		1		X	
18		1		X	
19		1		X	
20		1		X	
21		1		X	
22		1		X	
23		1		X	New supports; early signs of corrosion
24		1		X	
25		1		X	
26		1		X	
27		1		X	
28		1		X	
29		1		X	
30		1		X	
31		1		X	
32		1		X	
33		1		X	
34		1		X	
35		1		X	
36		1		X	
37		1		X	
38		1		X	
39	X	3		X	
40		1		X	
41		1		X	
42	X	3		X	

* Corrosion Ratings: 1- Minor Corrosion 2- Moderate Corrosion 3- Severe Corrosion

WILSON TUNNEL CEILING SUPPORT RODS

Honolulu Side (Outbound)

ROD #	CRACKS	CORROSION	DYE	PICTURES	COMMENTS
43	X	3		X	
44		1		X	
45		1		X	
46		1		X	
47		1		X	
48		1		X	
49		1		X	
50		1		X	
51		1		X	
52		1		X	
53		1		X	
54		1		X	
55		1		X	
56		1		X	
57	X	3		X	
58		1		X	
59		1		X	
60		1		X	
61	X	3		X	
62		2		X	
63		1		X	
64		1		X	
65		1		X	
66		1		X	
67		1		X	
68		1		X	
69	X	3		X	
70		1		X	
71		1		X	
72		1		X	
73		1		X	
74		1		X	
75		1		X	
76		1		X	
77		1		X	
78		2		X	
79		1		X	
80		1		X	
81	X	3		X	
82		1		X	
83		1		X	
84		1		X	

* Corrosion Ratings: 1- Minor Corrosion 2- Moderate Corrosion 3- Severe Corrosion

WILSON TUNNEL CEILING SUPPORT RODS

Honolulu Side (Outbound)

ROD #	CRACKS	CORROSION	DYE	PICTURES	COMMENTS
85		1		X	
86		1		X	
87		1		X	
88		1		X	
89		1		X	
90		1		X	
91		1		X	
92		2		X	
93		2		X	
94		1		X	
95		1		X	
96		1		X	
97	X	3		X	
98		1		X	
99		2		X	
100		2		X	
101		1		X	
102		1		X	
103		1		X	
104		1		X	
105		1		X	
106		1		X	
107		1		X	
108		1		X	
109	X	3		X	
110	X	3		X	
111		1		X	
112		1		X	
113	X	3		X	
114		1		X	
115		2		X	
116		1		X	
117		2		X	
118		2		X	
119		2		X	
120		1		X	
121		2		X	
122		2		X	
123	X	3		X	
124		2		X	

* Corrosion Ratings: 1- Minor Corrosion 2- Moderate Corrosion 3- Severe Corrosion

WILSON TUNNEL CEILING SUPPORT RODS

Kaneohe Side (Outbound)

ROD #	CRACKS	CORROSION	DYE	PICTURES	COMMENTS
1		1	X	X	
2		1	X	X	
3		1		X	
4		1		X	
5		1		X	
6		3		X	Deep holes near interface
7		2		X	
8		2		X	
9		2		X	
10		1		X	
11		2		X	
12		1		X	
13		2		X	
14		3		X	Deep holes near interface
15		2		X	
16		2		X	
17		2		X	
18		1		X	New supports; early signs of corrosion
19		3		X	
20	X	3		X	
21		2		X	
22		3		X	
23		3		X	
24		3		X	
25		2		X	
26		2		X	
27		2		X	
28		2		X	
29		2		X	
30	X	3		X	
31		2		X	
32		2		X	
33		2		X	
34		3		X	
35		2		X	
36		2		X	
37		2		X	
38		2		X	
39		2		X	
40		3		X	
41		2		X	
42	X	3		X	

* Corrosion Ratings: 1- Minor Corrosion 2- Moderate Corrosion 3- Severe Corrosion

WILSON TUNNEL CEILING SUPPORT RODS

Kaneohe Side (Outbound)

ROD #	CRACKS	CORROSION	DYE	PICTURES	COMMENTS
43		3		X	
44	X	3		X	
45		2		X	
46	X	3		X	
47		2		X	
48		3		X	Hole in concrete next to pole
49		2		X	
50		3		X	
51		3		X	
52	X	3		X	
53		3		X	
54		2		X	
55	X	3		X	
56		2		X	
57	X	3		X	
58		2		X	
59	X	3		X	
60	X	3		X	
61	X	3		X	
62	X	3		X	
63	X	3		X	
64		3		X	Hole in concrete next to pole
65	X	3		X	
66		3		X	
67	X	3		X	
68		3		X	
69	X	3		X	
70		2		X	
71	X	3		X	
72		1		X	
73	X	3		X	
74	X	3		X	
75	X	3		X	
76	X	3		X	
77	X	3		X	
78	X	3		X	
79	X	3		X	
80		3		X	
81	X	3		X	
82	X	3		X	
83	X	3		X	
84		3		X	

* Corrosion Ratings: 1- Minor Corrosion 2- Moderate Corrosion 3- Severe Corrosion

WILSON TUNNEL CEILING SUPPORT RODS

Kaneohe Side (Outbound)

ROD #	CRACKS	CORROSION	DYE	PICTURES	COMMENTS
85	X	3		X	
86	X	3		X	
87	X	3		X	
88	X	3		X	
89	X	3		X	
90	X	3		X	
91	X	3		X	
92	X	3		X	
93	X	3		X	
94		2		X	
95	X	3		X	
96	X	3		X	
97	X	3		X	
98	X	3		X	
99	X	3		X	
100	X	3		X	
101	X	3		X	
102	X	3		X	
103	X	3		X	
104	X	3		X	
105	X	3		X	
106	X	3		X	
107	X	3		X	
108	X	3		X	
109	X	3		X	
110	X	3		X	
111	X	3		X	
112	X	3		X	
113	X	3		X	
114	X	3		X	
115	X	3		X	
116	X	3		X	
117	X	3		X	
118	X	3		X	
119	X	3		X	
120	X	3		X	
121	X	3		X	
122	X	3		X	
123	X	3		X	
124	X	3		X	
125	X	3		X	
126	X	3		X	

* Corrosion Ratings: 1- Minor Corrosion 2- Moderate Corrosion 3- Severe Corrosion

WILSON TUNNEL CEILING SUPPORT RODS

Kaneohe Side (Outbound)

ROD #	CRACKS	CORROSION	DYE	PICTURES	COMMENTS
127	X	3		X	
128	X	3		X	
129	X	3		X	
130	X	3		X	
131	X	3		X	
132	X	3		X	
133	X	3		X	
134	X	3		X	
135	X	3		X	
136	X	3		X	
137	X	3		X	
138	X	3		X	
139	X	3		X	
140	X	3		X	
141	X	3		X	
142	X	3		X	
143	X	3		X	
144	X	3		X	
145	X	3		X	
146	X	3		X	
147	X	3		X	
148	X	3		X	
149	X	3		X	
150	X	3		X	
151	X	3		X	
152	X	3		X	
153	X	3		X	
154	X	3		X	
155	X	3		X	
156	X	3		X	
157	X	3		X	
158	X	3		X	
159	X	3		X	
160	X	3		X	
161	X	3		X	
162	X	3		X	
163	X	3		X	
164	X	3		X	
165	X	3		X	
166	X	3		X	
167	X	3		X	
168	X	3		X	
169	X	3		X	

* Corrosion Ratings: 1- Minor Corrosion 2- Moderate Corrosion 3- Severe Corrosion

WILSON TUNNEL CEILING SUPPORT RODS

Kaneohe Side (Outbound)

ROD #	CRACKS	CORROSION	DYE	PICTURES	COMMENTS
170	X	3		X	
171	X	3		X	
172	X	3		X	
173	X	3		X	
174	X	3		X	
175	X	3		X	
176	X	3		X	
177	X	3		X	
178	X	3		X	
179	X	3		X	
180	X	3		X	
181	X	3		X	
182	X	3		X	
183	X	3		X	
184	X	3		X	
185	X	3		X	
186	X	3		X	
187	X	3		X	
188	X	3		X	
189	X	3		X	
190	X	3		X	
191	X	3		X	
192	X	3		X	
193	X	3		X	
194	X	3		X	
195	X	3		X	
196	X	3		X	
197	X	3		X	
198	X	3		X	
199	X	3		X	
200	X	3		X	
201	X	3		X	
202	X	3		X	
203	X	3		X	
204	X	3		X	
205	X	3		X	
206	X	3		X	
207	X	3		X	
208	X	3		X	
209	X	3		X	
210	X	3		X	
211	X	3		X	
212	X	3		X	

* Corrosion Ratings: 1- Minor Corrosion 2- Moderate Corrosion 3- Severe Corrosion

WILSON TUNNEL CEILING SUPPORT RODS

Kaneohe Side (Outbound)

ROD #	CRACKS	CORROSION	DYE	PICTURES	COMMENTS
213	X	3		X	
214	X	3		X	
215	X	3		X	
216	X	3		X	
217	X	3		X	
218	X	3		X	
219	X	3		X	
220	X	3		X	
221	X	3		X	
222	X	3		X	
223	X	3		X	
224	X	3		X	
225	X	3		X	
226	X	3		X	
227	X	3		X	
228	X	3		X	
229	X	3		X	
230	X	3		X	
231	X	3		X	
232	X	3		X	
233	X	3		X	
234	X	3		X	
235	X	3		X	
236	X	3		X	
237	X	3		X	
238	X	3		X	
239	X	3		X	
240	X	3		X	
241	X	3		X	
242	X	3		X	
243	X	3		X	
244	X	3		X	
245	X	3		X	
246	X	3		X	
247	X	3		X	
248	X	3		X	
249	X	3		X	
250	X	3		X	

* Corrosion Ratings: 1- Minor Corrosion 2- Moderate Corrosion 3- Severe Corrosion



End of report

Appendix D

E&I Rod Fracture Survey Report

Investigation into Fractures of Stainless Steel Hanger Rods in Hawaii's Wilson Tunnel

January 2016

TECHNICAL REPORT DOCUMENTATION PAGE

1. Report No. Unassigned	2. Government Accession No.	3. Recipient's Catalog No.
4. Title and Subtitle Investigation into Fractures of Stainless Steel Hanger Rods in Hawaii's Wilson Tunnel.		5. Report Date. January 2016
		6. Performing Organization Code:
7. Author(s) Justin M. Ocel, Jason Provines, Terry Arnold, and Sheila Rimal Duwadi		8. Performing Organization Report No.
9. Performing Organization Name and Address Office of Infrastructure Research and Development Federal Highway Administration 6300 Georgetown Pike McLean, VA 22101-2296		10. Work Unit No.
		11. Contract or Grant No.
12. Sponsoring Agency Name and Address Office of Infrastructure Research and Development Federal Highway Administration 6300 Georgetown Pike McLean, VA 22101-2296		13. Type of Report and Period Covered
		14. Sponsoring Agency Code HRDI-01
15. Supplementary Notes This investigation was conducted by staff at the Turner-Fairbank Highway Research Center at the request of the Hawaii Department of Transportation led by Sheila Duwadi with work performed by Justin Ocel and Jason Provines of the Structures Laboratory and Terry Arnold of the Chemistry Laboratory. Jason Provines is a contract engineer with Professional Service Industries, Inc. of Herndon, VA working in the Structures Laboratory under FHWA's Support Services for the Structures Laboratories contract (DTFH61-10-D-00017). We would like to thank the staff from the Structures and the Chemistry laboratories and our colleagues for their assistance and insight especially Dr. Rontang Liu and Dr. Richard Meininger.		
16. Abstract During a routine inspection on September 25, 2015, the Hawaii Department of Transportation (HDOT) found eight fractured hanger rods which support the ceiling slab of the Wilson Tunnel that connects Kane'ohe to Honolulu on the island of O'ahu. Subsequently they identified 22 other rods that were similarly fractured. Through the local FHWA Division office, the state requested that FHWA conduct an investigation to determine what caused the failures. This report outlines the work conducted as part of that investigation. Two rods received at the Turner-Fairbank Highway Research Center were examined including a determination of mechanical properties, chemical properties, metallography of the steel, and analysis of the fracture surface. Additionally, chemical analysis of the concrete was conducted near the site of the fractures. The chemical analysis of the steel found high levels of sulfur indicating that the rods were most likely type 303 stainless steel, and the tensile and hardness properties indicated they were likely in a cold-finished state. Each rod had pitting corrosion evident through its entire length and transverse cross sections near the fracture revealed numerous branching, "tree-root" cracks throughout the cross-section, mostly originating from corrosion pits. Analysis of the steel microstructure and of the fracture surface found the cracking was a combination of trans- and intergranular fracture, which, coupled with the presence of numerous branching cracks, indicated that failure was due to stress corrosion cracking. The driving force of the stress-corrosion cracking was from chlorine contamination of the concrete, likely believed to be from the use of beach sand in the concrete mix at the time of construction.		
17. Key Words Stress corrosion cracking, tunnel, hanger rod, corrosion, chloride, bromide, beach sand, fracture, inspection		18. Distribution Statement This report was prepared for the Hawaii DOT

19. Security Classif. (of this report) Unclassified	20. Security Classif. (of this page) Unclassified	21. No. of Pages 38	22. Price N/A
--	--	------------------------	------------------

Form DOT F 1700.7 (8-72)

Reproduction of completed page authorized

SI* (MODERN METRIC) CONVERSION FACTORS

APPROXIMATE CONVERSIONS TO SI UNITS

Symbol	When You Know	Multiply By	To Find	Symbol
LENGTH				
in	inches	25.4	millimeters	mm
ft	feet	0.305	meters	m
yd	yards	0.914	meters	m
mi	miles	1.61	kilometers	km
AREA				
in ²	square inches	645.2	square millimeters	mm ²
ft ²	square feet	0.093	square meters	m ²
yd ²	square yard	0.836	square meters	m ²
ac	acres	0.405	hectares	ha
mi ²	square miles	2.59	square kilometers	km ²
VOLUME				
fl oz	fluid ounces	29.57	milliliters	mL
gal	gallons	3.785	liters	L
ft ³	cubic feet	0.028	cubic meters	m ³
yd ³	cubic yards	0.765	cubic meters	m ³
NOTE: volumes greater than 1000 L shall be shown in m ³				
MASS				
oz	ounces	28.35	grams	g
lb	pounds	0.454	kilograms	kg
T	short tons (2000 lb)	0.907	megagrams (or "metric ton")	Mg (or "t")
TEMPERATURE (exact degrees)				
°F	Fahrenheit	5 (F-32)/9 or (F-32)/1.8	Celsius	°C
ILLUMINATION				
fc	foot-candles	10.76	lux	lx
fl	foot-Lamberts	3.426	candela/m ²	cd/m ²
FORCE and PRESSURE or STRESS				
lbf	poundforce	4.45	newtons	N
lbf/in ²	poundforce per square inch	6.89	kilopascals	kPa
APPROXIMATE CONVERSIONS FROM SI UNITS				
Symbol	When You Know	Multiply By	To Find	Symbol
LENGTH				
mm	millimeters	0.039	inches	in
m	meters	3.28	feet	ft
m	meters	1.09	yards	yd
km	kilometers	0.621	miles	mi
AREA				
mm ²	square millimeters	0.0016	square inches	in ²
m ²	square meters	10.764	square feet	ft ²
m ²	square meters	1.195	square yards	yd ²
ha	hectares	2.47	acres	ac
km ²	square kilometers	0.386	square miles	mi ²
VOLUME				
mL	milliliters	0.034	fluid ounces	fl oz
L	liters	0.264	gallons	gal
m ³	cubic meters	35.314	cubic feet	ft ³
m ³	cubic meters	1.307	cubic yards	yd ³
MASS				
g	grams	0.035	ounces	oz
kg	kilograms	2.202	pounds	lb
Mg (or "t")	megagrams (or "metric ton")	1.103	short tons (2000 lb)	T
TEMPERATURE (exact degrees)				
°C	Celsius	1.8C+32	Fahrenheit	°F
ILLUMINATION				
lx	lux	0.0929	foot-candles	fc
cd/m ²	candela/m ²	0.2919	foot-Lamberts	fl
FORCE and PRESSURE or STRESS				
N	newtons	0.225	poundforce	lbf
kPa	kilopascals	0.145	poundforce per square inch	lbf/in ²

*SI is the symbol for the International System of Units. Appropriate rounding should be made to comply with Section 4 of ASTM E380.
(Revised March 2003)

TABLE OF CONTENTS

INTRODUCTION.....	1
SCOPE OF WORK.....	2
CHEMICAL AND MECHANICAL TESTS OF THE RODS.....	3
AS RECEIVED CONDITION.....	3
TESTING FOR SURFACE CONTAMINANTS.....	7
DESTRUCTIVE TESTING.....	8
Tensile Testing.....	9
Chemical Analysis.....	12
Hardness Testing.....	13
METALLOGRAPHIC AND FRACTOGRAPHIC EXAMINATION.....	15
PRELIMINARY EVALUATION.....	15
CLEANING.....	18
TRANSVERSE SECTIONS NEAR FRACTURES.....	20
TYPICAL MICROSTRUCTURE.....	23
FRACTOGRAPHY OF FRACTURE SURFACES.....	25
CHLORIDE ANALYSIS OF TUNNEL CONCRETE.....	28
CONCLUSIONS.....	37
RECOMMENDATIONS.....	38
APPENDIX A – ROD SURFACE CRACKS.....	40
APPENDIX B – TABLE OF ROCKWELL B HARDNESS TEST RESULTS.....	49
REFERENCES.....	50

LIST OF FIGURES

FIGURE 1.	SCHEMATIC. ELEVATION VIEW OF TUNNEL CROSS-SECTION.....	2
FIGURE 2.	PHOTO. CLOSE-UP PICTURES OF ROD 1.	4
FIGURE 3.	PHOTO. CLOSE-UP PICTURES OF ROD 2.	5
FIGURE 4.	PHOTO. ROD 1 FRACTURE SURFACE.	6
FIGURE 5.	PHOTO. ROD 2 FRACTURE SURFACE.	6
FIGURE 6.	PHOTO. INJECTION OF FLUID INTO BRESLE PATCH.....	7
FIGURE 7.	SCHEMATIC. CUT PLAN FOR ROD 1.	8
FIGURE 8.	SCHEMATIC. CUT PLAN FOR ROD 2.	9
FIGURE 9.	SCHEMATIC. DETAILING OF TENSILE COUPON.....	9
FIGURE 10.	GRAPH. ENGINEERING STRESS VERSUS STRAIN CURVES FOR ALL TENSILE SPECIMENS.....	12
FIGURE 11.	SCHEMATIC. LOCATIONS OF HARDNESS TESTS FOR RODS 1 AND 2	14
FIGURE 12.	GRAPH. CONSTANT RADIUS AVERAGE ROCKWELL B HARDNESS OF BOTH RODS.	14
FIGURE 13.	IMAGE. EDX IMAGES OF ROD 1 FRACTURE SURFACE (AT 3 O’CLOCK).	16
FIGURE 14.	PHOTO. ROD 1 FRACTURE SURFACE AFTER CLEANING.....	19
FIGURE 15.	PHOTO. ROD 2 FRACTURE SURFACE AFTER CLEANING.....	19
FIGURE 16.	PHOTO. DIRECTIONALITY OF FRACTURE PROGRESSION IN ROD 1.	20
FIGURE 17.	SCHEMATIC. CUT PLAN FOR TRANSVERSE SLICES OF F1 AND F2 FRACTURE SECTIONS.	21
FIGURE 18.	PHOTO. TRANSVERSE CRACKS IN FRACTURE SURFACE SECTIONS; ROD 1 (LEFT), ROD 2 (RIGHT).	21
FIGURE 19.	PHOTO. ROD 2 POLISHED IMAGE SHOWING MAJOR CRACK AND SMALLER BRANCHING CRACKS.....	22
FIGURE 20.	PHOTO. ROD 2 TRANSVERSE SECTION AT 50X MAGNIFICATION. ELECTROLYTIC OXALIC ACID ETCH FOR 30 S.	22
FIGURE 21.	PHOTO. ZOOMED IN VIEW OF A CRACK BRANCH IN FIGURE 20 AT 500X MAGNIFICATION.....	23
FIGURE 22.	PHOTO. TYPICAL GRAIN STRUCTURE ON M2 SECTION AT 200X MAGNIFICATION AFTER 30 SECOND ELECTROLYTIC ETCH IN OXALIC ACID.	24

FIGURE 23.	PHOTO. LONGITUDINAL MICROETCH FROM ROD 2 AT 200X MAGNIFICATION AFTER 30 S. ELECTROLYTIC ETCH IN OXALIC ACID.	24
FIGURE 24.	IMAGE. POLISHED LONGITUDINAL SECTION VIEWED WITH SEM AND EDX, ELECTRON BEAM IMAGE (TOP), SULFUR IMAGE (BOTTOM-LEFT), MANGANESE IMAGE (BOTTOM-RIGHT).	25
FIGURE 25.	ROD 2 CLEANED FRACTURE SURFACE SHOWING MORE FEATURES OF TRANSGRANULAR FRACTURE.....	26
FIGURE 26.	ROD 2 CLEANED FRACTURE SURFACE SHOWING MORE FEATURES OF INTERGRANULAR FRACTURE.....	27
FIGURE 27.	ROD #13 - INBOUND (IB) WILSON TUNNEL	28
FIGURE 28.	ROD #31 IB WILSON TUNNEL	29
FIGURE 29.	ROD #34 - IB WILSON TUNNEL	30
FIGURE 30.	ROD 40 - IB WILSON TUNNEL	31
FIGURE 31.	ROD #18 - OUTBOUND (OB) WILSON TUNNEL.....	32
FIGURE 32.	ROD #40 OB - WILSON TUNNEL	33
FIGURE 33.	LOCATION OF WILSON TUNNEL HANGER REPAIRS	34
FIGURE 34.	PHOTO. ROD 1 AT ZERO DEGREES.	41
FIGURE 35.	PHOTO. ROD 1 AT 45 DEGREES.....	41
FIGURE 36.	PHOTO. ROD 1 AT 90 DEGREES.....	42
FIGURE 37.	PHOTO. ROD 1 AT 135 DEGREES.....	42
FIGURE 38.	PHOTO. ROD 1 AT 180 DEGREES.....	43
FIGURE 39.	PHOTO. ROD 1 AT 225 DEGREES.....	43
FIGURE 40.	PHOTO. ROD 1 AT 270 DEGRESS.	44
FIGURE 41.	PHOTO. ROD 1 AT 315 DEGREES.....	44
FIGURE 42.	PHOTO. ROD 2 AT ZERO DEGREES.	45
FIGURE 43.	PHOTO. ROD 2 AT 45 DEGREES.....	45
FIGURE 44.	PHOTO. ROD 2 AT 90 DEGREES.....	46
FIGURE 45.	PHOTO. ROD 2 AT 135 DEGREES.....	46
FIGURE 46.	PHOTO. ROD 2 AT 180 DEGREES.....	47
FIGURE 47.	PHOTO. ROD 2 AT 225 DEGREES.....	47
FIGURE 48.	PHOTO. ROD 2 AT 270 DEGREES.....	48
FIGURE 49.	PHOTO. ROD 2 AT 315 DEGREES.....	48

LIST OF TABLES

TABLE 1.	SURFACE CONTAMINATION RESULTS.....	8
TABLE 2.	RESULTS OF ROD 1 TENSILE TESTS	11
TABLE 3.	RESULTS OF ROD 2 TENSILE TESTS	11
TABLE 4.	CHEMICAL COMPOSITION (PERCENT BY WEIGHT)	13
TABLE 5.	CHLORIDE CONTENT OF CONCRETE SAMPLES	35
TABLE 6.	ROCKWELL B HARDNESS TEST RESULTS FOR RODS 1 AND 2	49

INTRODUCTION

During routine inspection on September 25, 2015, the Hawaii Department of Transportation (HDOT) found eight fractured hanger rods which support the ceiling of the Wilson Tunnel connecting Kane'ohe to Honolulu on the island of O'ahu. Subsequently they identified 22 other rods that were similarly fractured.

Figure 1 shows a cross-section of the tunnel where the tunnel lining and ceiling slab are integrally cast together creating an upper ventilation plenum. Stainless steel rods are used to support the central part of the ceiling slab. These 1-1/4 inch diameter rods are spaced every 98 inches along the length of the tunnel.

The Hawaii DOT reached out to the FHWA Division and Headquarters offices, who contacted the Turner-Fairbank Highway Research Center (TFHRC) for assistance in the investigation of the failure, and guidance on non-destructive evaluation (NDE) methodologies to use in their evaluation of the remaining hanger rods. They also stated their inspection report had indicated vibrations of ceiling slabs at the location of the anchors, possibly caused by airflow, and expressed concerns on whether this could have played a role in the fractures.

The FHWA provided general guidance on NDE methods to use, and indicated that in addition to investigating the failed rods and the fractured surfaces, there may be value in conducting vibration analysis through the use of super computers, and testing the concrete for corrosive elements in the areas of the fractured and near still intact rods. Request was made to the State for the following:

1. Samples of as many fractured hanger rods as possible. Each of these samples would preferably include the fracture surfaces with as long a length as possible, if not the entire rod.
2. Samples of any unused stainless steel rods, which the State has in reserve, to confirm type.
3. Connection details for stainless rods embedded from concrete liner to ceiling slab.
4. Representative samples of concrete from the ceiling slab and liner around the hanger, both at the failed and intact hangers.

On October 28, TFHRC received two of the fractured rods, and on December 15 seven concrete samples from the Hawaii DOT. This report documents the investigation conducted on the rods, and concrete; and presents the findings.

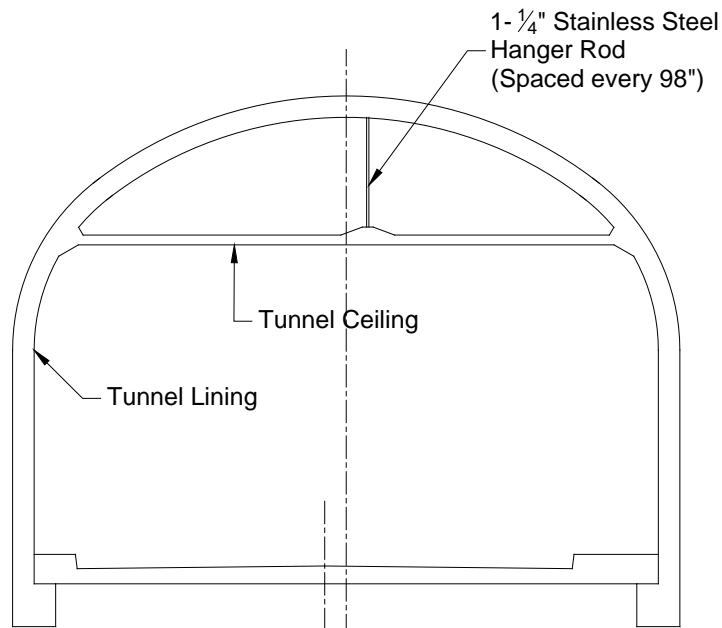


Figure 1. Schematic. Elevation view of tunnel cross-section.

SCOPE OF WORK

The scope of work presented herein includes forensic investigation of the two fractured hanger rods and analysis of the concrete samples to include the following:

- Documentation of the as-received condition of rods – measuring, photographing, and recording any anomalies.
- Determination of the presence and concentration of surface contaminants.
- Determination of chemical properties of the rods and ascertaining the material type.
- Determination of mechanical properties of the rods.
- Metallographic evaluation of the steel and evaluation of the fracture surface.
- Determination of composition of any contaminants on concrete
- Determination of the composition of the dirt on the fractured face of the broken rods.
- Determination of the chloride content of the concrete samples

This report is organized into the following main sections that outline chemical and mechanical tests and evaluation, metallographic and fractographic examination, concrete analysis, conclusion, and recommendations.

CHEMICAL AND MECHANICAL TESTS OF THE RODS

This chapter discusses the documentation of the as-received condition of the two rods, the procedures and results from chemical and mechanical evaluation of the rods, and surface contamination measurements on the rods.

AS RECEIVED CONDITION

Each rod was approximately 80 inches long; and no documentation was provided regarding the location of the rods in the tunnel. However, it was verbally communicated by HDOT that the two rods came from the inbound tunnel. Each rod had an obvious fracture on one end closest to the ceiling slab, and the opposite end appeared to be saw cut. Neither rod was attracted to a magnet indicating it was a form of austenitic stainless steel.

Visually, the rods had surface corrosion product on them in distinct patches. Figure 2 and 3 show a series of close-up photos along the length of each of the rods, which were denoted as “Rod 1” and “Rod 2”. A tape measure is provided in each photo for reference; the cut end is zero inches, and the fractured end is at approximately 80 inches.

Pictures of the actual fracture surfaces on Rod 1 and 2 are shown in Figures 4 and 5 respectively. Each fracture surface was heavily corroded and no features were observable on the macroscale to determine if the fracture was brittle or ductile. However, since the rod was in direct tension and the fracture surface was generally flat and normal to the load, it was concluded that the fracture was brittle at the macroscale.



Figure 2. Photo. Close-up pictures of Rod 1.



Figure 3. Photo. Close-up pictures of Rod 2.



Figure 4. Photo. Rod 1 fracture surface.



Figure 5. Photo. Rod 2 fracture surface.

TESTING FOR SURFACE CONTAMINANTS

Before the rods were destructively tested, three surface contamination measurements (e.g., chlorides) were taken on each of the rods, one as close to the fracture as possible, one in the middle, and the third as close to the cut end as possible. The Bresle method was used, which consists of placing a self-sticking patch, with a sampling surface area of 12.25 cm², to the rod. An empty syringe with a fine needle was used to evacuate the air from inside the patch. Then a proprietary extraction fluid (Chlor*Rid) was injected into the patch. The needle was slid back and the cell was massaged around for 15 to 20 seconds (see Figure 6). Tapping and rubbing the cell helps extract soluble salts into the solution. The needle was then used to extract the solution from the cell, which process was repeated three times before the solution was removed from the patch and analyzed using an ion chromatography (IC) machine.



Figure 6. Photo. Injection of fluid into Bresle patch.

The IC has the ability to detect small amount of ions in a solution, however the only two ions that had reportable concentrations were chloride (Cl⁻) and sulfate (SO₄⁻). The results of the measurements at the three locations on each rod are shown in Table 1. In both rods, the highest ion measurements were near the fractured end of the rod, and in all locations there was a higher concentration of sulfate than chloride. The anion concentrations were higher in Rod 1, but no conclusion can be derived since their locations in the tunnel were not known.

Table 1. Surface Contamination Results

Rod	Sample Location	Chloride Concentration ($\mu\text{g}/\text{cm}^2$)	Sulfate Concentration ($\mu\text{g}/\text{cm}^2$)
1	Near fracture	19.6	30.9
	Middle	10.7	16.7
	Near cut end	11.2	23.2
2	Near fracture	6.7	11.1
	Middle	5.1	10.0
	Near cut end	5.7	8.9

DESTRUCTIVE TESTING

The schematics shown in Figure 7 and 8 depict the cutting plan for each of the rods, along with the naming convention of the various samples to be tested. Approximately one inch of the fractured end was removed for metallographic and fractographic examination as described in more detail in the next chapter. Three 12-inch long samples were removed to fabricate tensile coupons for mechanical property evaluation. A piece approximately 3/8-inch thick was removed for chemical testing at an external laboratory. Finally, a section approximately 1” long was removed to conduct metallography tests (described further in the next chapter).

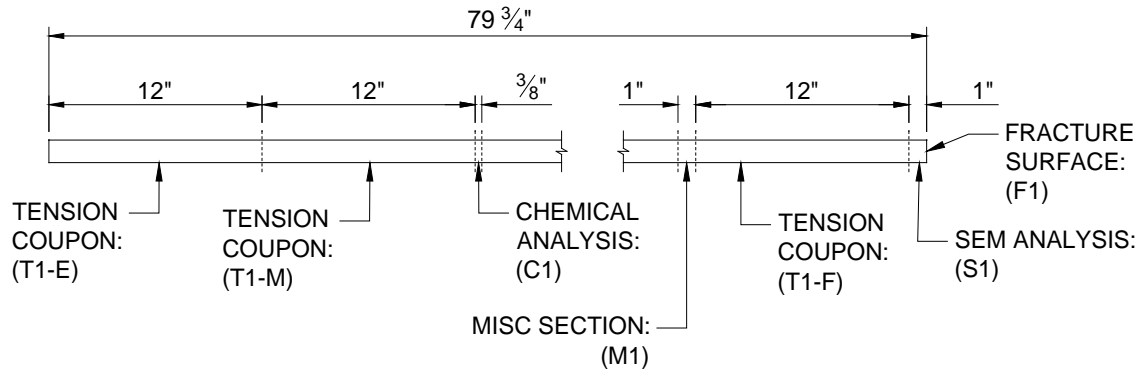


Figure 7. Schematic. Cut plan for Rod 1.

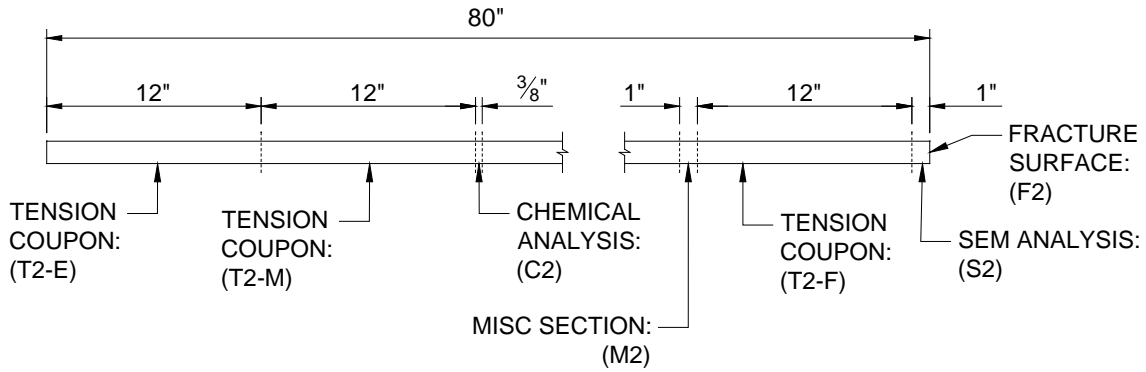


Figure 8. Schematic. Cut plan for Rod 2.

Tensile Testing

The tensile coupons were detailed according to the proportions of round bar specimens as specified in ASTM E8/E8M-13a “*Standard Test Methods for Tension Testing of Metallic Materials.*” However, some dimensions were modified such that the bar could be tested as close to its full diameter as possible. This resulted in a reduced diameter of 7/8 inch and a length of the reduced section of 5 inches. A tapered reduced diameter was machined into the specimens in accordance with ASTM E8/E8M-13a to ensure failure in the middle of the specimen. The dimensions of the coupons are shown in Figure 9.

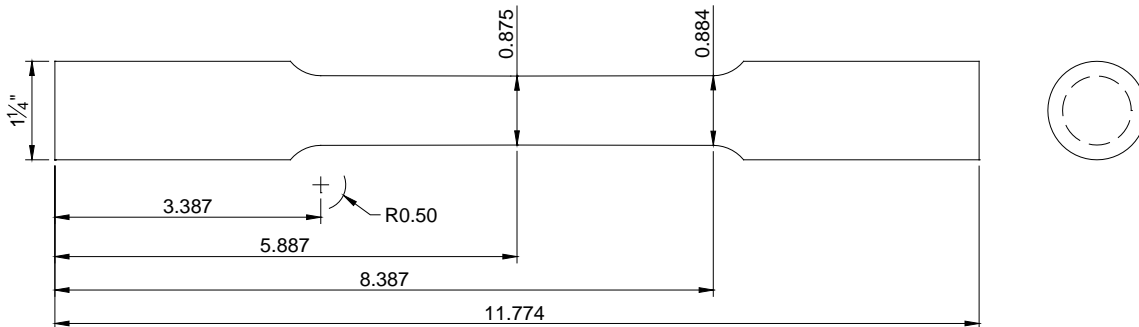


Figure 9. Schematic. Detailing of tensile coupon.

The testing was performed in a digitally controlled servovalve hydraulic test frame with hydraulic grips. Testing was performed according to ASTM E8/E8M-13a. The loading rate for determining yield properties was based on Method C which equated to a crosshead speed of 0.075 inch/minute based on the specimen dimensions. After 3 percent strain had been achieved,

the loading rate was increased to 0.53 inch/minute and this rate was used until bar fracture¹. Strain was measured with a clip-on extensometer measuring over a 4.0000 inch gauge length.

The results are reported in Tables 2 and 3, respectively for Rod 1 and Rod 2, with average yield strength of 74.5 ksi and a tensile strength of 100.9 ksi for Rod 1; and average yield strength of 68.5 ksi and a tensile strength of 97.3 ksi for Rod 2. The elongations of both rods were greater than 43 percent, and the reduction in area was more than 50 percent. The high yield and tensile properties of these rods suggests that they were cold-finished material, as the annealed condition of stainless steel would have corresponding values roughly half of that measured.

Plots of the six stress versus strain curves from tensile testing are shown in Figure 10. The results from Rod 1 are plotted with a heavy black line, and those for Rod 2 are with a heavy dashed red line. The three plots for each rod plot right on top each other so there was no noticeable difference in tensile properties along the length of either rod.

¹ For the original reduced length of the specimens, 5 inches, E8/E8M allows the crosshead speed to be 0.25 to 2.5 inches per minute to determine tensile properties.

Table 2. Results of Rod 1 Tensile Tests

Specimen^a	Modulus (ksi)	0.2% Offset Yield Stress (ksi)	Tensile Strength (ksi)	Elongation^b	Percent Reduction in Area
T1_E	27199	74.4	100.8	43.4	54
T1_M	27213	74.5	100.8	42.8	53
T1_F	27247	74.6	101.1	43.0	55
Average	27220	74.5	100.9	43.1	54

^a – Specimen names correlate to the locations shown in Section A-A of Figure 7.

^b – Elongation is reported on a 3.5 inch gauge length, which is the four bar diameter requirement in ASTM E8/E8M.

Table 3. Results of Rod 2 Tensile Tests

Specimen^a	Modulus (ksi)	0.2% Offset Yield Stress (ksi)	Tensile Strength (ksi)	Elongation^b	Percent Reduction in Area
T2_E	27185	68.2	97.2	46.5	54
T2_M	27463	68.8	97.2	46.8	54
T2_F	27918	68.5	97.5	46.2	55
Average	27522	68.5	97.3	46.5	54

^a – Specimen names correlate to the locations shown in Section A-A of Figure 8.

^b – Elongation is reported on a 3.5 inch gauge length, which is the four bar diameter requirement in ASTM E8/E8M.

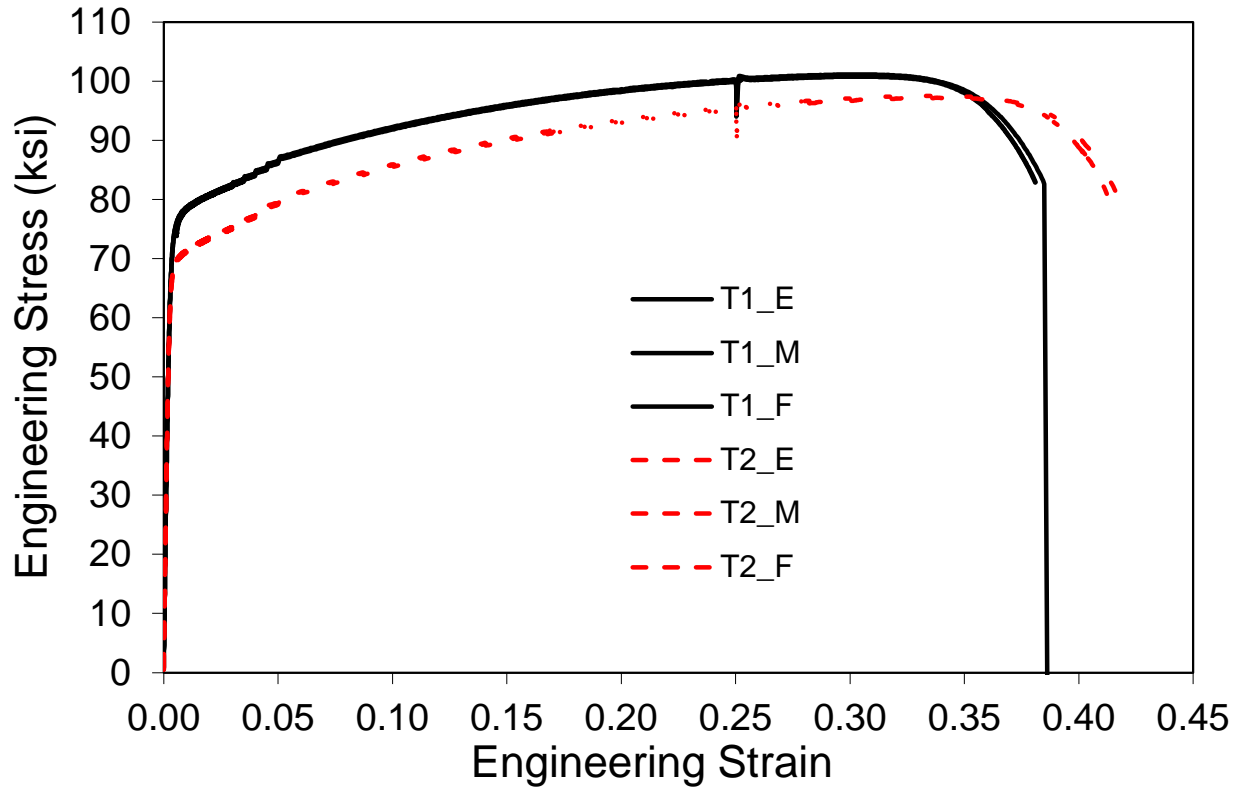


Figure 10. Graph. Engineering stress versus strain curves for all tensile specimens.

Chemical Analysis

The two 3/8" specimens (C1 and C2) were sent to an outside laboratory to conduct chemical analysis. Chemical analysis was performed in accordance with ASTM E1086 and ASTM E1019 for carbon and sulfur. The results of the chemical analysis are shown in Table 4 for each rod. Also shown in the table are the chemical requirements for Type 303 stainless steel from the ASTM A 276 "Standard Specification for Hot-Rolled and Cold-Finished Corrosion-Resistant Steel Bars." The plans for the tunnel provided by Hawaii only specified the hanger rod material as "stainless steel"; for this time period, A 276 is the most likely used ASTM standard. This tentative specification from 1949 was adopted as a standard in 1954; regardless, the chemical composition of Type 303 was the same between these two editions. The high level of sulfur present in the rods excluded the possibility of any other 300 series alloys. Elevated levels of sulfur are added to steel to increase its machinability and are sometimes referred to as "free-machining" grades. The shaded cells for the phosphorus levels represent the values that were out of specification, assuming ASTM A 276 Type 303. Lastly, the chemical composition between the two rods was very close indicating that these two rods were likely from the same heat of steel.

Table 4. Chemical Composition (Percent by Weight)

Element	Rod 1	Rod 2	ASTM A 276 – 49T (Type 303)
C	0.09	0.09	0.15 max
Mn	1.48	1.53	2.00 max
P	0.020	0.020	0.07 min
S	0.309	0.316	0.07 min
Si	0.53	0.53	1.00 max
Ni	9.22	9.21	8.00 to 10.00
Cr	17.67	17.92	17.00 to 19.00
Mo	0.49	0.47	0.60 max
Cu	0.27	0.27	—

— not applicable to the standard.

Max = maximum.

Min = minimum.

Hardness Testing

Hardness tests were performed on 1.0-inch-thick cross sections removed from each rod. Tests were conducted using a 1/16-inch-diameter steel sphere using the Rockwell B scale. Figure 11 shows the locations of the 28 hardness tests taken on each rod cross-section. Test locations were laid out using a polar coordinate system and were selected to determine how the hardness varied through the radius of each rod. Sampling was generally performed near the center of the rod, the mid-radius, and near the outer perimeter. Test locations were determined based on ASTM E18, which requires that hardness readings be spaced at least 3 indent diameters apart, or 2.5 indent diameters from edges. All individual hardness measurements from both rods can be found in Appendix B.

Results from the hardness tests are compiled into Figure 12. In the plot, hardness values at a common radial distance were averaged and reported for each rod. The center and outer surface of the rods are shown on the figure as vertical dashed lines. Overall, both rods displayed hardness values ranging from 82-97 HRB. Rod 1 consistently showed slightly larger hardness values than Rod 2. This supports the tensile testing results which suggested that Rod 1 had larger yield and tensile strengths than Rod 2. Both rods exhibited a similar trend of increasing hardness from the center of the rod to the outer surface. The non-uniform hardness suggests there was some type of treatment process applied to the rods after rolling. Based on ASTM A 276 and considering the chemical analysis, tensile testing, and hardness tests, it appears the rods were cold-finished, though the exact process is unknown. Neither the 1949 or 1955 versions of ASTM A 276 specify any hardness requirements for Type 303 cold-finished steel. Both versions do specify minimum hardness values for chromium grade steels, but not for chromium-nickel grades, to which Type 303 belongs.

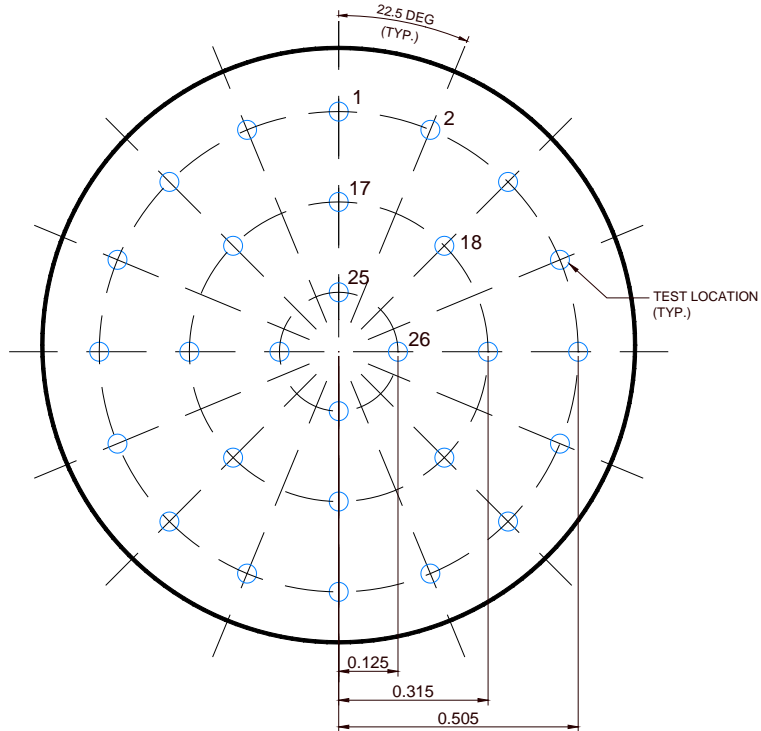


Figure 11. Schematic. Locations of hardness tests for Rods 1 and 2

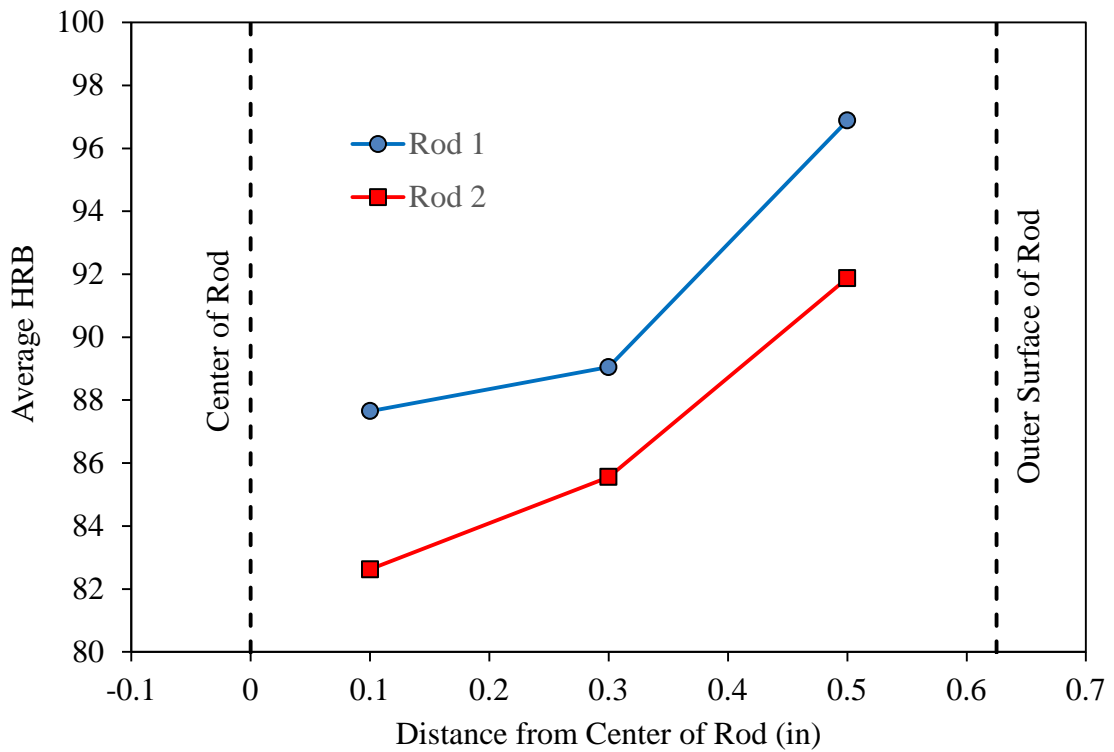


Figure 12. Graph. Constant radius average Rockwell B hardness of both rods.

METALLOGRAPHIC AND FRACTOGRAPHIC EXAMINATION

This chapter discusses the procedures and findings of the metallographic and fractographic examinations. Metallographic examination describes the analysis of crystal microstructures and presence of internal defects on select cross-sections of the rods. Fractographic examination is the analysis of fracture surfaces. In both cases, a high powered microscope is used.

PRELIMINARY EVALUATION

Before the fractured surfaces (F1 and F2) were cleaned, each was placed in the scanning electron microscope (SEM), and four typical areas were analyzed with the energy dispersive x-ray (EDX) detector. This detector has the ability to see elements that are present in the viewing area and represent them in a color contour plot. The areas were roughly at the mid radius at the 12, 3, 6, and 9 o'clock positions relative to how the specimen was loaded into the microscope. Figure 13 displays the elements detected through the EDX at a particular point on the fracture surfaces of Rod 1. For the purposes of scale, each image is roughly 0.045 inches square. The electron beam image represents the surface at high magnification; and it shows a mud-cracked looking surface where there are corrosion products. As expected of steel, the EDX detected alloying elements of iron, chromium, and nickel with oxygen on the surfaces, which indicates the amount of oxides. There were also traces of chlorine and bromine, which correlate with contaminants found in a marine environment such as seawater. These EDX spectra are considered "typical" for each of the rod fractures; that is, four positions were examined with the EDX on each rod, but the overall findings presented in Figure 13 was not significantly different between the eight positions examined.

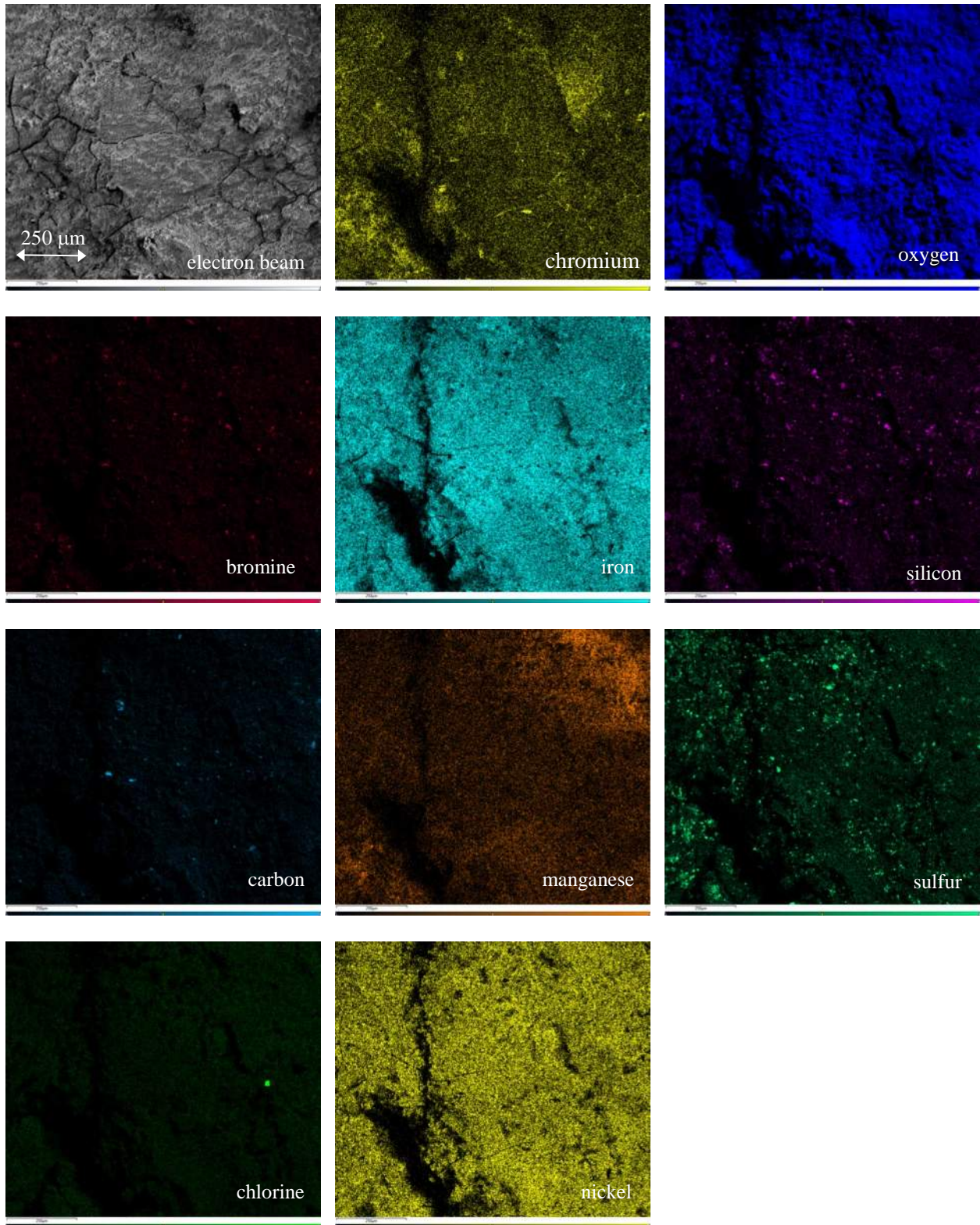


Figure 13. Image. EDX images of Rod 1 fracture surface (at 3 o'clock).

CLEANING

Figures 4 and 5 showed the as-received pictures of the fracture surfaces with heavy corrosion products. Before they could be analyzed further, the surfaces had to be cleaned. The first attempt at cleaning was to place the rods in an ultrasonic bath for 30 minutes in an alkaline solution; this was not effective in removing any of the corrosion product. A second attempt was made with Rod 1 to cathodically clean the surface in a sodium carbonate solution, with and without ultrasonic agitation, which also proved unsuccessful. In the third attempt, Rod 1 was cleaned using a solution of weak nitric and acetic acids. This was successful in removing the rust product and the final cleaned fracture surface can be seen in Figure 14. A less aggressive method was attempted on Rod 2 by continuing ultrasonic cleaning in the alkaline solution, though the rod was periodically removed and brushed with a toothbrush. Many cycles of brushing and ultrasonic cleaning resulted in the cleaned fracture surface in Figure 15.

After cleaning it was also quite evident that each rod had a multitude of cracks that could visibly be seen around the perimeter of the rods. Eight photos were taken around each rod perimeter to show these cracks; all of these photos are presented in Appendix A. The pictures were taken by starting at one position (denoted zero degrees) then each subsequent picture was taken by rotating the specimen 45 degrees about its longitudinal axis.

Both of the fracture surfaces appeared to be macroscopically brittle, but no clear initiation points could be identified. Since Rod 1 was cleaned better, it is easier to visualize the fracture surface having radial directionality. This can be further described with the assistance of Figure 16 which shows the cleaned fracture surface of Rod 1 and a side view of the Rod 1 fracture section. The fracture surface itself had obvious impact damage along one strip of the fracture surface outlined with a yellow line. The side view shows this area of impact damage that was likely the last ligament of the rod suffering final ductile overload. This is clear because of the obvious necking shown in the side view photo. As for the directionality of the fracture surface, there are no clear chevron marks pointing back to the initiation point, but overall the crack growth appeared to spiral around the center of the rod, beginning and ending from the ligament with the impact damage. The following sections will show that there were multiple cracks growing that likely coalesced, but it was the growth of the individualized cracks that appears to grow in a spiral that left this characteristic directionality on the fracture surface. The same directionality can be seen in Rod 2, though it is more difficult to see in Figure 15 since Rod 2 was not cleaned as thoroughly. There was also no evidence of a final overload or necking in Rod 2.



Figure 14. Photo. Rod 1 fracture surface after cleaning.

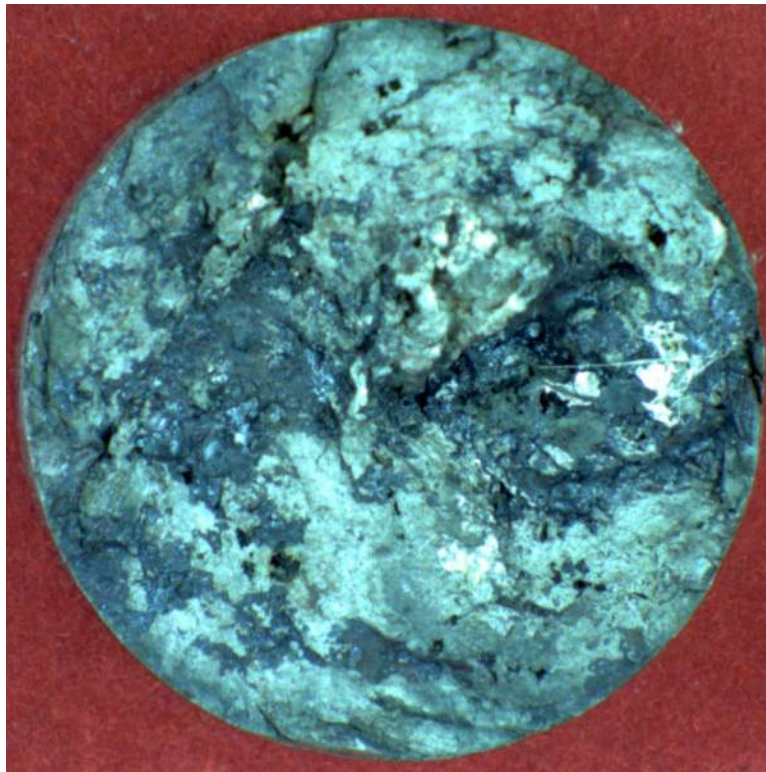


Figure 15. Photo. Rod 2 fracture surface after cleaning.

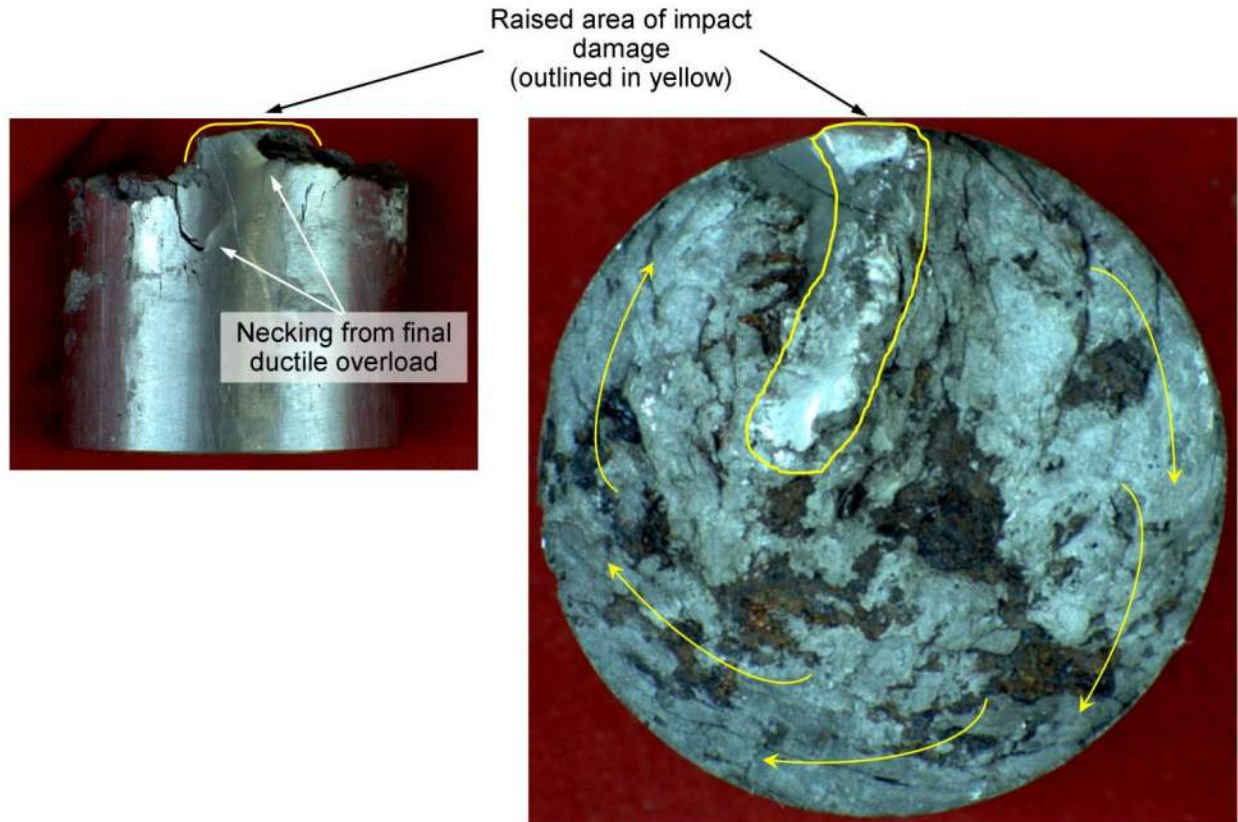


Figure 16. Photo. Directionality of fracture progression in Rod 1.

TRANSVERSE SECTIONS NEAR FRACTURES

When the Rod 2 fracture was saw cut from the overall rod, many cracks were observed on the cut edge. To investigate this further, an additional 3/16 inch thick cross-section was removed from the ends of the fracture sections of F1 and F2, then polished to expose any cracks. Figure 17 shows a schematic of where these transverse sections were removed. A suitable picture could not be attained in the polished condition because of the surface reflectivity; therefore the pictures shown in Figure 18 from each rod transverse section have been roughened with 60 grit sandpaper. The picture of the transverse sections clearly show that there are multiple cracks originating from various points on the surface and into the depth of the rod, and that the group of cracks in each section are oriented in a general clockwise direction around the rod center.

Figure 19 is a 50x magnification micrograph of an area near the outer perimeter of Rod 2 taken with an inverted microscope. The larger crack near the top of this image is one that is more visible in Figure 18. However, at this higher magnification, finer “tree-root,” branching cracks can be seen growing through other parts of the cross-section. The polished surface was electrolytically etched for 30 seconds in oxalic acid and a micrograph taken near the ends of a “tree-root” crack at 50x magnification are shown in Figure 20. At this low magnification, the multiple branching of the cracks is very evident; this is typical of a stress corrosion cracking mechanism. Increasing the magnification to 500x, as shown in Figure 21, reveals that the cracks are both inter- and trans-granular (i.e., the cracks propagate along grain boundaries, and through

grains), another typical feature of SCC in austenitic stainless steels. The round, black inclusions seen in this micrograph are the manganese sulfide inclusions to be discussed in a following section. These features discussed thus far are not unique to just Rod 2, the images from Rod 1 look very similar and are not shown for brevity.

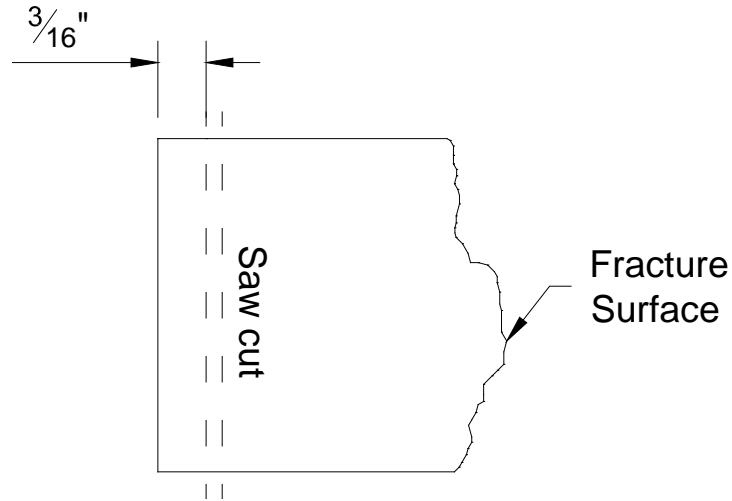


Figure 17. Schematic. Cut plan for transverse slices of F1 and F2 fracture sections.

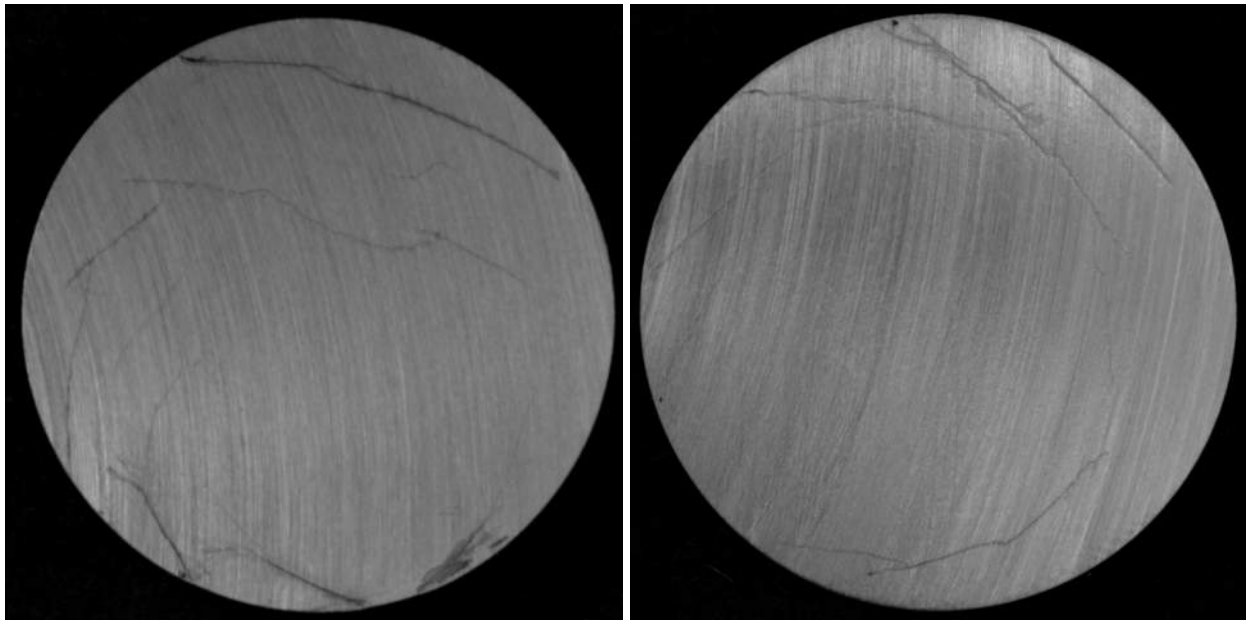


Figure 18. Photo. Transverse cracks in fracture surface sections; Rod 1 (left), Rod 2 (right).

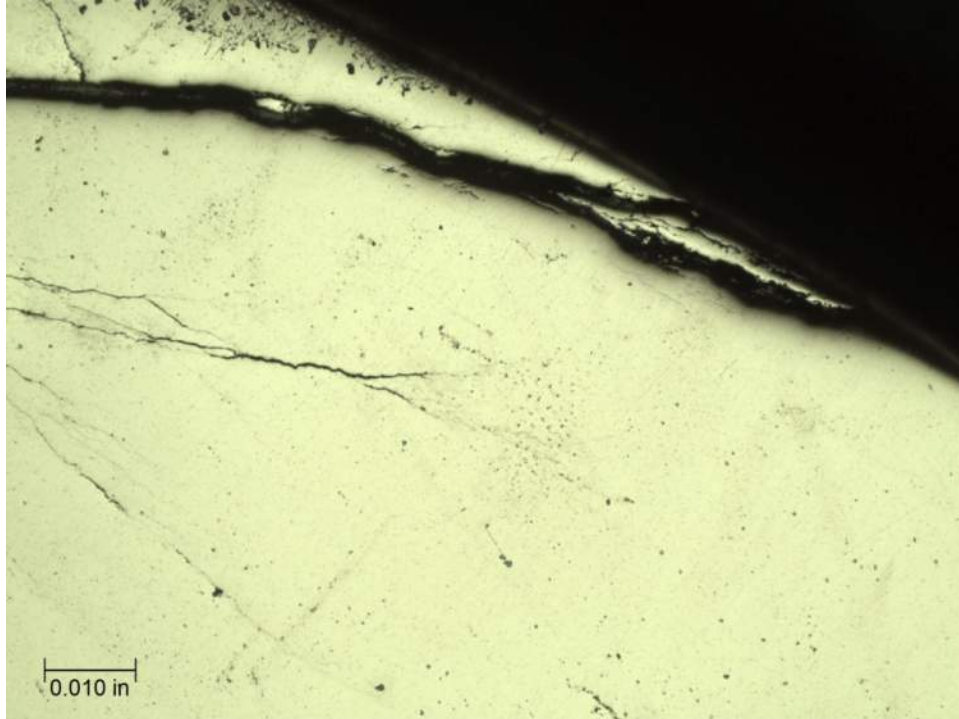


Figure 19. Photo. Rod 2 polished image showing major crack and smaller branching cracks.

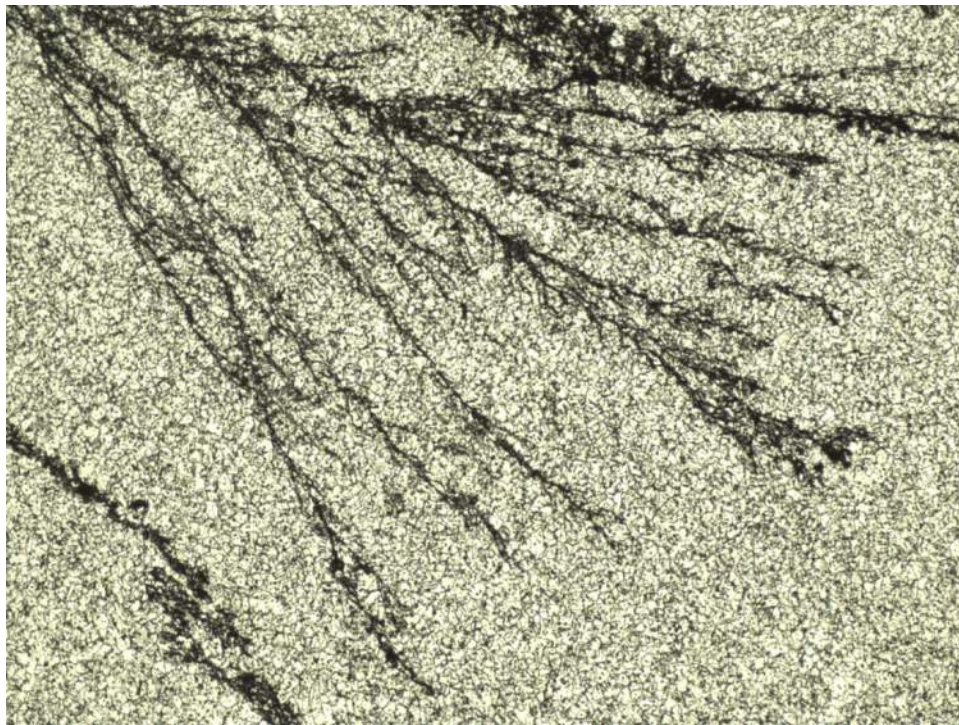


Figure 20. Photo. Rod 2 transverse section at 50x magnification. Electrolytic oxalic acid etch for 30 s.

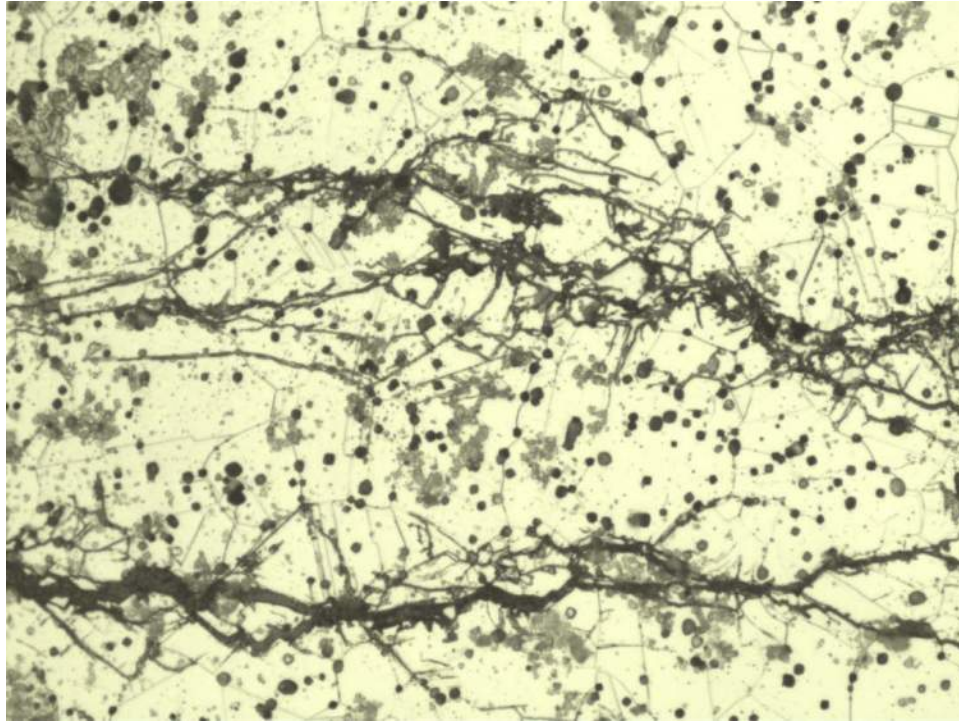


Figure 21. Photo. Zoomed in view of a crack branch in Figure 20 at 500x magnification.

TYPICAL MICROSTRUCTURE

Transverse and longitudinal sections were polished and etched to reveal the microstructure. The transverse sections were the M1 and M2 sections as depicted in Figures 7 and 8. The longitudinal sections were taken from the ends which were gripped during the tensile testing of the T1-F and T2-F specimens. The microstructures between the two rods were identical and thus only the microstructure from Rod 2 will be presented. Figure 22 shows the transverse microstructure at 200x magnification after a 30 seconds electrolytic etch in oxalic acid. The grain boundaries can be faintly seen, but the most dominant feature in the micrograph is the black, round inclusions speckled throughout the transverse cross-section. The longitudinal section in Figure 23 shows a similar grain structure however the black inclusions are elongated in the longitudinal axis of the rod. The inclusions were analyzed with the EDX (see Figure 24) and were confirmed to be manganese sulfide. Their amount is not surprising for this free-machining grade of stainless steel. Manganese sulfides are typical inclusions in steel, and their transverse and longitudinal shapes are typical for a hot-rolled, or cold-drawn product where they become elongated in the direction of roll or drawing.

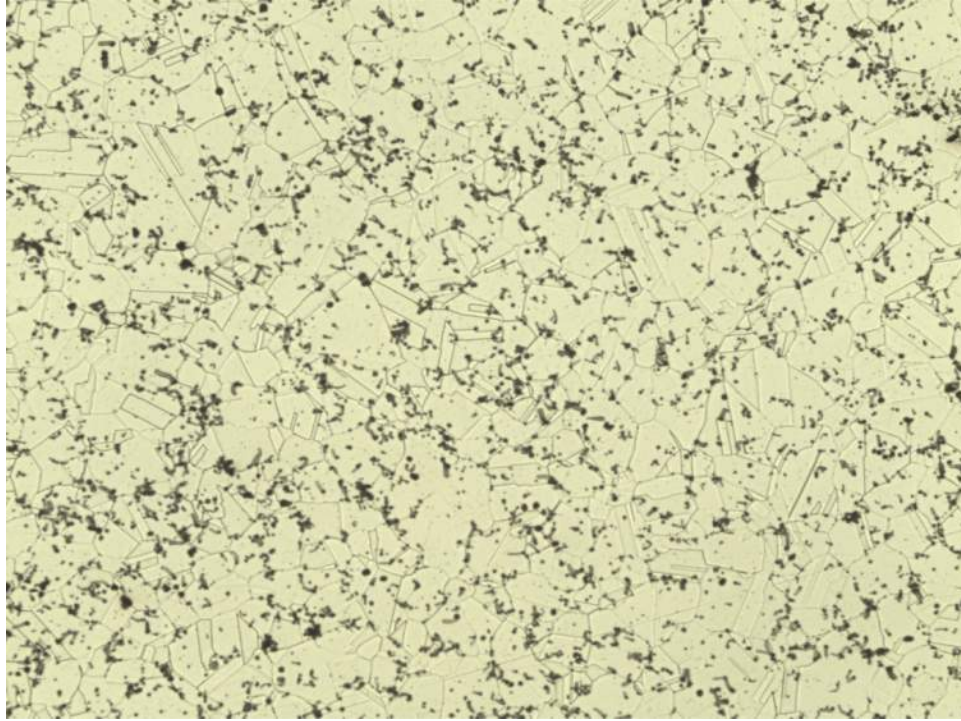


Figure 22. Photo. Typical grain structure on M2 section at 200x magnification after 30 second electrolytic etch in oxalic acid.

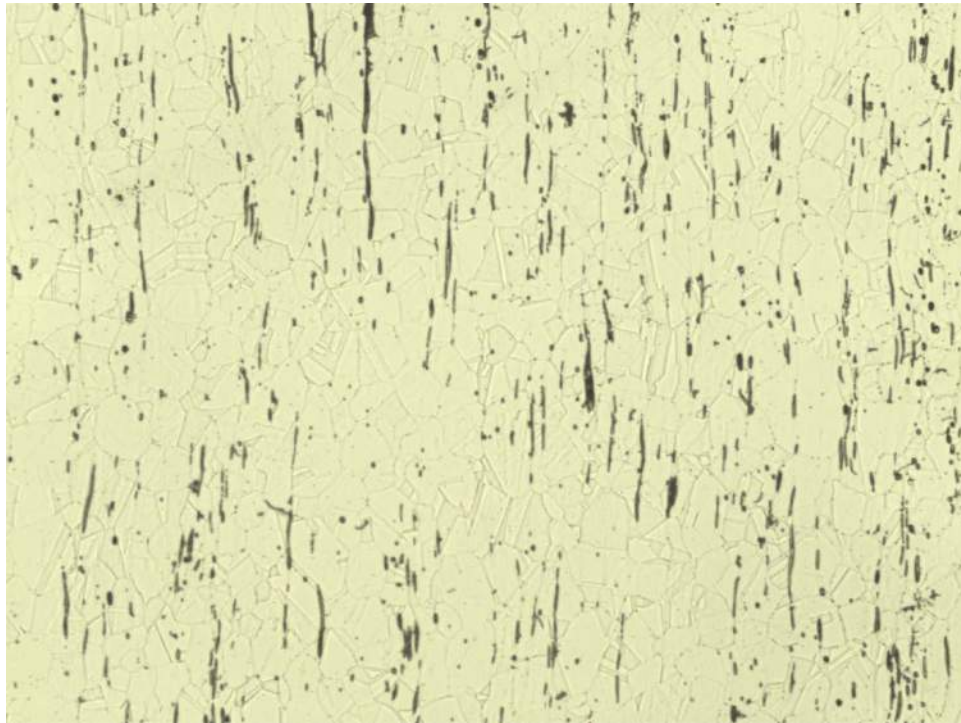


Figure 23. Photo. Longitudinal microetch from Rod 2 at 200x magnification after 30 s. electrolytic etch in oxalic acid.

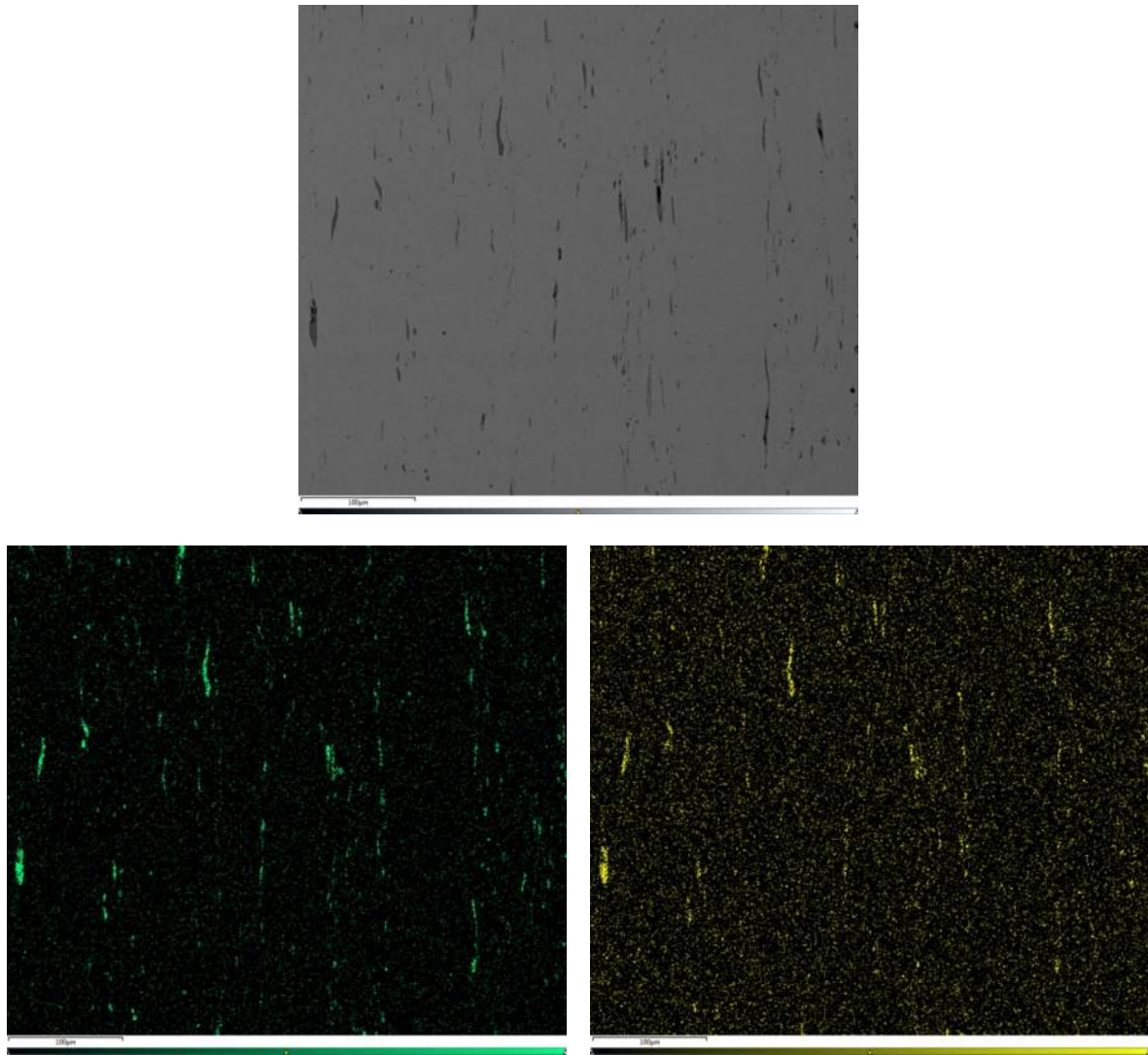


Figure 24. Image. Polished longitudinal section viewed with SEM and EDX, electron beam image (top), sulfur image (bottom-left), manganese image (bottom-right).

FRACTOGRAPHY OF FRACTURE SURFACES

The fracture surfaces were heavily corroded and it was presumed that any fine features that could help to identify the mode of fracture had been lost. Both rod surfaces were analyzed in the SEM under high magnification. Only the images from Rod 2 are presented because the acid cleaning of the Rod 1 surface appeared to etch the surface more than was apparent in Rod 2. A variety of positions on the fracture surface were examined and each position was unique; however, evidence of both trans- and intergranular fracture could be seen. Two typical images of the surface are presented in Figures 25 and 26. Figure 25 shows more features of transgranular, or cleavage fracture, oriented around a corrosion pit (white arrows point to some locations that have more cleavage features). Figure 26 shows grain facets in the center vertical section that is more in focus, which is indicative of intergranular fracture. White arrow points to the exposed grain facets that look more like “rock candy.” The fractography confirms the findings presented in

figures 18 and 19 that the cracks grew in a mixed mode between trans- and intergranular cracking.

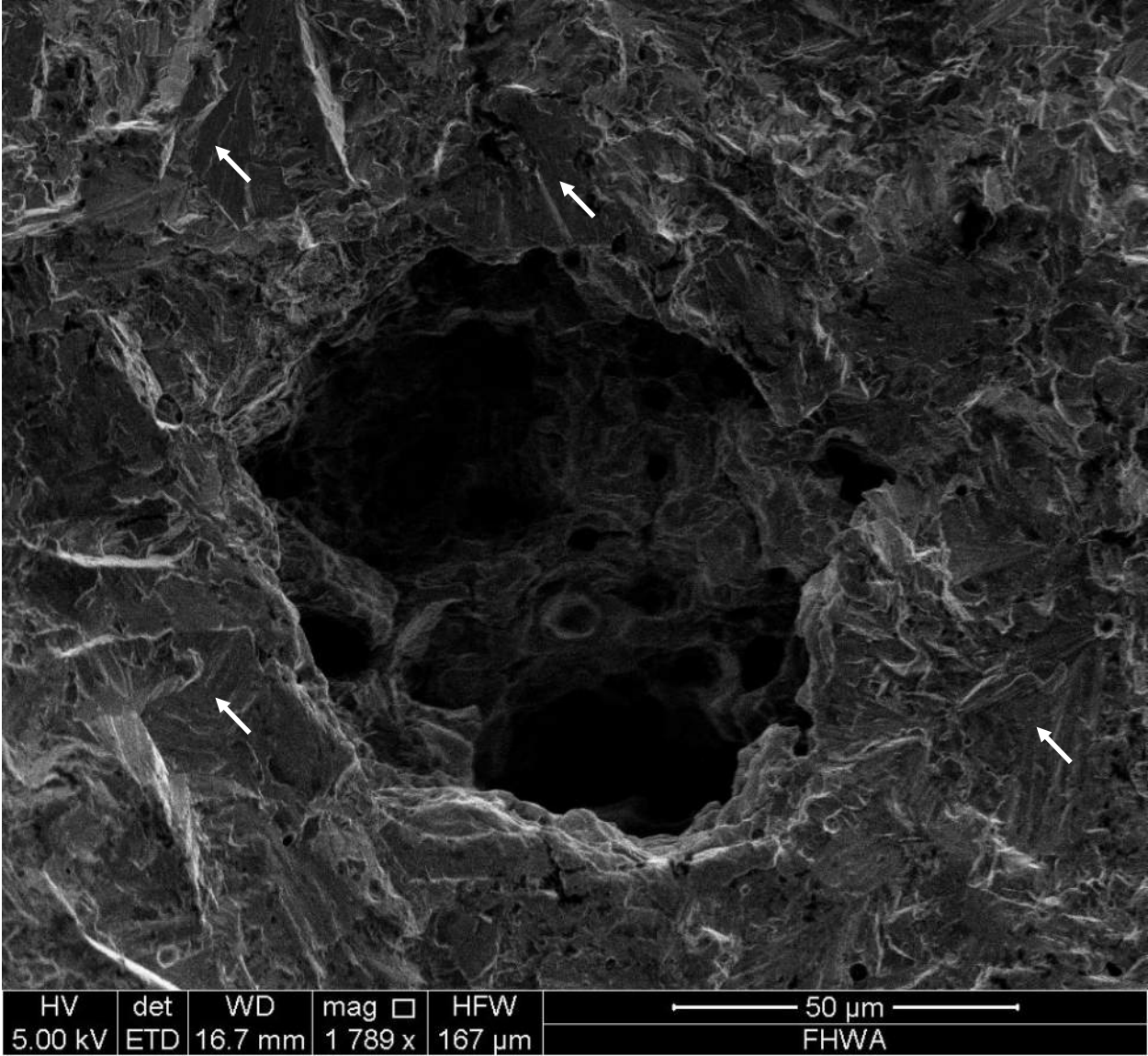


Figure 25. Rod 2 cleaned fracture surface showing more features of transgranular fracture.

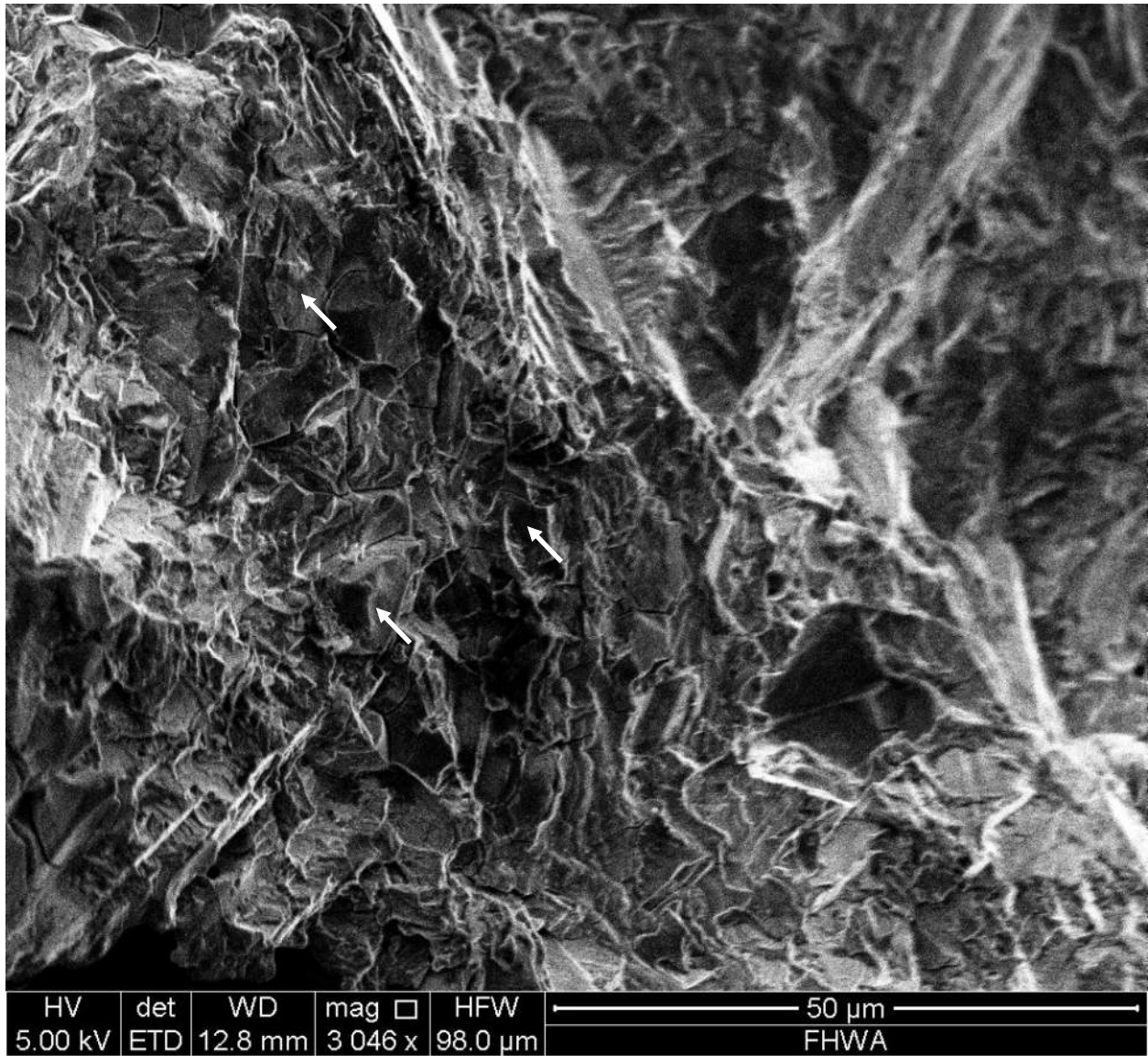


Figure 26. Rod 2 cleaned fracture surface showing more features of intergranular fracture.

CHLORIDE ANALYSIS OF TUNNEL CONCRETE

The prior chapter provided evidence that the hanger rods fractured from stress corrosion cracking, a phenomena that affects austenitic stainless steels (like the type 303 stainless used in the tunnels) in a chlorine rich environment. However, the surface chloride measurements on the rods revealed relatively low concentrations of chloride, and another source of the chlorine was sought with the hypothesis being that it was trapped within the concrete. As the State was concerned about the extent of corrosion on the rods that have not broken they provided samples of concrete that was cut from locations around hanger rods to help better understand the distribution of chloride throughout the tunnel. Seven samples of concrete cut from the topside of the ceiling were received from the Hawaii DOT. Accompanying the samples were two documents. One had six pictures (Figures 27 to 32) showing the locations where six of the seven samples were removed. The other is a drawing of the hanger repairs in the tunnel, (Figure 33). The drawing had blue circles at 100, 1600, 2200, 2400 feet inbound (IB) and 500, 1500, 2400 outbound (OB) tunnel locations. This chapter presents the findings of the chloride analysis conducted on the concrete samples.

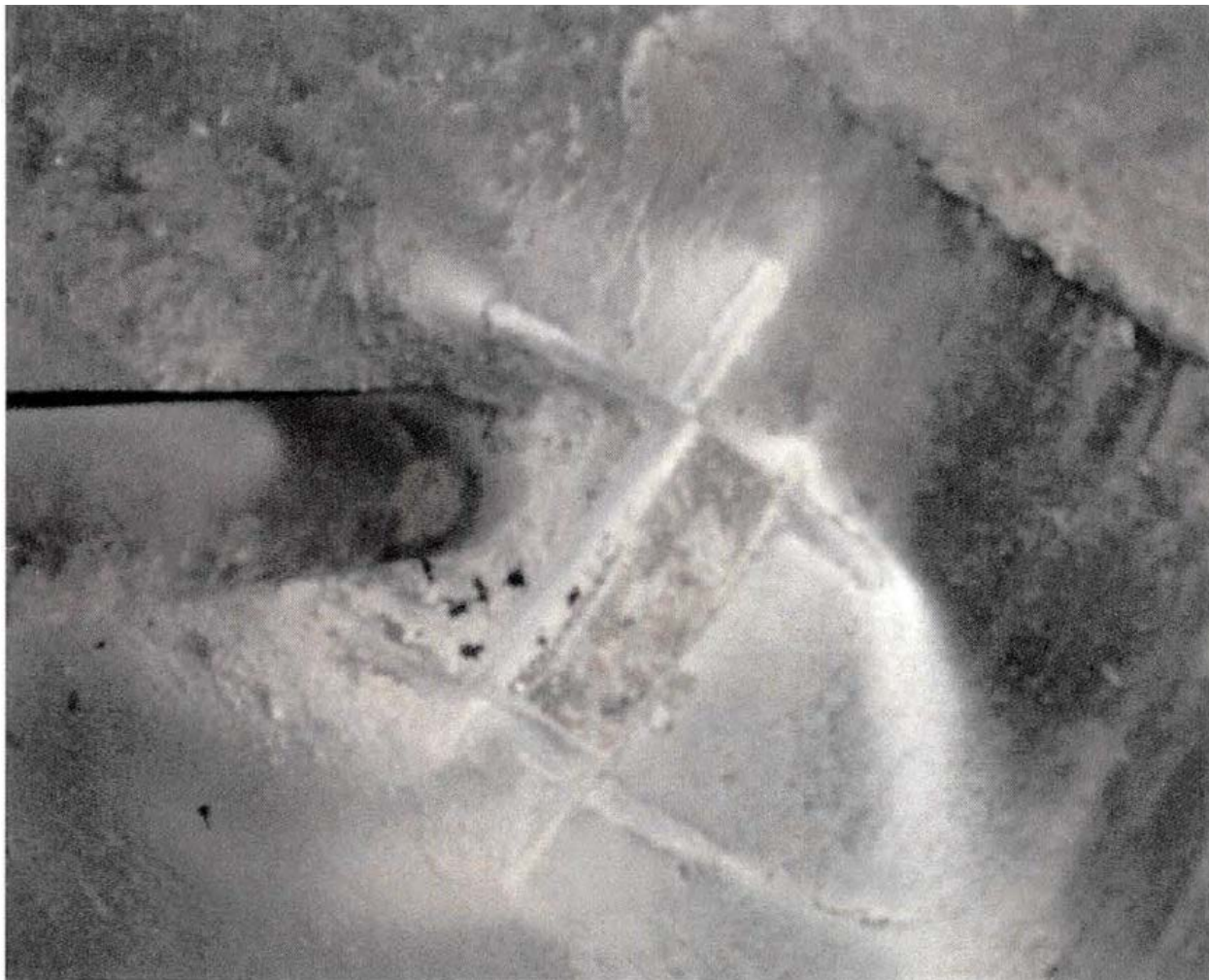


Figure 27. Rod #13 - Inbound (IB) Wilson Tunnel



Figure 28. Rod #31 IB Wilson Tunnel



Figure 29. Rod #34 - IB Wilson Tunnel

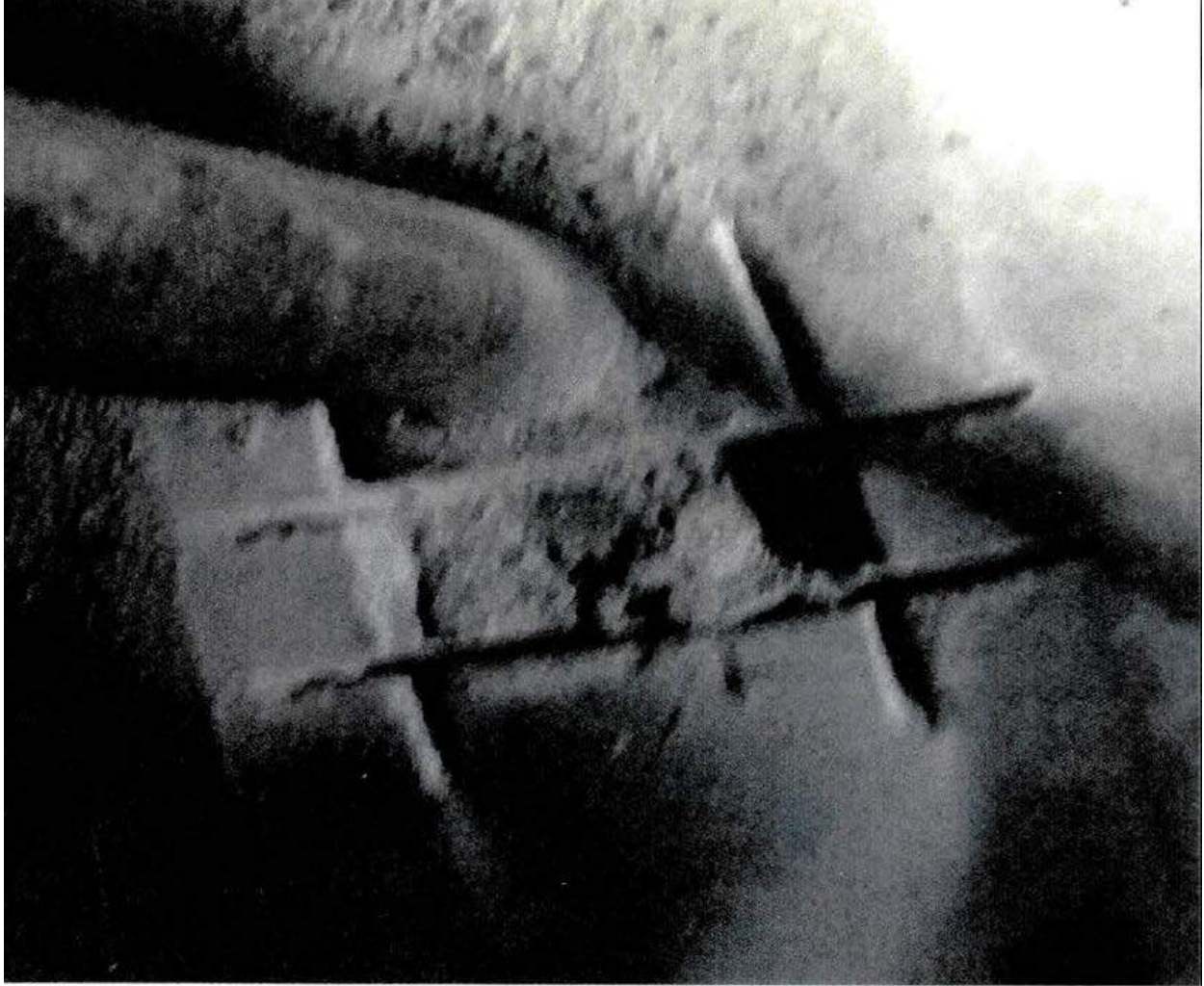


Figure 30. Rod 40 - IB Wilson Tunnel



Figure 31. Rod #18 - Outbound (OB) Wilson Tunnel



Figure 32. Rod #40 OB - Wilson Tunnel

The samples were weighed between 50 and 100 grams. They were broken with a hammer, then placed in the Retsch puck mill and ground to a fine powder. The total chloride content was determined in accordance with ASTM C1152.

The results in Table 5 show that all seven samples contained chloride. Since the test was carried out after acidification, the result gives the total chloride present whether they are bound, or are soluble and available to cause corrosion.

Table 5. Chloride Content of Concrete Samples

Rod #	FHWA Reference	Sample Weight (gram)	Chloride by % Weight of Concrete
13 IB	TSA1/19/1	52.62	0.161
18 OB	TSA1/19/2	105.48	0.184
20 IB	TSA1/19/3	58.67	0.137
31 IB	TSA1/19/4	50.55	0.151
34 IB	TSA1/19/5	53.5	0.202
40 IB	TSA1/19/6	80.3	0.170
65 OB	TSA1/19/7	68.39	0.058

To put the concrete chloride concentrations into context, a couple facts will be presented. The facts pertain to steel reinforcing bars in concrete, which is admittedly different than the stainless steel hanger rods from the tunnel, but will help provide a reference. ASTM C1152 states that the initiation of corrosion occurs when the chloride concentration at reinforcing steel exceeds the threshold concentrations typically in the range of 0.05 to 0.1% by weight of concrete. This however only applies to steel reinforcing bars and no information is given on a threshold for stainless steel. The National Ready Mixed Concrete Association (NRMCA) suggests that between 50 and 75% of the total chloride in concrete will be water soluble and will impact the corrosion process. The TFHRC has also been involved in the deck assessment of the Arlington Memorial Bridge in Washington, DC which is in very poor condition. This bridge was built in 1932 and is subjected to frequent deicing chemicals. ASTM C1152 analysis of cores removed from the deck found chlorine content in the range of 0.019-0.048% at the level of the top mat of reinforcing bars. Therefore, the concentrations measured from the ceiling slab of the Wilson Tunnel are certainly high enough to cause reinforcing bars to corrode, and were at places up to 10 times higher than that measured in an 80 year bridge deck subject to deicing chemicals.

It appears that the chlorine driving the SCC phenomena in the stainless steel hanger rods is trapped within the concrete ceiling slab. This would also explain why the fractures are only found at the concrete interface with the rod, and why SCC cracks were only limited to within approximately one inch of the concrete interface. There are only two plausible explanations of how the chlorine got there. One, Hawaii being in a marine environment can have trade winds

carry salt from the ocean inland. Over the lifetime of the tunnel, airborne salts can deposit in the upper plenum, and be absorbed into the concrete through the wet/dry cycles. The EDS analysis of the broken rod end shows the presence of both chloride and bromide (The ASTM C1152 test method employs titration with silver nitrate and therefore it does not differentiate between chloride and bromide since they react similarly). The only place that chlorine and bromine could have come from is seawater. Two, in the era when the tunnel was constructed, beach sand may have been used to make the concrete, and this sand would have inevitably had a substantial concentration of chlorine². TFHRC cannot definitively rule out which scenarios is correct, although it is believed that beach sand in the concrete mix was the most likely reason.

² <http://www.deseretnews.com/article/695205225/Hawaii-concrete-firms-forced-to-import-sand.html?pg=all>

CONCLUSIONS

The results of the mechanical, chemical, microstructural, and concrete analyses lead to the following conclusions:

- Based on chemical test results the hanger rods were likely a type 303 stainless steel based on comparison with the tentative edition of ASTM A 276 “*Hot Rolled and Cold Finished Corrosion Resisting Steel Bars*” published in 1949, the timeframe of construction of the tunnel. The type 303 stainless steel purposely has a large amount of sulfur which makes the steel easier to machine, but virtually unweldable.
- The tensile properties of both rods had yield strengths around 70 ksi and tensile strengths around 100 ksi. These are higher than expected for a type 303 stainless steel in the annealed condition, and it is assumed that the hanger rods were cold-finished (likely cold drawn). Hardness testing also supported the belief that the rods were cold-finished.
- Each rod had clear evidence of pitting corrosion along its entire length.
- Each rod had multiple branching cracks that could be identified along the perimeter of the rods and on transverse cross-sections near the fracture, which is an indication of stress corrosion cracking (SCC). Cracks appear to originate from corrosion pits and propagate through both grains and their boundaries (i.e., inter- and transgranular) which is typical for SCC in austenitic stainless steels.
- There was evidence of chlorine and bromine on the fracture surfaces which likely results from the marine environment of Hawaii.
- The level of chloride found in the concrete was up to ten times higher than found in concrete for the Arlington Memorial Bridge in Washington, D.C., which has been likely subjected to harsh deicing salts for prolonged periods possibly dating back to its construction in 1932. It is believed that this high level of chloride was likely from the use of beach sand in concrete mix.

RECOMMENDATIONS

The following recommendations are presented for consideration for Hawaii DOT:

1. Since 21 other hanger rod were found to be fractured, it should be assumed that the remaining intact hanger rods have some level of Stress Corrosion Cracking (SCC); as such, it may only be a matter of time before the remaining rods fracture. An in-depth inspection of all hanger rods is recommended. Dye penetrant testing (PT) is advised. The corrosion product should be cleaned away before PT using water and steel wool. The cracks could be seen with the naked eye within about 1 inch of the fracture surface for the two rods in this analysis, and PT should be used to assist this visual inspection within the plenum.
2. A redundancy analysis should be conducted of the ceiling slab and hanger system to determine the impact of subsequent rod failures. This analysis can be used to determine when a “critical finding” needs to be reported to the FHWA as per the requirements of the National Tunnel Inspection Standards.
3. Austenitic stainless steels should be avoided for future use in high chloride environments because of their susceptibility to pitting and stress corrosion cracking. Hawaii, being a marine environment, certainly has the susceptibility to have high chloride concentrations. Type 303 stainless has the lowest resistance to pitting corrosion of all the austenitic stainless steel grades and represents the last choice austenitic steel for this environment. However, it took 60 years for the fractures to be observed indicating that the chloride charge in the environment is not as high as expected, and even though the lowest grade of austenitic was chosen, it probably met the design life intent for the period in which it the tunnel was designed. The State should consider a duplex grade of stainless for possible future retrofits as they have higher resistance to SCC than the austenitic grades. However, if austenitics are continued, consider using Type 316L as it has more resistance to pitting corrosion and SCC than Type 303 which has a demonstrated life of approximately 60 years in this environment.
4. Consider performing a ventilation study using computational fluid dynamics to model the air flow in the tunnel to determine if the ceiling slab can be removed altogether to eliminate the possibility of the overhead structure from failing and falling onto traffic below. This option could serve to eliminate the use of hangers all together along with the important safety concerns for overhead structures.
5. In the extreme, consider abandoning all existing hanger rods and retrofit the tunnel with new hanger rod(s). When retrofitting, use inert material between the replacement rod(s) and the contaminated concrete to prevent contact of the new rod(s) with chlorine-rich concrete.
6. To confirm the extent of chlorine contamination throughout the thickness of the concrete, consider sampling of the ceiling slab and liner at more locations along the length of the tunnel. This data could then confirm whether the chlorine was present from construction (e.g. beach sand used in the mix), or from the accumulation of airborne salts. If the data

show uniformly high chlorine concentrations everywhere, this would substantiate the beach sand theory and raise concerns for the rebar used in the concrete ceiling.

APPENDIX A – ROD SURFACE CRACKS

This appendix shows pictures taken around the perimeter of each rod section containing the fracture surface. The first picture taken of each rod section is referred to as the zero degree position, and then the subsequent seven pictures for each rod section are taken after rotating the section 45 degrees about its longitudinal axis. Visually, many cracks and pits can be seen on the outer perimeter; however, black arrows are used to highlight those that are cracks (as some are faint and could be confused with scratches), and orange arrows call out corrosion pits.

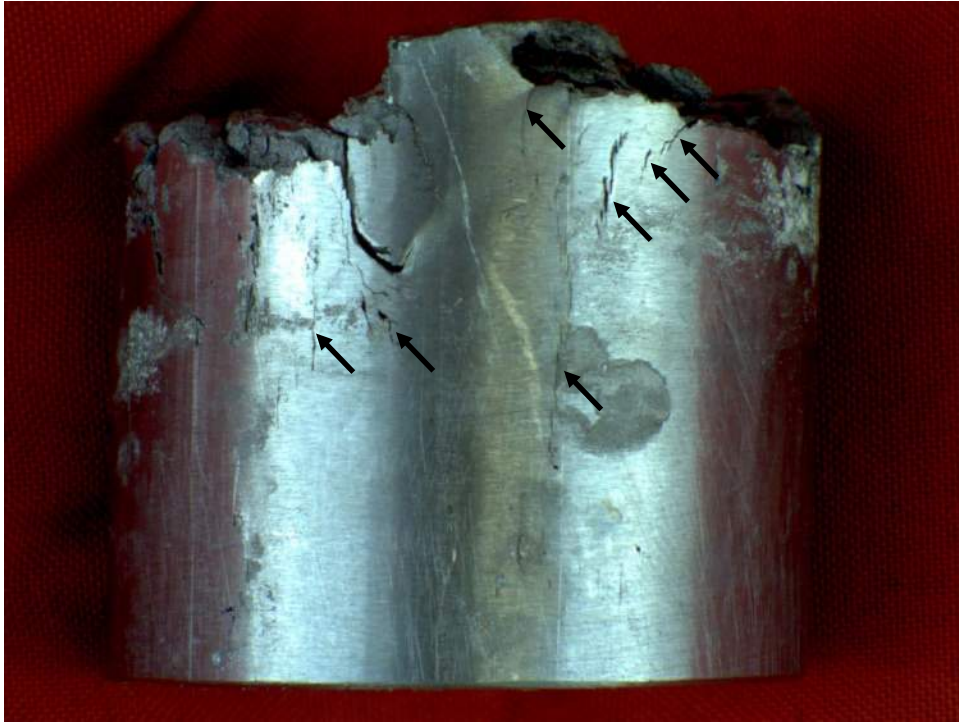


Figure 34. Photo. Rod 1 at zero degrees.



Figure 35. Photo. Rod 1 at 45 degrees.

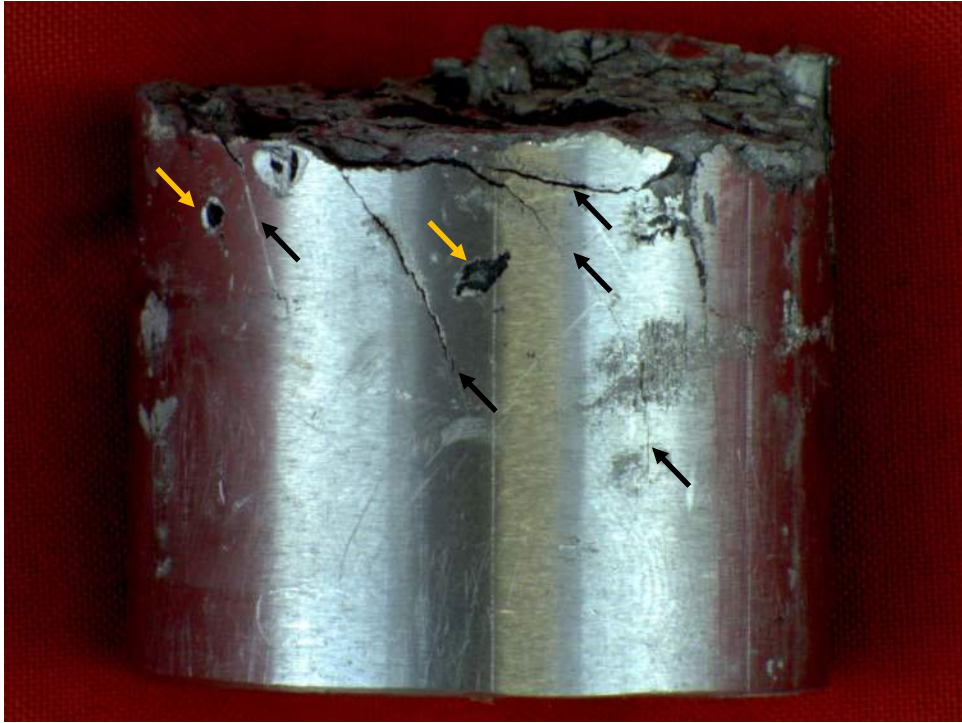


Figure 36. Photo. Rod 1 at 90 degrees.



Figure 37. Photo. Rod 1 at 135 degrees.



Figure 38. Photo. Rod 1 at 180 degrees.

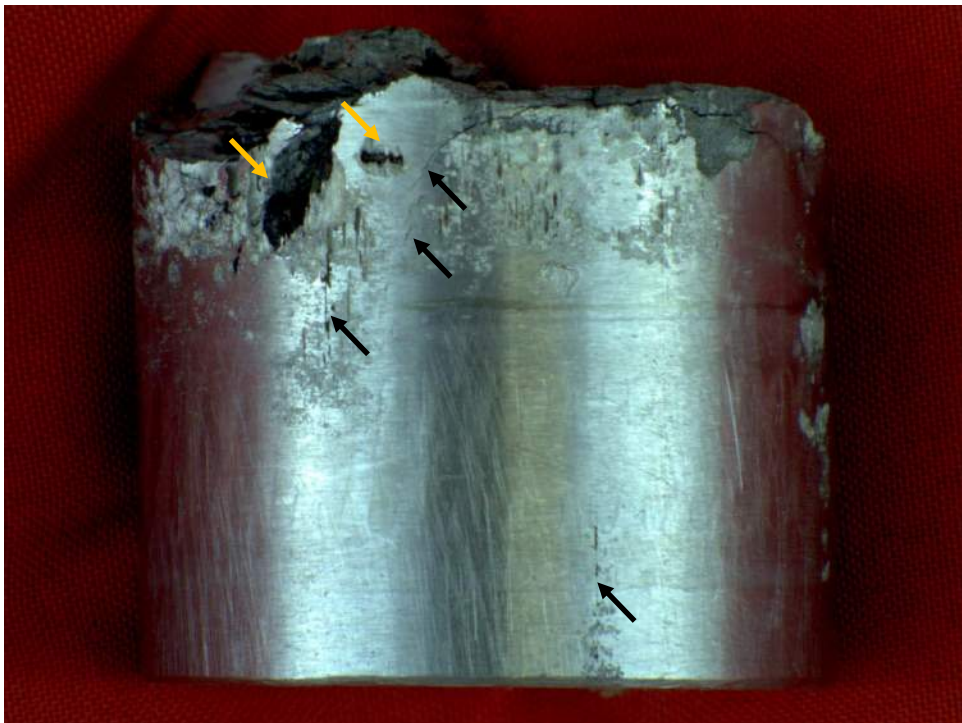


Figure 39. Photo. Rod 1 at 225 degrees.



Figure 40. Photo. Rod 1 at 270 degrees.

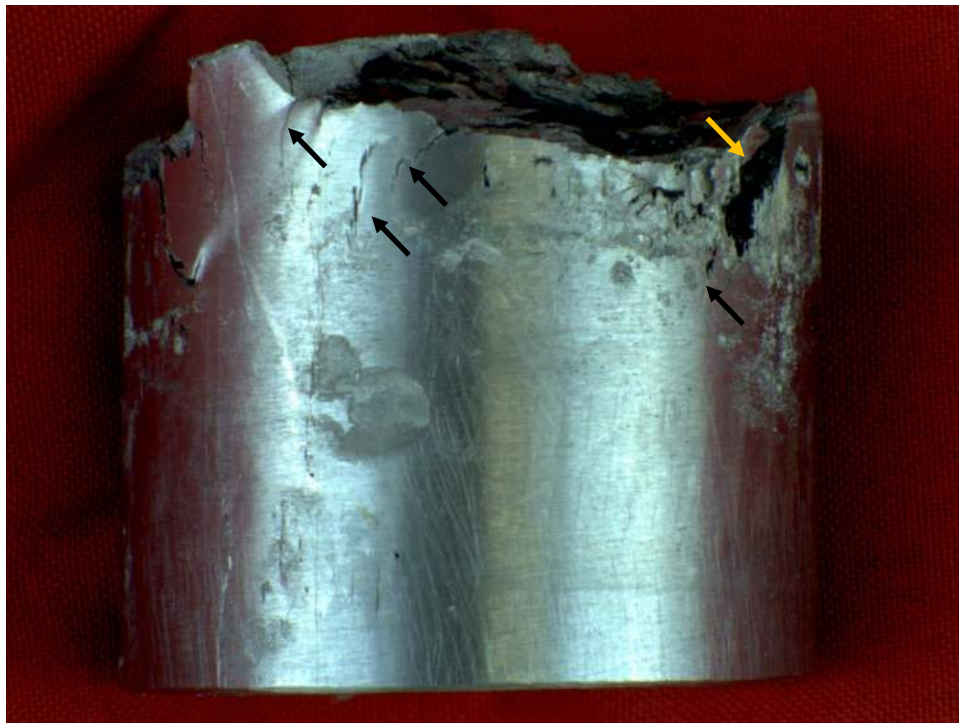


Figure 41. Photo. Rod 1 at 315 degrees.

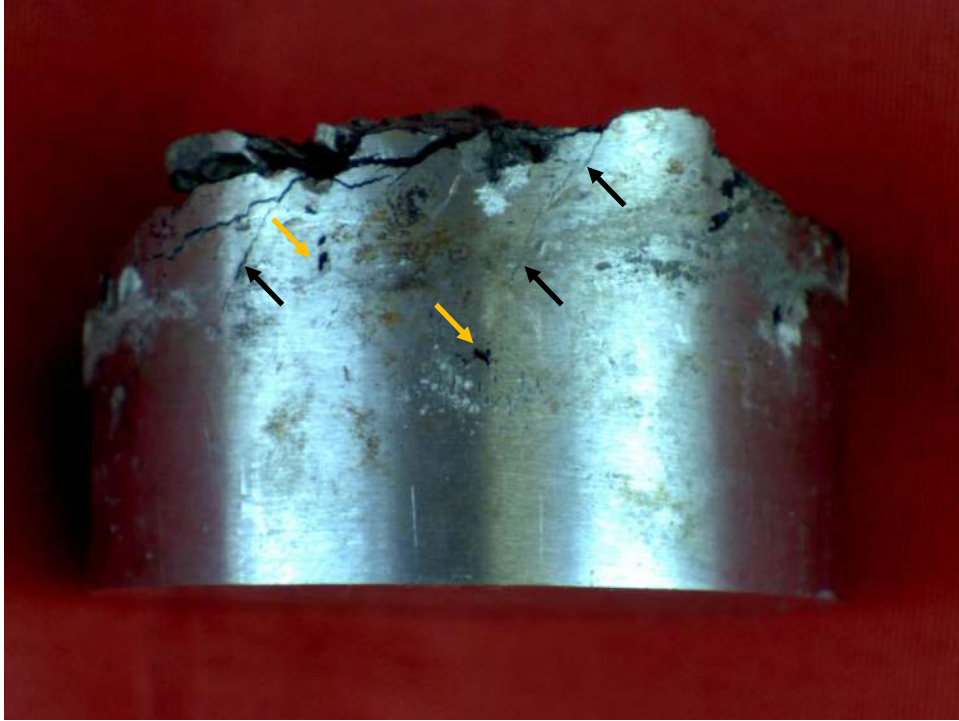


Figure 42. Photo. Rod 2 at zero degrees.

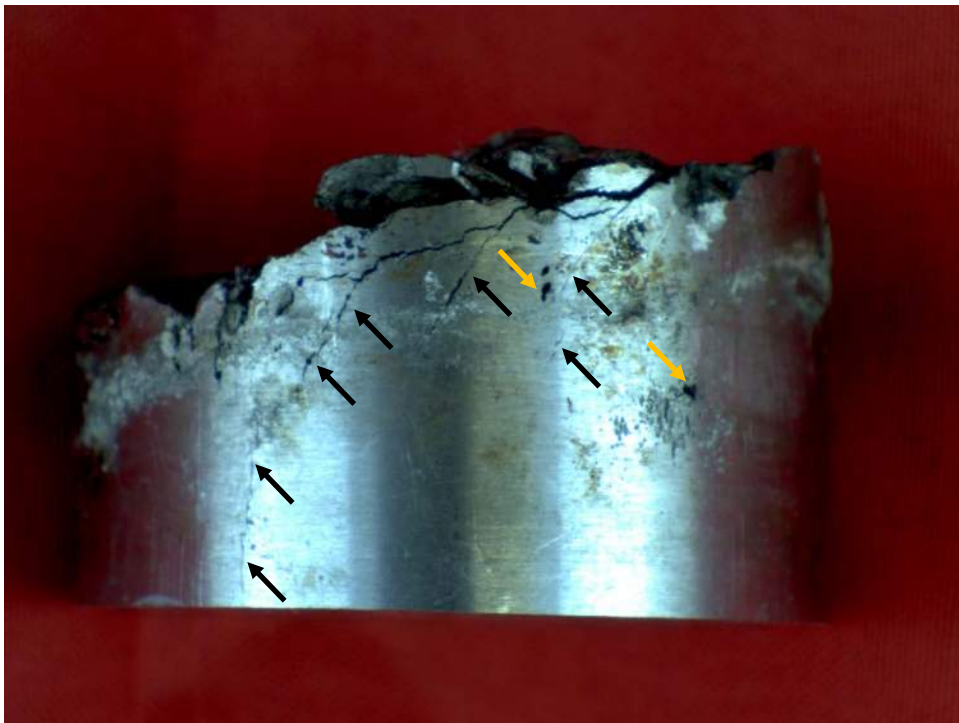


Figure 43. Photo. Rod 2 at 45 degrees.



Figure 44. Photo. Rod 2 at 90 degrees.

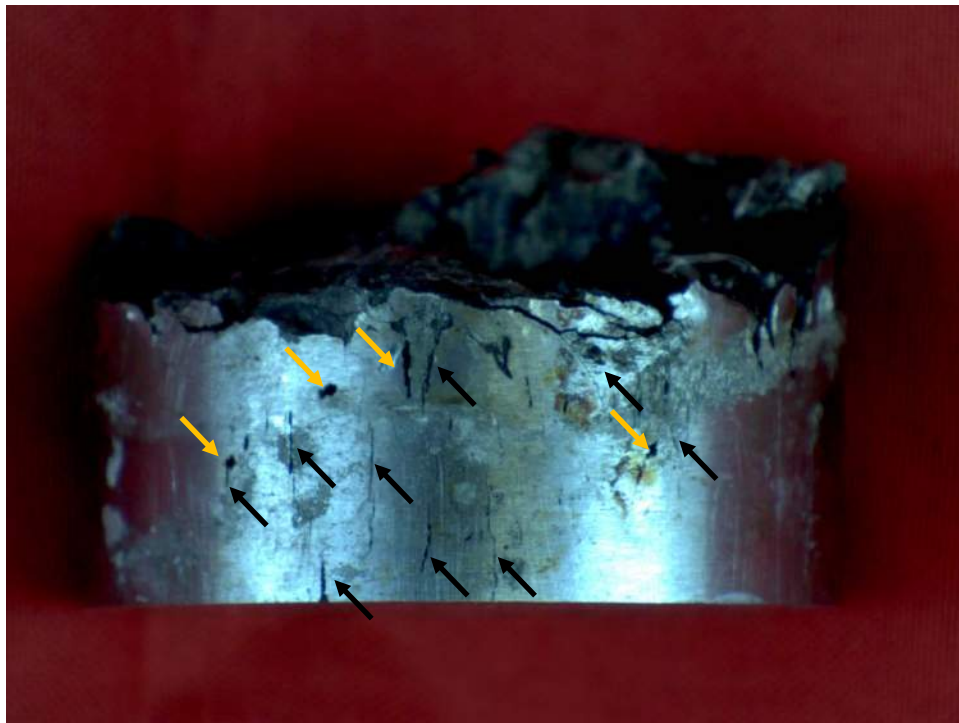


Figure 45. Photo. Rod 2 at 135 degrees.



Figure 46. Photo. Rod 2 at 180 degrees.

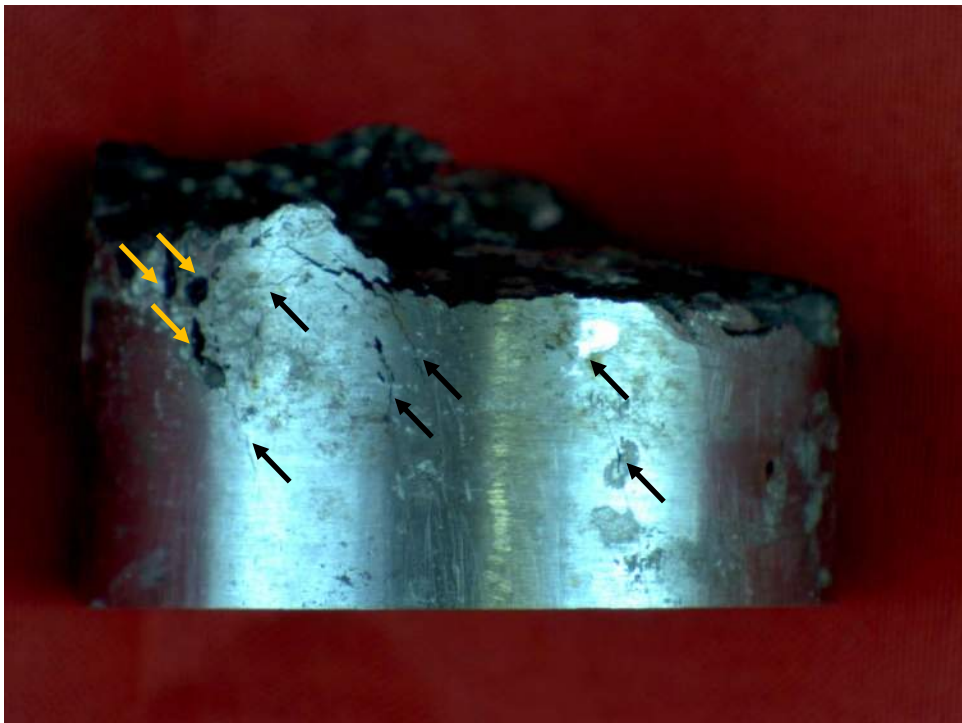


Figure 47. Photo. Rod 2 at 225 degrees.

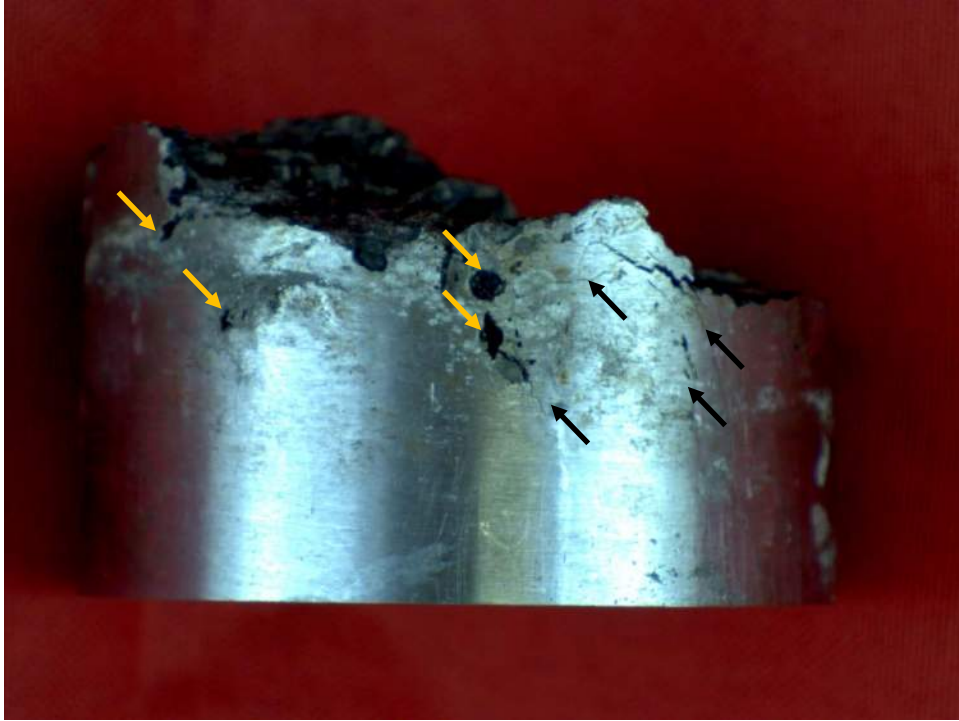


Figure 48. Photo. Rod 2 at 270 degrees.

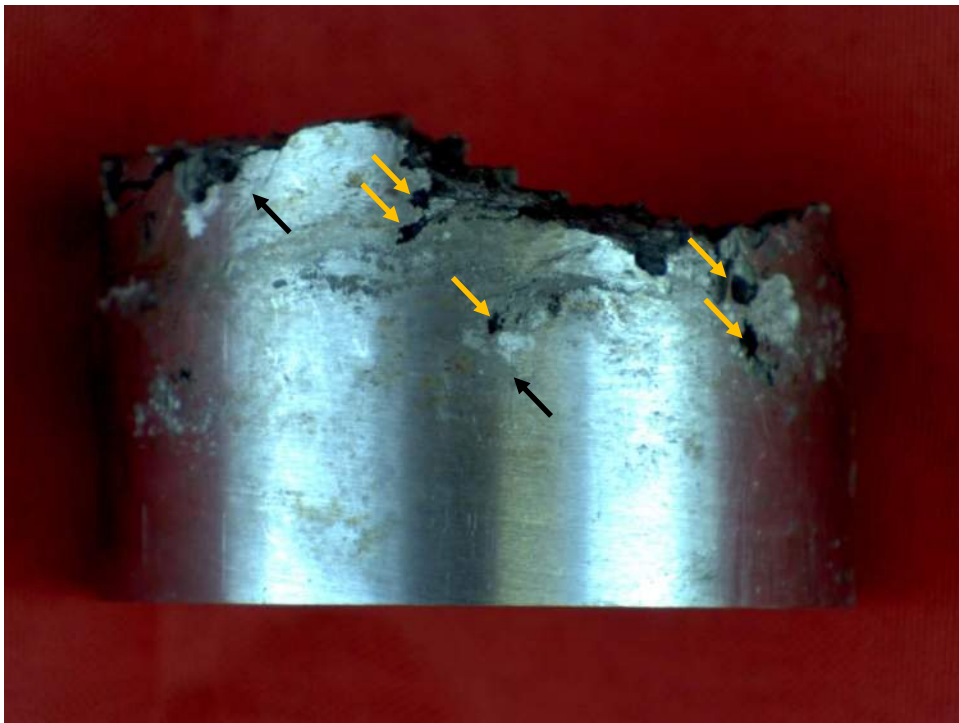


Figure 49. Photo. Rod 2 at 315 degrees.

APPENDIX B – TABLE OF ROCKWELL B HARDNESS TEST RESULTS

This appendix contains a table of data representing the raw hardness measurements taken on Rods 1 and 2. The location numbers in the table correlate to those shown in Figure 11, but additional columns are provided in the table to represent the polar coordinates of each hardness test. The Rockwell B hardness scale was used for these measurements.

Table 6. Rockwell B hardness test results for Rods 1 and 2

Location	Rod 1 HRB Value	Rod 2 HRB Value	Polar Coordinate Radius (inch)	Polar Coordinate Angle (degree)
1	98.25	95.89	0.505	0.0
2	98.54	95.08	0.505	22.5
3	97.87	91.87	0.505	45.0
4	97.77	89.28	0.505	67.5
5	95.32	89.91	0.505	90.0
6	95.50	92.32	0.505	112.5
7	97.59	92.59	0.505	135.0
8	99.06	92.88	0.505	157.5
9	98.73	92.52	0.505	180.0
10	96.93	92.70	0.505	202.5
11	97.43	90.88	0.505	225.0
12	96.77	90.26	0.505	247.5
13	97.37	91.54	0.505	270.0
14	94.20	89.33	0.505	292.5
15	93.48	90.37	0.505	315.0
16	95.30	92.61	0.505	337.5
17	88.27	88.06	0.315	0.0
18	90.52	86.20	0.315	45.0
19	88.71	84.60	0.315	90.0
20	88.47	85.69	0.315	135.0
21	89.52	83.51	0.315	180.0
22	88.97	84.39	0.315	225.0
23	88.67	85.48	0.315	270.0
24	89.27	86.52	0.315	315.0
25	87.03	84.37	0.125	0.0
26	87.20	82.18	0.125	90.0
27	89.32	82.27	0.125	180.0
28	87.05	81.67	0.125	270.0

REFERENCES

1. ASTM E8/E8M. (2013). "Standard Test Methods for Tension Testing of Metallic Materials," *Book of Standards Volume 03.01*, ASTM International, West Conshohocken, PA.
2. ASTM E1086. (2014). "Standard Test Method for Analysis of Austenitic Stainless Steel by Spark Atomic Emission Spectrometry," *Book of Standards Volume 03.05*, ASTM International, West Conshohocken, PA.
3. ASTM E1019. (2011). "Standard Test Methods for Determination of Carbon, Sulfur, Nitrogen, and Oxygen in Steel, Iron, Nickel, and Cobalt Alloys by Various Combustion and Fusion Techniques," *Book of Standards Volume 03.05*, ASTM International, West Conshohocken, PA.
4. ASTM A 276. (1949). Tentative Specification for Hot-Rolled and Cold-Finished Corrosion-Resisting Steel Bars. American Society for Testing and Materials (ASTM). Philadelphia, PA.
5. ASTM A 276. (1955). Standard Specification for Hot-Rolled and Cold-Finished Corrosion-Resisting Steel Bars. American Society for Testing and Materials (ASTM). Philadelphia, PA.
6. ASTM C1152. (2012). Standard Test Method for Acid-Soluble Chloride in Mortar and Concrete. *Book of Standards Volume 04.02*, ASTM International, West Conshohocken, PA.